From cell to nerve in regional anesthesia

ten Hoope, W.

Publication date
2024
Document Version
Final published version

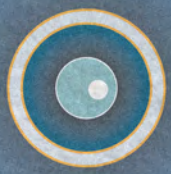

FROM CELL TO NERVE

IN REGIONAL ANESTHESIA

Werner ten Hoope

FROM CELL TO NERVE
IN REGIONAL ANESTHESIA

Werner ten Hoope

FROM CELL TO NERVE IN REGIONAL ANESTHESIA

ISBN 978-94-6483-969-2

Provided by thesis specialist Ridderprint, ridderprint.nl
Printing: Ridderprint
Layout and design: Erwin Timmerman, persoonlijkproefschrift.nl

Financial support for printing of this thesis was kindly provided by B. Braun Medical, Pajunk, and University of Amsterdam.

From cell to nerve in regional anesthesia

ACADEMISCH PROEFSCHRIFT

ter verkrijging van de graad van doctor
aan de Universiteit van Amsterdam
op gezag van de Rector Magnificus
prof. dr. ir. P.P.C.C. Verbeek
ten overstaan van een door het College voor Promoties ingestelde commissie,
in het openbaar te verdedigen in de Agnietenkapel
op vrijdag 17 mei 2024, te 13.00 uur

door Werner ten Hoope
geboren te 's-Gravenhage

Promotiecommissie

Promotores:	prof. dr. M.W. Hollmann	AMC-UvA
	prof. dr. J. Hermanides	AMC-UvA
Copromotores:	dr. ir. A.O. Verkerk	AMC-UvA
	dr. M.L. van Zuylen	AMC-UvA
Overige leden:	prof. dr. J.H. de Vries	AMC-UvA
	prof. dr. M.B. Vroom	AMC-UvA
	prof. dr. A.P.J. Vlaar	AMC-UvA
	prof. dr. J. Bruhn	Radboud Universiteit
	prof. dr. M.M.P.J. Reijnen	Universiteit Twente
	dr. E.M.E. Bos	AMC-UvA

Faculteit der Geneeskunde

TABLE OF CONTENTS

Chapter 1

General introduction and thesis outline

SECTION 1

REGIONAL ANESTHESIA AND DIABETIC NEUROPATHY

The Western World faces escalating challenges with Diabetes Mellitus (DM) and accompanying Diabetic Peripheral Neuropathy (DPN). Predictions consistently underestimate their prevalence, but current projections for 2040 anticipate 642 million patients with DM globally [1]. Approximately 10% of these patients exhibit symptomatic DPN, with an expected increase to 60 million neuropathic patients by 2040 [2]. DM patients have a twofold higher likelihood of requiring surgery compared to patients without DM [3]. Although generally considered safe, the suitability of regional anesthesia and the choice of local anesthetics (LA) for individuals with DPN remains uncertain, serving as the focal point of this thesis.

In Section 1 of this thesis, we delve into the clinical significance of having DM in the context of receiving regional anesthesia.

Chapter 2 provides a concise overview of the current literature to improve understanding of factors contributing to the development of DPN and their implications for regional anesthesia practice. **Chapter 3** focuses on the interaction of neuropathy and regional anesthesia, employing a rodent model to simulate neuropathy secondary to Type 2 DM. Clinical and experimental evidence suggests that peripheral nerve blocks exhibit prolonged duration in the presence of DPN [4]. This phenomenon could be attributed to either an increased sensitivity of diabetic nerve fibers to LA (pharmacodynamic hypothesis) [5,6] or a slower decline in LA concentration within the diabetic nerve (pharmacokinetic hypothesis) [7,8]. In this chapter we aimed to determine the minimum effective dose for a nerve block with lidocaine in DPN, quantify lidocaine's impact on nerve currents, and assess intraneural lidocaine concentrations over time.

SECTION 2

TRANSLATIONAL RESEARCH AND REGIONAL ANESTHESIA

Applications of regional anesthesia, including fascial plane blocks and peripheral nerve blocks, have assumed a pivotal role within modern multimodal analgesic approaches [9]. The theoretical advantages encompass enhanced pain management,

heightened patient contentment, prevention of postoperative delirium, and diminished opioid consumption. The significance of regional anesthesia is particularly pronounced in the context of surgeries of extremities characterized by inherent painful procedures. A multitude of injection techniques have been devised to specifically target regions such as the hip, anterior thigh, and knee. Notably, the fascia iliac compartment block (FICB) and the saphenous nerve block stand out as useful approaches. The continued exploration and refinement of these RA techniques shapes the evolving landscape of modern analgesic strategies.

In Section 2 of this thesis, we study the nerve anatomy of the lower limb to comprehend the distribution of analgesia for two regional anesthetic techniques in hip and knee surgery.

Historically, the femoral nerve block (FNB) was the preferred method for regional anesthesia in patients undergoing knee surgery. However, alternative approaches like the adductor canal block (ACB), including low and high-volume mid-thigh and distal adductor canal approaches, have emerged as alternatives, offering the advantage of reduced motor blockade [10]. While the objective of the ACB is to distribute the injected LA within the adductor canal, there have been reports of excessive spread toward the popliteal fossa (PF). This could potentially enhance analgesia for knee surgeries but also poses risks, including coverage of the main motor branches of the sciatic nerve (SCN), leading to adverse events such as postoperative falls. Current anatomical knowledge of distal injectate spread patterns is limited, and the existing literature is challenging to interpret as they primarily focus on single nerve block techniques, whereas clinical practice often involves combined techniques. **Chapter 4** address a radiological cadaveric study investigating the impact of different ACB techniques, involving low and high-volume mid-thigh and distal AC approaches, on the coverage of the main branches of the SCN.

For pain relieve in the upper extremity, numerous injection techniques targeting the hip, anterior thigh and knee have been developed, one of which is the fascia iliac compartment block (FICB). Originating from Winnie's 3-in-1 block, a lumbar plexus approach targeting the femoral nerve (FN), lateral femoral cutaneous nerve (LFCN), and obturator nerve (ON), the FICB employs an infra- (I-FICB) and a suprainguinal (S-FICB) approach. Although the S-FICB has been developed to improve consistency over the I-FICB, debates persist regarding their clinical superiority in providing cov-

erage of the ON [11]. To address this, we conducted a radiological cadaveric study in **Chapter 5,** using both needle insertion approaches with randomized advancements to assess ON coverage, cranial injectate spread, and involvement of FN and LFCN. Our hypothesis posited that S-FICB-H would achieve the most cranial injectate spread, but none of the nerve block techniques would reliably cover the ON.

SECTION 3

CLINICAL RESEARCH AND REGIONAL ANESTHESIA

Section 3 of this thesis focusses on determining the minimal volume dose for a saphenous nerve block *in vivo*, and the clinical relevance of this nerve block in ambulatory knee surgery.

The saphenous nerve, a purely sensory branch of the femoral nerve, plays a role in knee and lower leg innervation and is recognized for its potential in achieving analgesia without motor function loss [12]. Despite this, a structured assessment of the anesthetic spread of the selective saphenous nerve block has not yet been performed, and the minimum effective volume of LA needed to perform the block is not known. **Chapter 6** determines the minimum LA volumes required to achieve an effective block in 50% (eD50) and 95% (eD95) of healthy volunteers.

Efficient pain management is pivotal for the timely discharge of patients undergoing outpatient surgery. Regional anesthesia, specifically peripheral nerve blocks, have been implemented to enhance postoperative pain control and to expedite discharge processes. The adductor canal block (ACB) is suggested as a safe analgesic block that preserves motor function [13]. Studies have reported comparable pain relief and reduced loss of quadriceps motor strength in favor of ACB compared to femoral nerve block (FNB) [13] [14]. However, conflicting findings have been published regarding pain outcomes [15] and quadriceps function [16]. In the context of outpatient surgery, readiness for discharge encompasses various factors such as pain control, side effects, mobility, vital parameters, and surgical complications. **Chapter 7** aims to compare the impact of ACB versus FNB on readiness for discharge in patients undergoing outpatient anterior cruciate ligament (ACL) reconstruction. The hypothesis posits that ACB will provide effective pain control, preserve motor

strength, demonstrate a favorable safety profile, and thereby contribute to an earlier readiness for discharge.

SECTION 4

RESEARCH PROSPECTIVES: ROLE FOR STEM CELLS IN REGIONAL ANESTHESIA

In section 4 of this thesis, we discuss a novel approach for researching regional anesthesia, using a stem cell technique. Historically, in vitro investigations into peripheral regional anesthesia have predominantly relied on animal cell types due to the inherent challenges associated with obtaining human adult or fetal dorsal root ganglion neurons. Translation of findings from animal studies to humans is frequently hindered by significant genetic differences between the two species [17]. The introduction of human induced pluripotent stem cells (iPSC) has the potential to overcome the challenges associated with accessing human neuronal tissue. iPSC technology allows for the reprogramming of conventional human cells into nociceptive DRG neurons, presenting a valuable and ethical approach to conducting in vitro research into regional anesthesia in a human context. This advancement holds promise for more accurate and clinically relevant insights, minimizing the limitations associated with animal models.

Despite its increasing prominence, the field stands to gain from a research model that more accurately mirrors the complex neurobiological intricacies of pain signaling in humans, as compared to existing animal models. This discrepancy underscores the need for a more refined and human-centric approach to study regional anesthesia. By elucidating the principles of iPSC technology, **Chapter 8** aims to explain its potential in enhancing drug research and modeling diseases associated with (chronic) pain. Moreover, it could facilitate a more individualized strategy for regional anesthesia by preserving the genetic code, including mutations and variations, during the iPSC reprogramming process. The exploration of iPSC technology holds promise for bridging the translational gap and fostering a more precise understanding of RA mechanisms, thereby contributing to improved clinical outcomes.

In **Chapter 9** we investigate an induced pluripotent stem cell (iPSC) technology, that offers a means to acquire human cells that are challenging to access, including nociceptive dorsal root ganglion (DRG) neurons, facilitating their utilization in model development and pharmacological research. We briefly demonstrate the suitability of a human iPSC-derived nociceptive DRG neuron model for investigating in regional anesthesia, presenting a case study involving the examination of lidocaine.

References

1. Zimmet PZ, Alberti KG. Epidemiology of Diabetes-Status of a Pandemic and Issues Around metabolic Surgery. Diabetes Care 2016; 39:878-883
2. Said G. Diabetic neuropathy--a review. Nat Clin Pract Neurol 2007; 3:331-340
3. Dhatariya K, Levy N, Kilvert A et al. NHS Diabetes guideline for the perioperative management of the adult patient with diabetes. Diabet Med 2012; 29:420-433
4. Lirk P, Birmingham B, Hogan Q: Regional anesthesia in patients with preexisting neuropathy. Int Anesthesiol Clin 2011; 49: 144-65
5. Craner MJ, Klein JP, Renganathan M, Black JA, Waxman SG: Changes of sodium channel expression in experimental painful diabetic neuropathy. Ann Neurol 2002; 52: 786-92
6. Meerupally R, Singh JN, Sharma SS: Diabetic-induced increased sodium channel activity attenuated by tetracaine in sensory neurons in vitro. Biochem Biophys Res Commun 2014; 453: 296-301
7. Williams BA: Toward a potential paradigm shift for the clinical care of diabetic patients requiring perineural analgesia: strategies for using the diabetic rodent model. Reg Anesth Pain Med 2010; 35: 329-32
8. Pop-Busui R, Marinescu V, Van Huysen C, Li F, Sullivan K, Greene DA, Larkin D, Stevens MJ: Dissection of metabolic, vascular, and nerve conduction interrelationships in experimental diabetic neuropathy by cyclooxygenase inhibition and acetyl-L-carnitine administration. Diabetes 2002; 51: 2619-28
9. Wick, E. C., Grant, M. C. & Wu, C. L. Postoperative Multimodal Analgesia Pain Management With Nonopioid Analgesics and Techniques: A Review. JAMA Surg 152, 691-697, doi:10.1001/jamasurg.2017.0898 (2017)
10. Vora MU, Nicholas TA, Kassel CA, et al. Adductor canal block for knee surgical procedures: review article. J Clin Anesth. 2016;35:295-303
11. Bendtsen, T. F. et al. Suprainguinal fascia iliaca block: does it block the obturator nerve? Reg Anesth Pain Med 46, 832, doi:10.1136/rapm-2021-102712 (2021)
12. Andersen HL, Gyrn J, Moller L, Christensen B, Zaric D. Continuous Saphenous Nerve Block as Supplement to Single-Dose Local Infiltration Analgesia for Postoperative Pain Management After Total Knee Arthroplasty. Reg Anesth Pain Med. 2013 Dec 7;38(2):106-11
13. Sullivan, J.P., In ACL Reconstruction with Patellar Tendon Autograft, Adductor Canal Nerve Blockade Reduced Quadriceps Function Deficits Compared with Femoral Nerve Blockade, but Did Not Differ for Postoperative Pain. J Bone Joint Surg Am, 2019. 101(22): p. 2061
14. Faiaz, A. and S. Kamath, Randomised Controlled Trial between Ultrasound Guided Femoral Nerve Block and Adductor Canal Block for Postoperative Pain and Functional Outcome in Anterior Cruciate Ligament Reconstruction. Journal of Clinical and Diagnostic Research, 2019. **13**: p. 11-14
15. 15. Seangleulur A, M.S., Chernchujit B, Worathongchai S, Sorin T. , Comparison of Post-Operative Analgesia between Adductor Canal Block and Femoral Nerve Block after Arthroscopic Anterior Cruciate Ligament Reconstruction: A Randomized Controlled Trial. J Med Assoc Thai 2019;102:335-42.

16. Ogura, T., et al., Femoral nerve versus adductor canal block for early postoperative pain control and knee function after anterior cruciate ligament reconstruction with hamstring autografts: a prospective single-blind randomised controlled trial. Arch Orthop Trauma Surg, 2021. **141**(11): p. 1927-1934
17. Rostock C, Schrenk-Siemens K, Pohle J, Siemens J. Human vs. Mouse Nociceptors - Similarities and Differences. Neuroscience 2018; 387: 13-27

Section 1

Regional anesthesia and diabetic neuropathy

Chapter 2

Regional anesthesia in diabetic peripheral neuropathy

Based on: Werner ten Hoope, Marjolein Looije, Philipp Lirk
Curr Opin Anaesthesiol. 2017 Oct;30(5):627-631

Abstract

Purpose of review: To summarize recent relevant literature regarding regional anesthesia in the diabetic patient and formulate recommendations for clinical practice.

Recent findings: Diabetic neuropathic nerves, but not nerves of diabetic patients per se, exhibit complex functional changes. As a result, they seem more sensitive to the local anesthetics, and are more difficult to stimulate. When catheters are used postoperatively, diabetes is an independent risk factor for infection.

Summary: The pathophysiologic mechanisms underlying diabetic polyneuropathy are complex. Several pathways are thought to contribute to the development of diabetic neuropathy, triggered most importantly by chronic hyperglycemia. The latter induces inflammation and oxidative stress, causing microvascular changes, local ischemia and decreased axonal conduction velocity. Regional anesthesia is different in patients with diabetic neuropathy in several regards. First, the electric stimulation threshold of the nerve is markedly increased whereby the risk for needle trauma in stimulator-guided nerve blocks is theoretically elevated. The diabetic nerve is also more sensitive to local anesthetics, which results in longer block duration. Local anesthetics have been conjectured to be more toxic in diabetic neuropathy, but the evidence is equivocal and should not be a cause to deny regional anesthesia to patients with a valid indication. When peripheral nerve catheters are used, diabetes is an independent predisposing factor for infection.

Introduction

In the Western World, Diabetes Mellitus (DM) and Diabetic Peripheral Neuropathy (DPN) are two major and steadily increasing problems. Over the years, predictions on its prevalence have consistently underestimated the number of diabetics. For example, the number of more than 350 million diabetics worldwide, originally predicted for the year 2030, was already reached in 2011, and the current 2040 estimate already predicts 642 million diabetics.[1] Approximately 10% of diabetics are symptomatic for diabetic neuropathy,[2] and along these lines, the number of neuropathic patients worldwide would increase to 60 million by 2040. Diabetic patients are estimated to require surgery at least twice as often as non-diabetics,[3] and due to their comorbidities and the types of surgery performed, they are predestined to undergo many procedures such as, e.g., arteriovenous fistula creation under regional anesthesia.[4]

Regional anesthesia is generally thought to be safe, but neuropathy may change the way nerves respond to nerve blocks or neuraxial techniques. [5] There is currently no consensus on whether regional anesthesia techniques should be avoided or adapted in these patients. In a survey among European anesthesiologists, enormous heterogeneity was noted when answering on treating these patients, and more than 80% of respondents stated that more and better research is urgently needed to prepare the clinicians to care for these patients. [5]

In this review, we will focus on the recent advances in knowledge regarding the development of DPN, and the consequences for regional anesthesia.

Pathophysiology of Diabetic Polyneuropathy

The pathophysiologic mechanisms of diabetic polyneuropathy (DPN) are multifactorial and primary based on inflammation, oxidative stress and mitochondrial dysfunction induced by long-standing hyperglycemia. These factors lead to impaired blood vessel functionality in the vicinity of the nerve, immune system and metabolic adjustments, along with alterations in the expression of sodium and calcium channels.[6]

When chronic hyperglycemia is present, the normal cellular glycolysis pathway becomes saturated. Glucose is then processed by alternative oxidation pathways, such as the polyol pathway. These glucose oxidation pathways cause oxidative stress and produce free radicals causing neuron cell damage, and plays a key role in several mechanisms regarding the pathophysiology of DPN. [6, 7]

Microvascular changes and local ischemia

Cell damage is not the only pathologic mechanism. In diabetic neuropathy, the microcirculation is altered and tissue perfusion reduced with resulting nerve hypoxia. Mitochondrial dysfunction leads to a decline of production of nitrous oxide. Lack of NO will result in microvascular vasoconstriction, and lead to local ischemia. In DPN the total number of microvascular vessels is not changed but the quality of the vessels is decreased [6]. Recent animal studies show that vasorelaxation and nerve blood flow are impaired much sooner than previously assumed during the course of diabetic.[8, 9]

Neuroaxonal conduction velocity

Another result of polyol pathway activation is decreased uptake of myo-inositol, a precursor that influences Na/K/ATPase pump activity. The net effect is a decreased drive of sodium out of the cell, which results leads to less depolarization upon stimulation, and a decrease in conduction velocity of the neuron [6, 10]. A less understood phenomenon seen in neural membranes is a differential expression and/or phosphorylation of various sodium channel subtypes, including Nav1.3, Nav1.6, Nav1.7, Nav1.8 and Nav1.9 on primary sensory neurons.[7].

Novel pathophysiologic hypotheses

More recent research has shown that the Central Nervous System (CNS) in patients with diabetes and diabetic neuropathy exhibits profound morphological changes. These changes affect all CNS levels from the spinal cord through thalamic areas, all the way to the cortex. As an example, the gray matter in somatosensory areas of diabetic neuropathic subjects was significantly reduced as compared to non-diabetic and diabetic patients, and even patients with diabetic retinopathy, suggesting a strong relationship between cortical atrophy and diabetic neuropathy.[11] Furthermore, the involvement of sodium channels was revisited by Waxman and colleagues. These authors hypothesized that sodium channels with altered functions might contribute to the development of diabetic neuropathy rather than the traditional viewpoint that neuropathy causes sodium channel dysfunction. Following this hypothesis, sodium channel dysfunction and the diabetic state would be the main pathogenic factors for the development of neuropathy.[12] Also, the involvement of microglia is beginning to be better understood, particularly in cases of painful diabetic neuropathy, which affects up to half of diabetic neuropathic patients and still represents a substantial chronic pain treatment challenge.[13]

Consequences of Diabetic Neuropathy for Regional Anesthesia

The above-mentioned pathophysiological processes potentially influence nerve localization, and the pharmacodynamics and pharmacokinetics of local anesthetics when performing a nerve block in diabetic neuropathic nerve.

Nerve localization/stimulation

Electrical stimulation of nerves and peripheral nerve identification with ultrasound are well-established methodologies for administering peripheral nerve blocks. Recent evidence has called into question the reliability (accuracy) of nerve stimulation to guide correct needle position during regional anesthesia.[14] Theoretically, nerve stimulation is even more problematic in patients with diabetic neuropathy, because their baseline rheobase, the major determinant of stimulation threshold, is increased.[10] The first (experimental) evidence was provided by Rigaud et al., who performed sciatic nerve block in dogs, and showed a high likelihood of intraneural needle position in diabetic, but not healthy control animals. [15] Later, the first clinical evidence was contributed by Bigeleisen and colleagues, who showed increased stimulation thresholds in diabetic versus healthy patients for the brachial plexus.[16] Keyl et al. [17] compared a small group of DM patients scheduled for ischemic limb surgery to non-diabetic controls scheduled for ankle surgery. Both groups received popliteal sciatic nerve block before surgery under double guidance with stimulation and ultrasound. Stimulation thresholds at needle-nerve contact for control patients (mean 0.26 mA) were comparable to commonly accepted ranges for correct needle position of 0,3-0,5 mA. In the DM patients, assumed to be at high risk of DNP, the mean stimulation current needed to provoke a motor response at needle-nerve contact was almost 7-fold higher (mean 1,9mA) with considerable inter-individual variation. More recently, Heschl and colleagues [18] studied the stimulation threshold in healthy, diabetic and diabetic neuropathic patients undergoing lower limb surgery requiring sciatic nerve block. The authors found higher inter-patient variability in stimulation threshold than had been reported by Keyl [17] both for patients with or without DM. Diabetic neuropathy, but not diabetes per se, was associated with an increased stimulation threshold. The correlation with nerve conduction velocity was significant but weak. In the clinical situation, when using nerve stimulation as sole guidance, the precise degree of neuropathy and stimulation change is not known, so choosing the right cut-off level for stimulation can be difficult. Selecting a stimulation threshold too low may theoretically result in nerve trauma, while accepting a high stimulation threshold will most likely result in a share of failed blockades. The

number of patients in whom stimulation thresholds above >2mA were necessary were predominantly diabetic (12/55 vs 2/52 patients in the diabetic versus control group, respectively). Especially these outliers are, theoretically, at risk for intraneural injections of local anesthetics.

In summary, evidence shows that diabetic neuropathic nerves require, on average, a higher stimulation threshold than healthy nerves, but the precise value cannot be predicted accurately from anamnesis, or even detailed neurological testing.

Nerve sensitivity

In accordance to the postulated pathophysiologic mechanisms, it is expected that neuropathic nerves would be more sensitive to local anesthetics and therefore the success rate of nerve block would be higher in patients with DPN. Gebhard [19] performed a retrospective study in patients receiving supraclavicular nerve blocks. The success rate was higher in patients with diabetes than in nondiabetics (96% in DM vs 87% in NDM, p<0,001), independent of sex or BMI. It has long been hypothesized that lower doses of local anesthetics would be needed in diabetic neuropathic patients, but evidence is very limited.

Block duration

Several experimental studies have investigated the effect of diabetic neuropathy on block duration. While Kalichman and Calcutt reported no difference in block duration between diabetic and control animals, Kroin and Lirk reported longer block duration in diabetic neuropathic animals.[20-22] Kroin [23] further examined whether it was neuropathy or hyperglycemia that causes increases in block duration. The authors found that long-term glucose control with attenuation of neuropathy normalized block duration, whereas acute glucose control or hyperglycemia control did not.

In clinical studies, Cuvillon [24] and Salviz [25] reported that onset time of sciatic or axial nerve blocks was not significantly different between diabetics and non-diabetics whereas Sertoz [26] reported that onset of block duration is longer and the block regression time is substantially longer in poorly controlled diabetes. The decrease in nerve blood flow long recognized in diabetic neuropathy [27] would theoretically lead to a prolonged wash-out phase. Three clinical studies support this theory. Cuvillon [24] showed that well-regulated non-insulin dependent DM patients without apparent clinical DPN or neuropathy still have longer sciatic sensory block durations then non-DM controls (median 21h vs 17h). There was no difference in age between groups so the results are not likely to be biased by ageing nerves. Salviz

[25] confirmed the same principle in upper extremity blocks (median 13h vs 6h block duration). They also found a strong correlation between block duration and time since diagnosis DM, but not with HbA1c levels, although all participants seemed to have well-regulated blood glucoses (mean 6.6% ±0.1). Sertoz [26] further investigated the influence of HbA1c on block duration. The theory is that inadequately controlled blood glucose levels increase the likelihood of microvascular damage or damage of nerves, even though patients in this study were not tested specifically for neuropathy. The authors included 48 patients with diabetes mellitus, which were split into 3 groups based on their HbA1c (i.e. 5-6%, 7-8%, 9-10%). After popliteal nerve block both motor as sensory block regression time increased significantly in the 9-10% HbA1c group. The reasons for the prolonged block duration have not been clarified, but both pharmacodynamic (sodium currents are more sensitive) and pharmacokinetic (decreased nerve blood flow leads to extended duration of local anesthetics within the nerve) mechanisms have been conjectured.[22]

In conclusion, diabetic neuropathy leads to prolonged block duration. The precise mechanism has not been elucidated.

Complications of local anesthetics in DPN

Nerve toxicity

The idea that diabetic nerves are more vulnerable for toxic effects is based on the two-hit hypotheses, claiming that a nerve at risk, like a DPN nerve, who is subjected to a second hit, in this case LA, will be at higher risk to remain permanently damaged. The first landmark study was published by Kalichman and Calcutt, who showed that with 4% lidocaine, but not 2% lidocaine, nerves in patients with diabetes mellitus exhibited more damage compared to control patients. Kroin [20] explored various combinations of local anesthetics for their impact on histologic changes in rats with (type 1, streptozotocin model) and without diabetes mellitus. The diabetic rats showed increased neuronal damage with lidocaine/clonidine or ropivacaine, then with 10mg/ml lidocaine. It was questionable if the histology was illustrative for nerve damage as result of the medication, for the control animals injected with saline and the naïve healthy animals also had some small degree of nerve damage, possibly due to aging. Lirk [22] focused also on the differences in animals with early and advanced DM (type 2, ZDF rats), but found no clinically significant increase in neurotoxicity in diabetic animals.

Lirk et al [28] reviewed the literature of patients with diabetes mellitus who had possible nerve damage after local anesthetics. Nerve damage in patients with diabetes mellitus after peripheral nerve block was reported in six cases. Similarly, the epidemiology of nerve injury after regional anesthesia in diabetic neuropathic patients is unclear. In the only epidemiologic study, two patients out of 567 (0.4%) undergoing neuraxial anesthesia and analgesia suffered from new-onset neurologic deficit, but these numbers are too small on their own to allow conclusions on whether local anesthetics are more toxic on diabetic or diabetic neuropathic nerves. The authors believe that when a valid indication has been set for peripheral or central blockade, diabetic neuropathy should not be a reason to withhold regional anesthesia from the patient.

Infection

When catheters are placed for postoperative pain relief, the risk of infection increases over time. Nicolotti et al [29] performed a review on infection complication after perineural catheter placement, identifying postoperative hyperglycemia and diabetes mellitus as independent risk factors. Aveline et al [30] prospectively assessed 747 cases of locoregional anesthesia with ultrasound. They showed mostly low (10% and 0.13%) bacterial colonization and catheter infection, however diabetes mellitus was associated with an increased incidence (OR 2.32(95% CI 1.43-9.58) p0.004). Similarly, Bomberg and colleagues demonstrated diabetes as a risk factor for postoperative infection of peripheral nerve bock catheters.[31]

Conclusion

The mechanism of diabetic polyneuropathy is not completely understood, while we now understand that DPN and other end-organ failure is mainly the result of oxidative pathways. The threshold of nerve stimulation is markedly increased and ultrasound as alternative to (blind) electric nerve stimulation is most likely safer. Regional anesthesia in patients with DPN is characterized by longer block duration. Using clinically relevant doses, no excessive toxicity of local anesthetics has been demonstrated in animal models of diabetic neuropathy.

References

1. Zimmet PZ, Alberti KG. Epidemiology of Diabetes-Status of a Pandemic and Issues Around Metabolic Surgery. Diabetes Care 2016; 39:878-883.
2. Said G. Diabetic neuropathy--a review. Nat Clin Pract Neurol 2007; 3:331-340.
3. Dhatariya K, Levy N, Kilvert A *et al.* NHS Diabetes guideline for the perioperative management of the adult patient with diabetes. Diabet Med 2012; 29:420-433.
4. Aitken E, Jackson A, Kearns R *et al.* Effect of regional versus local anaesthesia on outcome after arteriovenous fistula creation: a randomised controlled trial. Lancet 2016; 388:1067-1074. ****** One of the few studies demonstrating improvement in functional outcome with Regional anesthesia.
5. Lirk P, Rutten MH, Haller I *et al.* Management of the patient with diabetic peripheral neuropathy presenting for peripheral regional anesthesia: a European survey and review of literature. Minerva Anestesiol 2013; 79:1039-1048.
6. Roman-Pintos LM, Villegas-Rivera G, Rodriguez-Carrizalez AD *et al.* Diabetic Polyneuropathy in Type 2 Diabetes Mellitus: Inflammation, Oxidative Stress, and Mitochondrial Function. J Diabetes Res 2016; 2016:3425617.

** Very good review article on diabetic neuropathy.

7. Schreiber AK, Nones CF, Reis RC *et al.* Diabetic neuropathic pain: Physiopathology and treatment. World J Diabetes 2015; 6:432-444.
8. Oltman CL, Coppey LJ, Gellett JS *et al.* Progression of vascular and neural dysfunction in sciatic nerves of Zucker diabetic fatty and Zucker rats. Am J Physiol Endocrinol Metab 2005; 289:E113-122.
9. Coppey LJ, Gellett JS, Davidson EP *et al.* Changes in endoneurial blood flow, motor nerve conduction velocity and vascular relaxation of epineurial arterioles of the sciatic nerve in ZDF-obese diabetic rats. Diabetes Metab Res Rev 2002; 18:49-56.
10. Nodera H, Kaji R. Nerve excitability testing and its clinical application to neuromuscular diseases. Clin Neurophysiol 2006; 117:1902-1916.
11. Tesfaye S, Selvarajah D, Gandhi R *et al.* Diabetic peripheral neuropathy may not be as its name suggests: evidence from magnetic resonance imaging. Pain 2016; 157 Suppl 1:S72-80.
12. Hoeijmakers JG, Faber CG, Merkies IS, Waxman SG. Channelopathies, painful neuropathy, and diabetes: which way does the causal arrow point? Trends Mol Med 2014; 20:544-550.
13. Cameron NE, Cotter MA, Low PA. Nerve blood flow in early experimental diabetes in rats: relation to conduction deficits. Am J Physiol 1991; 261:E1-8.
14. Sala-Blanch X, de Riva N, Carrera A *et al.* Ultrasound-guided popliteal sciatic block with a single injection at the sciatic division results in faster block onset than the classical nerve stimulator technique. Anesth Analg 2012; 114:1121-1127.
15. Rigaud M, Filip P, Lirk P *et al.* Guidance of block needle insertion by electrical nerve stimulation: a pilot study of the resulting distribution of injected solution in dogs. Anesthesiology 2008; 109:473-478.
16. Bigeleisen PE, Moayeri N, Groen GJ. Extraneural versus intraneural stimulation thresholds during ultrasound-guided supraclavicular block. Anesthesiology 2009; 110:1235-1243.

17. Keyl C, Held T, Albiez G *et al.* Increased electrical nerve stimulation threshold of the sciatic nerve in patients with diabetic foot gangrene: a prospective parallel cohort study. Eur J Anaesthesiol 2013; 30:435-440.
18. Heschl S, Hallmann B, Zilke T *et al.* Diabetic neuropathy increases stimulation threshold during popliteal sciatic nerve blockdagger. Br J Anaesth 2016; 116:538-545.
19. Gebhard RE, Nielsen KC, Pietrobon R *et al.* Diabetes mellitus, independent of body mass index, is associated with a "higher success" rate for supraclavicular brachial plexus blocks. Reg Anesth Pain Med 2009; 34:404-407.
20. Kroin JS, Buvanendran A, Williams DK *et al.* Local anesthetic sciatic nerve block and nerve fiber damage in diabetic rats. Reg Anesth Pain Med 2010; 35:343-350.
21. Lirk P, Flatz M, Haller I *et al.* In Zucker Diabetic Fatty Rats, Subclinical Diabetic Neuropathy Increases In Vivo Lidocaine Block Duration But Not In Vitro Neurotoxicity. Reg Anesth Pain Med 2012; 37:601-606.
22. Lirk P, Verhamme C, Boeckh R *et al.* Effects of early and late diabetic neuropathy on sciatic nerve block duration and neurotoxicity in Zucker diabetic fatty rats. Br J Anaesth 2015; 114:319-326.
23. Kroin JS, Buvanendran A, Tuman KJ, Kerns JM. Effect of Acute Versus Continuous Glycemic Control on Duration of Local Anesthetic Sciatic Nerve Block in Diabetic Rats. Reg Anesth Pain Med 2012; 37:595-600.
24. Cuvillon P, Reubrecht V, Zoric L *et al.* Comparison of subgluteal sciatic nerve block duration in type 2 diabetic and non-diabetic patients. Br J Anaesth 2013; 110:823-830.
25. Salviz EA, Onbasi S, Ozonur A *et al.* Comparison of Ultrasound-Guided Axillary Brachial Plexus Block Properties in Diabetic and Nondiabetic Patients: A Prospective Observational Study. J Hand Surg Am 2017; 42:190-197.
26. Sertoz N, Deniz MN, Ayanoglu HO. Relationship between glycosylated hemoglobin level and sciatic nerve block performance in diabetic patients. Foot Ankle Int 2013; 34:85-90.
27. Theriault M, Dort J, Sutherland G, Zochodne DW. Local human sural nerve blood flow in diabetic and other polyneuropathies. Brain 1997; 120 (Pt 7):1131-1138.
28. Lirk P, Rutten MV, Haller I *et al.* Management of the patient with diabetic peripheral neuropathy presenting for peripheral regional anesthesia: a European survey and review of literature. Minerva Anestesiol 2013; 79:1039-1048.
29. Nicolotti D, Iotti E, Fanelli G, Compagnone C. Perineural catheter infection: a systematic review of the literature. J Clin Anesth 2016; 35:123-128.
30. Aveline C, Le Hetet H, Le Roux A *et al.* Perineural ultrasound-guided catheter bacterial colonization: a prospective evaluation in 747 cases. Reg Anesth Pain Med 2011; 36:579-584.
31. Bomberg H, Kubulus C, List F *et al.* Diabetes: a risk factor for catheter-associated infections. Reg Anesth Pain Med 2015; 40:16-21.

Chapter 3

Pharmacodynamics and pharmacokinetics of lidocaine in a rodent model of diabetic neuropathy

Based on: Werner ten Hoope, Markus W. Hollmann, Kora de Bruin, Hein J. Verberne, Arie O. Verkerk, Hanno L. Tan MD PhD, Camiel Verhamme MD PhD, Janneke Horn MD PhD, Marcel Rigaud, Susanne Picardi, Philipp Lirk
Anesthesiology 2018 Mar;128(3):609-619

Abstract

Background

Clinical and experimental data show that peripheral nerve blocks last longer in the presence of diabetic neuropathy. This may occur because diabetic nerve fibers are more sensitive to local anesthetics, or because the local anesthetic concentration decreases more slowly in the diabetic nerve. The aim of this study was to investigate both hypotheses in a rodent model of neuropathy secondary to Type 2 Diabetes.

Methods

We performed a series of sciatic nerve block experiments in twenty-five Zucker Diabetic Fatty rats aged 20 weeks with a neuropathy component confirmed by neurophysiology, and control rats. We determined *in vivo* the minimum local anesthetic dose of lidocaine for sciatic nerve block. To investigate the pharmacokinetic hypothesis, we determined concentrations of radiolabeled (^{14}C) lidocaine up to 90 minutes after administration. Last, dorsal root ganglia were excised for patch clamp measurements of sodium channel activity.

Results

First, in vivo minimum local anesthetic dose of lidocaine for sciatic nerve motor block was significantly lower in diabetic (0.9%) as compared to control rats (1.4%). Second, at 60 minutes following nerve block, intraneural lidocaine was higher in the diabetic animals. Third, single cell measurements showed a lower inhibitory concentration of lidocaine for blocking sodium currents in neuropathic as compared to control neurons.

Conclusions

We demonstrate increased sensitivity of the diabetic neuropathic nerve towards local anesthetics, and prolonged residence time of local anesthetics in the diabetic neuropathic nerve. In this rodent model of neuropathy, both pharmacodynamic and pharmacokinetic mechanisms contribute to prolonged nerve block duration.

Introduction

Local anesthetics are widely used to block nerve conduction for surgical anesthesia, or to manage acute and chronic pain. However, diabetic neuropathic nerves may react differently to blockade than healthy nerves.[1] We have previously shown in Zucker Diabetic Fatty rats with neuropathy that nerve blocks last substantially longer as compared to healthy control rats.[2] This is in concordance with recent experimental [3] and clinical [4] literature, but the mechanism of block prolongation remains unknown.

There are two hypotheses why nerve blocks could last longer in diabetic neuropathy; the first is pharmacodynamic and states that nerve fibers are more susceptible because their sodium channel expression [5] and function [6] has changed. The second hypothesis is pharmacokinetic, and stipulates delayed washout of local anesthetic due to microangiopathy [7] and decreased nerve blood flow.[8] Both mechanisms have been assumed,[1] but never directly investigated in the context of regional anesthesia.

Using the local anesthetic lidocaine in a rodent model of diabetic neuropathy, we examined minimum local anesthetic dose of lidocaine for sciatic nerve block *in vivo*, used patch clamp measurements to quantify the effect of lidocaine on sodium currents *in vitro*, and determined intraneural concentrations of lidocaine *in vivo* over time. Our hypotheses were that as compared to healthy control nerves, 1) diabetic neuropathic neurons would be more sensitive to the blocking effects of lidocaine, and 2) the intraneural lidocaine concentration after nerve blockade would remain elevated over time.

Materials and Methods

The present study protocol was approved on December 18th, 2014 by the Institutional Animal Care and Use Committee of the Academic Medical Center, University of Amsterdam, protocol number LEICA75AA-1. Methods and results are reported according to ARRIVE guidelines.[9]

Experimental setup

Experiments were carried out in 25 male Zucker diabetic fatty and 25 control rats, obtained from Charles River Laboratories (L'Arbresle, France). Zucker diabetic fatty rats are an inbred model of Type II DM that combines a dietetic component (Purina

#5008 diet, Charles River, L'Arbresle, France) with a genetic predisposition. Diabetic animals exhibit a leptin receptor mutation (fa/fa, "diabetic"), while control animals carry a heterozygous mutation (fa/+, "CTRL or Control").[10]

Animals underwent two sets of experiments. In week 1, animals were tested for diabetic state and nerve conduction velocity, and subsequently we performed sciatic nerve block with varying concentrations of lidocaine to determine *in vivo* minimum local anesthetic dose for motor blockade in control versus diabetic animals. In week 2, we repeated and confirmed nerve conduction velocity measurements and performed sciatic nerve block with radiolabeled lidocaine to measure intraneural lidocaine concentrations over time. After these experiments were completed, 9 animals from both groups underwent excision of the lumbar dorsal root ganglia for patch-clamp experiments to determine the effects of lidocaine on sodium currents in diabetic versus healthy nerves.

Animals

Animals were obtained at 14 weeks of age and were given six weeks for acclimatization, with free access to water and diet. For all electrophysiological measurements, sciatic nerve block, and measurements of weight and glucose, animals were anesthetized using isoflurane (Baxter, Utrecht, The Netherlands) with an inspiratory concentration of 2-3 Vol% since this regimen least affects electrophysiological measurements in rodent models.[11] To minimize animal distress the electrophysiological measurements and nerve blocks were performed percutaneously. Buprenorphine (0.05 mg/kg body weight) was used as analgesic rescue.

Glucose was measured before experiments using a commercially available glucose meter (GlucoMen, Menarini Diagnostics, Valkenswaard, The Netherlands) able to detect glucose values of up to 33 mmol/L. If glucose values exceeded the upper detection limit, we set these values at 33 mmol/L.

Animal welfare (e.g. animal appearance and behavior) was assessed at least weekly by an animal care technician unaffiliated with the experimental team. Out of the fifty animals, one animal in the control group fulfilled predefined criteria for early termination of experiments (humane endpoints) when it developed a growing skin defect after percutaneous nerve block in week 1. The animal was euthanized. Further, one diabetic animal died during induction of anesthesia using isoflurane in week 2. Replacement of animals was done after consultation with the Animal Care and Use Committee. All other animals survived to the end of the experiment, no animal needed analgesic rescue, and welfare assessment showed no abnormal-

ities concerning appearance or behavior at any time point. All animals showed full recovery from sciatic nerve block after the experiments of week 1. After the last experiments, while still under isoflurane anesthesia, animals were euthanized using CO_2 narcosis. For additional patch clamp experiments requested during the Journal review process we received permission by the Animal Care and Use Committee to obtain additional four Zucker diabetic fatty rats and four control rats.

Sciatic nerve block

Nerve block was performed percutaneously combining the technique described by Thalhammer et al.[12] modified by nerve stimulation as described by Kroin et al.[13] In brief, a 25G needle was introduced just caudal to the sciatic notch in a cephalad direction, and connected with a clip to the electromyography system programmed to deliver a pulse of 0.1 ms duration, and 0.5 mA current, triggered manually. Ipsilateral hind-leg muscle contraction in the absence of local gluteal muscle stimulation was taken as sign of proximity of needle to nerve, and injection of 0.2 mL of lidocaine 2% was performed.[14] We defined a successful nerve block on the basis of two signs: successful nerve stimulation as described above before injection and subsequent behavioral testing showing absence of the toe-spreading reflex. The latter reflex, used to test sciatic nerve fibers, was evaluated as described before.[14] In brief, animals were gently lifted, resulting in a physiologic vestibular reflex where toes are extended and spread.

Electrophysiology

Animal temperature was maintained well above 34°C using a warming blanket (Harvard Apparatus, Zouterwoude, The Netherlands). We studied the sciatic nerve with monopolar needle electrodes as described previously,[15] using the PowerLab 4/25T nerve stimulator together with the Scope software package Version 3.8.7 (both from AD Instruments, Oxford, UK). In brief, for motor conduction studies of the sciatic nerve the recording cathode was placed in the muscles between the hallux and the second digit, and the recording anode was placed subcutaneously on the lateral surface of the fifth digit. Stimulating electrodes were inserted 3 mm apart at the medial ankle, and just cranial to the sciatic notch. A grounding electrode was attached between the stimulating and the recording electrodes. Supramaximal square-wave pulses of 0.1 ms duration were delivered. Supramaximal stimulation was achieved by increasing the intensity by 25-30% above the current that gave maximal muscle response. Motor nerve conduction velocity was calculated over the segment be-

tween the sciatic notch and the ankle.[15] Measurements were carried out by one investigator (P.L.), and neurophysiology graphs underwent blinded assessment and validation by an experienced neurophysiologist (C.V.).

Pharmacodynamics – *In vivo* minimum local anesthetic dose

For the determination of minimum local anesthetic dose, we performed sciatic nerve blocks using lidocaine (BBraun, Melsungen, Germany) in various dilution steps (in normal saline 0.9%, BBraun) in a total volume of 0.2 mL [14] and evaluated sciatic nerve motor block (yes/no) after 20 minutes. The starting concentration was 2% and according to the Dixon up-and-down method, when a successful block was observed, this concentration was decreased by 0.2% for the subsequent test animal. Conversely, failed block lead to subsequent increase of the dose by 0.2%. The concentration of lidocaine at which a successful block would be achieved in 50% of the test animals (ED50) was determined by calculating the mean dose from consecutive rats in which successful nerve block was followed by failed nerve block three times.[16] A priori, we determined that a difference of 0.25% in minimum local anesthetic dose would be considered relevant.

Pharmacodynamics – *In vitro* electrophysiology

Cell preparation

Single dorsal root ganglion (DRG) neurons were obtained by enzymatic dissociation following a protocol described previously.[17] In short, L4 and L5 dorsal root ganglia were excised and placed into cold (4ºC) solution containing (in mM): Na^+ 145, K^+ 4, Ca^{2+} 2.5, Mg^{2+} 1, L-malate$^-$ 5, acetate$^-$ 24, Cl^- 127 (Sterofundin, BBraun, Melsungen, Germany). The ganglia were dissected and stored in a modified Tyrode's solution (20°C) containing (in mM): NaCl 140, KCl 5.4, $CaCl_2$ 1.8, $MgCl_2$ 1.0, glucose 5.5, HEPES 5.0; pH 7.4 (NaOH). Next, the ganglion pieces were placed in nominally Ca^{2+}-free Tyrode's solution (37°C), *i.e.*, modified Tyrode's solution with 10 mM $CaCl_2$, which was refreshed two times before the addition of liberase IV (0.25–0.29 U/ml; Roche, Indianapolis, IN, USA) and elastase (2.4–0.7 U/mL; Serva, Heidelberg, Germany) for 10 min. During the incubation period, the tissue was triturated through a pipette (tip diameter: 2.0 mm). The dissociation was stopped by transferring the ganglion pieces into nominally Ca^{2+}-free Tyrode's solution (20°C). The tissue was triturated (pipette tip diameter: 0.8 mm) in Ca^{2+}-free Tyrode's solution for 4 min to obtain single cells. Finally, the nominally Ca^{2+}-free Tyrode's solution was replaced with normal Tyrode's solution in

three steps to increase the Ca^{2+} concentration. In each step, approximately 75% of the solution on top of the cells was carefully replaced with Tyrode's solution. The time interval between the solution changes was 10–15 min. For electrophysiological measurements, small aliquots of cell suspension were put in a recording chamber on the stage of an inverted microscope. DRG neurons were allowed to adhere for 5 minutes before superfusion was initiated.

Recording procedures.
Action potentials (APs) and the sodium current (I_{Na}) were recorded with the patch-clamp technique using an Axopatch 200B Clamp amplifier (Molecular Devices, Union City, CA) and custom-made acquisition software (Scope; kindly provided by J. Zegers). Membrane currents and potentials were low-pass filtered (cut off 5 kHz) and digitized at 40 kHz. APs and I_{Na} were analyzed offline using custom-made software (MacDaq; kindly provided by A. van Ginneken). Cell membrane capacitance (C_m) was estimated by dividing the decay time constant of the capacitive transient, in response to 5 mV hyperpolarizing voltage clamp steps from –40 mV, by the series resistance. Series resistance was compensated for by at least 80%.

Current clamp experiments.
APs were recorded at 36±0.2°C in modified Tyrode's solution by the amphotericin-perforated patch-clamp technique. Pipettes (borosilicate glass; resistance 1.5–2 MW) were filled with solution containing (mM): K-gluc 125, KCl 20, NaCl 10, amphotericin-B 0.44, HEPES 10; pH 7.2 (KOH). APs were elicited by applying 500 ms depolarizing current pulses of various amplitudes through the patch pipette. We analyzed the resting membrane potential (RMP) as the potential just before the depolarizing current pulses. In addition, from the first AP during the depolarizing pulse, we measured: 1) the the AP overshoot, i.e., the maximal potential of the AP above the 0 mV level, 2) the maximal upstroke velocity (dV/dt_{max}) by the first derivative of the AP, and 3) the AP duration (APD) at 50% repolarization (APD_{50}).

Voltage clamp experiments.
I_{Na} was recorded at 20°C with the whole-cell ruptured patch-clamp technique using a voltage-clamp protocol with a holding potential of -60 mV and 300-ms depolarizing pulses to 0 mV. This depolarizing test pulse was preceded by a 700-ms prepulse to -50 and -120 mV. We defined the I_{Na} recorded with the prepulse to -50 mV as tetrodotoxin (TTX)-resistant, while the TTX-sensitive I_{Na} was obtained by digital subtraction

of the TTX-resistant I_{Na} from the total I_{Na}, measured after the prepulse to -120mV. The cycle length was 5 sec. Extracellular solution contained (in mM): 20 NaCl, 120 CsCl, 1.8 $CaCl_2$, 1.2 $MgCl_2$, 0.1 $CdCl_2$, 11.0 glucose, 5.0 HEPES; pH 7.4 (CsOH). Pipettes were filled with solution containing (mM) 3.0 NaCl, 133 CsCl, 2.0 $MgCl_2$, 2.0 Na_2ATP, 2.0 TEACl, 10 EGTA, 5.0 HEPES; pH 7.2 (CsOH). I_{Na} was defined as the difference between peak current and the current at the end of the depolarizing voltage step. Dose–response curves of the effects of lidocaine on I_{Na} were fitted to the Hill equation: $I_{drug}/I_{control}=1/[1+(dose/IC_{50})^n]$, where $I_{drug}/I_{control}$ is the normalized I_{Na} current, dose is the bath concentration of the drug, IC_{50} is the concentration required for 50% current block, and n is the Hill coefficient.

Pharmacokinetics – Intraneural lidocaine

Nerve block was performed on 24 control and 25 diabetic rats using radiolabeled ^{14}C-lidocaine obtained from American Radiolabeled Chemicals (ARC, St. Louis, MO, United States). Nerves were harvested at 5, 10, 30, 60, and 90 minutes after injection. Animals with excision at 5 and 10 minutes were kept under anesthesia until tissue harvesting, and animals with excision at 30, 60 and 90 minutes were awakened and subjected to behavioral testing until tissue harvesting. Sciatic nerves were excised from a point proximal to the sciatic notch to the popliteal fossa guided by methylene blue injectate. Nerves were homogenized in 0.5 mL Solvable™ tissue solubilizer (Solvable® Packard Chemical Operations, The Netherlands), before being incubated with 5 mL InstaGel scintillation solution (Perkin Elmer, Groningen, The Netherlands). The radioactivity was determined after 10 min by liquid scintillation counting (2000CA, Packard, Amstelveen, The Netherlands) and corrected for background activity. The measured radioactivity is expressed in disintegrations per minute (DPM). Animals were assigned to treatment group (duration) using a pre-defined random number list (random.org List randomizer, accession date May 20th, 2015).

Statistical analysis

For single cell measurements, normality and equal variance assumptions were tested with the Kolmogorov-Smirnov and the Levene median test, respectively. Groups were compared with unpaired *t*-test or, in case of a failed normality and/or equal variance test, Mann-Whitney rank sum test. Paired *t*-tests were used to compare drug effects between groups of cells.

Data for motor blockade was not normally distributed. Therefore, means and bias corrected and accelerated 95% confidence intervals (BCa 95% CI) were derived

following bootstrapping, drawing 1,000 samples of the same size as the original samples. *P*<0.05 was considered statistically significant.

For measurements of intraneural lidocaine concentration, data not normally distributed were log transformed. Data are presented in scatterplots on a log scale by time in minutes, as median (log) with the interquartile range (25-75 percentile). Boxplots of the control arm and DM arm were constructed. The log transformed data were analyzed using a two-way ANOVA for repeated measurements. A post-hoc subgroup analysis at the different time points was performed using the Welch t-test for unequal variances in order to test for significant differences between the DM group and the control group. Considering the multiple testing of hypothesis (p values), we added Bonferroni adjusted p values for the 30 minutes and 60 minutes level. Therefore, we multiplied the unadjusted p-values by the number of hypotheses tested, 5. If the Bonferroni adjusted p-values are still less than the original alpha set for the study (0.05), we rejected the null hypothesis. A two-sided p-value<0.05 was considered to be statistically significant.

Sample size calculation

For the pharmacodynamic experiments (Dixon up-and-down method), no sample size calculation was applicable. We estimated between 10 and 20 subjects necessary to reliably determine minimum local anesthetic dose. Therefore, sample size was determined on basis of intraneural lidocaine experiments, and no corrections for further experiments were made for findings obtained during pharmacodynamic experiments. The number of test animals was determined on basis of earlier experiments [18] in which epinephrine was used to modify the intraneural concentration of local anesthetic. Since the effects of diabetic neuropathy and added epinephrine on nerve block duration are comparable,[14] and no preliminary results concerning diabetic lidocaine kinetics were available, we used the same group size of 10 nerves per measurement time point used by Sinnott et al.[18] This translated into 5 animals injected bilaterally (i.e. 10 nerves) per time point of analysis, resulting in 25 diabetic and 25 control animals being tested. This would allow detection of a difference in intraneural concentration of 30% between healthy and diabetic animals, with a Power of 80% and with an alpha of P < 0.05, assuming a common standard deviation of 20%, and one lost specimen per group. Also, this number would be high enough to allow for the pharmacodynamic experiments. Power analysis was done with the aid of nQuery Advisor® 7.0 (Statistical Solutions Ltd., Cork, Ireland).

Results

Diabetic model

At the time of experiments, diabetic animals were heavier and had markedly elevated plasma glucose concentrations (Table 1). These findings were consistent between week 1 and 2. Also, motor nerve conduction velocity was significantly slower in the diabetic group as compared to control animals at both time points (Table 1). There was no significant change in nerve conduction velocity in either group between experiments in week 1 and week 2.

Table 1.

Week 1	**Control (n=25)**	**Diabetic (n=25)**	**P-value**
Weight (g)	344 ± 24	387 ± 50	< 0.001
Glucose (mmol/L)	10 ± 2	30 ± 4	< 0.001
Nerve conduction velocity (m/s)	44 ± 6	36 ± 4	< 0.001
Week 2	**Control (n=24)**	**Diabetic (n=25)**	**P-value**
Weight (g)	355 ± 24	372 ± 41	< 0.05
Glucose (mmol/L)	13 ± 4	30 ± 4	< 0.001
Nerve conduction velocity (m/s)	46 ± 10	38 ± 5	< 0.01

Animal demographics (mean ± SD)

Nerve block duration

Motor block duration in both groups were obtained. The motor block duration was significantly extended in the diabetic rats as compared to the control group (p=0.036; Figure 1).

Pharmacodynamics – *In vivo* minimum local anesthetic dose

Minimum local anesthetic dose ED50 was investigated in diabetic and control rats according to the Dixon up and down method. Diabetic animals showed a minimum local anesthetic dose ED50 for lidocaine-induced motor block of 0.9%, compared to 1.4% in control animals (p < 0.018, CI 0.58- 0.57) (Figure 2).

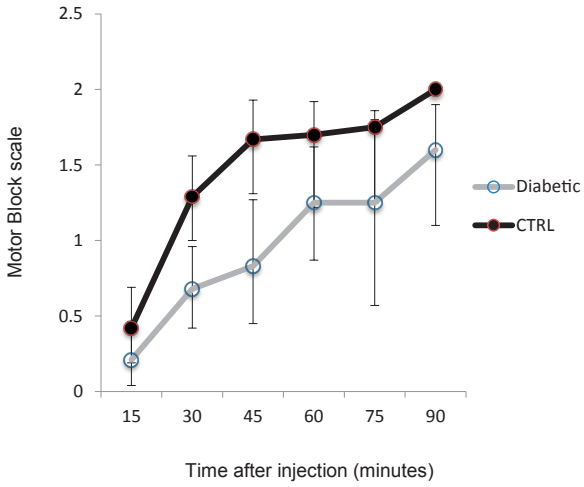

Figure 1 Motor blockade scale over time (minutes)

Values are shown as means with bias corrected and accelerated 95% confidence intervals (BCa 95% CI) measured in DM (n=25) and CTRL (n=25). *Motor block score*: 2: immediate and forceful reflex; 1: weak reflex; 0: no reflex. All animals were tested before experiments and found to have no signs of sensory or motor deficit.

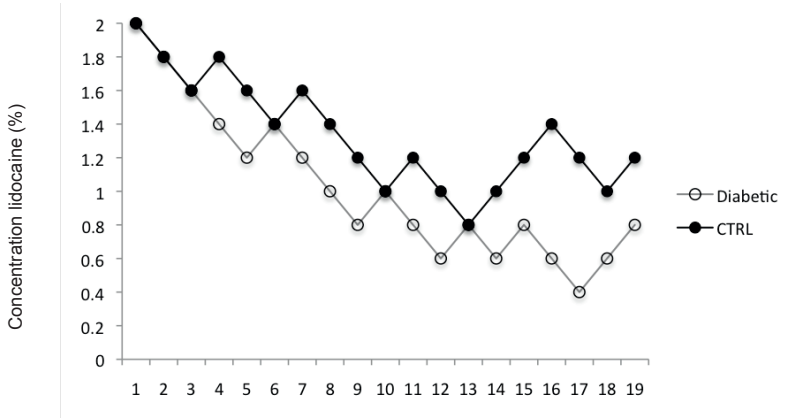

Figure 2. In vivo minimum local anesthetic dose of lidocaine in sciatic nerve block

Minimum local anesthetic dose was investigated in diabetic and control rats according to the Dixon up and down method. Nineteen diabetic and nineteen control rats were necessary to determine the minimum local anesthetic dose. All animals were tested before experiments and found to have no signs of motor deficit, and recovered fully after experiments.

Pharmacodynamics – *In vitro* electrophysiology

Figure 3 shows basic AP characterisics and I_{Na} densities of freshly isolated control and DM DRGs with a size smaller than 25 µM. Action potentials in response to 200 pA depolarizing pulses are shown in Figure 3A.

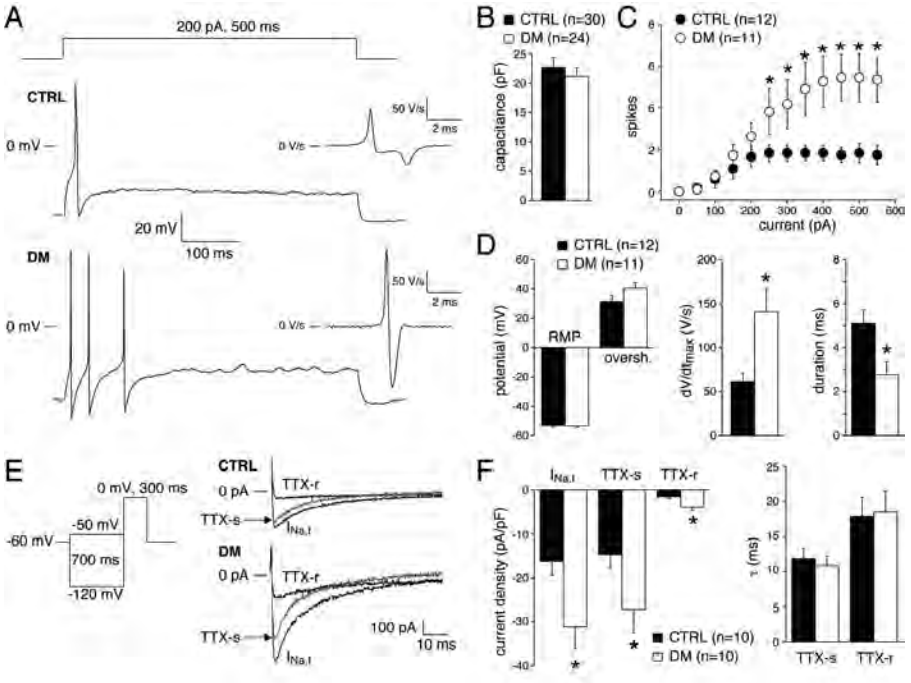

Figure 3. Action potential characteristics of freshly isolated dorsal root ganglions under basal conditions.

A, Examples of action potentials recorded from a control (CTRL) and diabetic mellitus (DM) DRG during a 200 pA, 500 ms-long depolarizing pulse. **Inset:** dV/dt of the first action potential. **B**, Average (SD) cell capacitance of CTRL (n=30) and DM (n=24) ganglia. **C**, Average (SD) number of spikes during depolarizing pulses of increasing amplitudes in CTRL (n=12) and DM (n=11) ganglia. **D**, Average (SD) action potential characteristics of CTRL (n=12) and DM (n=11) DRGs during a 200 pA depolarizing pulse. Asterisks indicate adjusted significant differences between control and DM ganglia. **E**, Typical Na^+ current (I_{Na}) in a CTRL and DM dorsal root ganglia recorded with the depicted protocol. Total sodium currents I_{Na} ($I_{Na,t}$) was recorded using the prepulse to -120 mV, while TTX-resistant (TTX-r) was defined as I_{Na} recorded using the prepulse to -50 mV. TTX-sensitive (TTX-s) was obtained by subtracting TTX-r from $I_{Na,t}$. F, Average current densities of CTRL (n=10) and DM (n=10) DRG's, and time constants (τ) of current inactivation obtained by monoexponential fits. Data are given as mean +/- standard deviation (SD).

C_m was 22 ± 12.7 pF (average ± SD, n=54), consistent with a previous finding in freshly isolated small diameter L4/L5 DRGs,[19] and did not differ significantly between CTRL and DM DRGs (Figure 3B). Average number of spikes and AP characteristics are shown in Figure 3C and 3D, respectively. DM DRG have more APs during depolarizing pulses compared to control DRGs. In addition, the maximum AP upstroke, dV/dt, was significantly higher and the duration was significantly shorter in DM DRGs.

Typical I_{Na} recordings and average I_{Na} densities are show in Figure 3, E and F. In DM DRGs, peak I_{Na} ($I_{Na,t}$) was significantly greater than in control DRGs, due to a significant increase of both TTX-resistant and TTX-sensitive currents. The TTX-resistant, i.e., the I_{Na} recorded using the -50 mV prepulse, is rather small in both control and DM DRGs compared to the TTX-sensitive I_{Na} and the relative contribution of TTX-sensitive is not altered due to DM (12±2.8% (CTRL) and 15.1±3.6% (DM). Thus these experiments demonstrate that DM results in hyperexcitability, due to an increased density of Na^+ currents, in freshly isolated DRGs, as described previously.[19-21]

To study whether DM changed the sensitivity of I_{Na} to blockade by lidocaine, a concentration–response curve was obtained by using concentrations between 1 and 1000 µM. Because the relative contribution of TTX-sensitive is small and not changed by DM (Figure 3E), we focused on the inhibition of total I_{Na}, rather than on separate dose–response curves of TTX-resistant and TTX-sensitive currents. Figure 4A shows typical peak I_{Na} recordings in the absence and presence of different lidocaine concentrations; average effects are summarized in Figure 4B. We found a significantly lower IC_{50} in DM compared to control DRGs, while the Hill coefficients were not significantly different. The higher I_{Na} sensitivity for lidocaine in DM DRGs suggests that the reduction of the action potential upstroke will be greater. To address this issue, we studied the effects of 10 µM lidocaine on action potentials. Figure 5A shows typical action potentials during 200 pA depolarizing pulses in the absence of lidocaine (CTRL), in the presence of lidocaine, and upon washout of the drug. Lidocaine reversibly decreased the action potential upstroke in both control and DM DRGs, but the magnitude of reduction was significantly higher in DM DRGs (Figure 5B). In addition, the AP overshoot was significantly decreased in DM, but not in control, DRGs (Figure 5B). The slower AP upstroke velocity resulted in a significantly increased action potential duration (APD_{50}) in DM DRGs (Figure 5B). Finally, we found a significantly lower number of spikes in diabetic neurons as lidocaine was added (Figure 5C). These single cell measurements demonstrate that DM DRGs have a higher sensitivity to lidocaine.

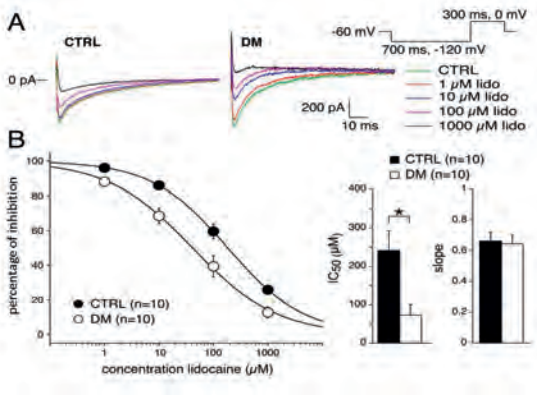

Figure 4. Concentration dependence of I_{Na} block by lidocaine in Control and Diabetic dorsal root ganglions.

A, Typical I_{Na} recordings in CTRL and DM dorsal root ganglia in absence and presence of 1 to 1000 µM lidocaine. Inset: voltage clamp protocol. **B**, Average effects of lidocaine in control (CTRL, n=10) and DM (n=10) DRG's. Please note that the currents are normalized to the current before application of the drug. Solid lines: Hill equation fits of average data. Data are given as mean +/- standard deviation (SD).

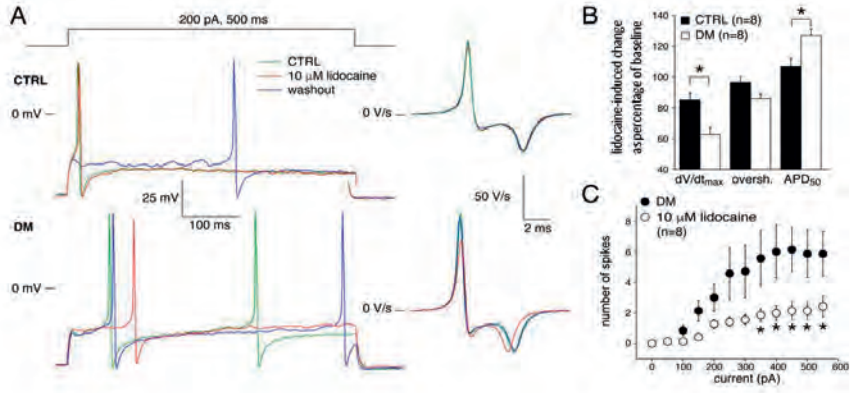

Figure 5. Effects of 10 µM lidocaine on action potential characteristics

A, Examples of action potentials during a 200 pA depolarizing pulse in absence of lidocaine, presence of lidocaine, and upon washout of the drug. **Inset:** dV/dt of the first action potential demonstrating a reversible decreased of the action potential upstroke in response to lidocaine. **B**, Average (SD) effects of lidocaine on the action potential upstroke (left), action potential overshoot (middle) and action potential duration (right) in CTRL and DM DRGs. **C**, Average (SD) number of spikes during depolarizing pulses of increasing amplitudes in DM (n=8) ganglia in absence and presence of lidocaine.

Pharmacokinetics – Intraneural lidocaine

While the absorption of radiolabeled lidocaine into the sciatic nerve at 5 minutes was similar between diabetic and control animals, we observed that at 60 mins the neural content in nerves of control animals was (mean log) 5.4 versus 7.1 in diabetic animals (p= 0.005 (CI -2.88 – 0.52)). Results are given in Figure 6.

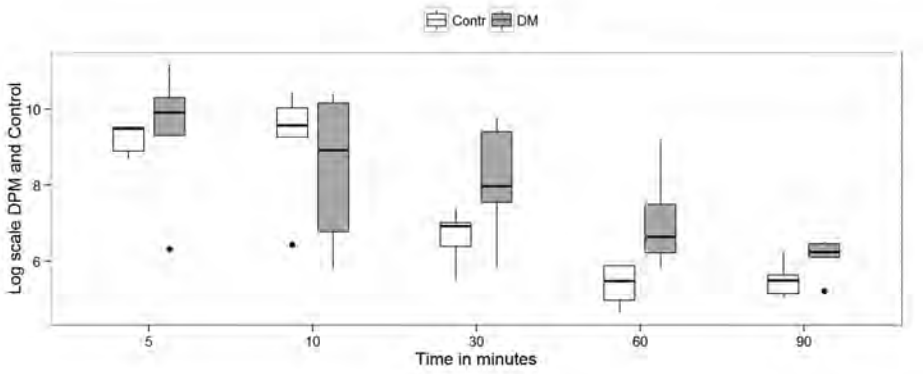

Figure 6. Intraneural lidocaine ^{14}C concentration over time.

Intraneural lidocaine ^{14}C concentration boxplot given as median (log) (interquartile range, 25-75 percentile) values: DM vs. CTRL (n= 10 measurements per timepoint). Asterisks indicate adjusted significant difference between CTRL and DM, a dot signifies a data outlier, defined as a data point that is located outside 1.5 times the interquartile range above the upper quartile and bellow the lower quartile.

Discussion

We demonstrate that both pharmacodynamic and pharmacokinetic mechanisms contribute to the overall phenomenon of prolonged nerve block duration.

Sodium channels in diabetic neuropathy

Next to being the main pharmacological target of local anesthetics, sodium channels play a substantial role in the pathophysiology of diabetic neuropathy. On a neuronal level, the expression of specific sodium channels is differentially influenced during diabetic neuropathy. Literature has been undecided on the exact pattern of sodium channel alterations. In general, an increase in sodium currents is reported, and this increase correlates with progression of neuropathy in experimental models.[6] De-

pending on the type of neurons investigated, and even on the specific location within the neuronal membrane, a variety of changes has been demonstrated. For example, while expression studies suggest that globally, Nav1.8 may be decreased in diabetic dorsal root ganglia,[5] others have observed no decrease in Nav1.8-mediated currents [21] or even an increase.[20] Notably, the latter increase was found in small-size neurons, comparable to those investigated here. Adding to the complexity, Hong further described that diabetic neuropathy also leads to changes in the spatial distribution of sodium channel isoforms, with the nodal regions featuring decreased levels of Nav1.6 and Nav1.8.[21] An increase in the current density measured in cell soma coupled with a decrease in axonal (nodal) Na^+ currents suggests that transport of channels down the axon may be impaired in diabetic animals. Also, this finding may reconcile our findings of reduced nerve conduction velocity and increased excitability, since these two effects were measured at separate locations, the cell body versus the axon, which are differentially affected by neuropathic changes. Finally, expressed channels may be further modified in their functionality, e.g. inactivation, by secondary mechanisms such as methylglyoxal modification,[22] as well as serine-threonine or tyrosine phosphorylation.[23]

On the neuroanatomical level, diabetic neuropathy is characterized by the loss of nerve fibers, predominantly of unmyelinated sensory axons, in the setting of hyperexcitability. This leads to the unique combination of negative symptoms (loss of sensitivity to touch, pinprick and temperature) and positive symptoms (hyperalgesia, allodynia and ongoing pain) [24] combined with motor deficit.[25]

The clinical relevance of these changes for regional anesthesia is underlined by a recent report correlating a prolonged stimulus strength-duration time constant, which is strongly indicative of sodium channel (dys)function, with severity of neuropathy and decreased quality of life in diabetic neuropathic patients.[26]

Pharmacodynamics

We report that the *in vivo* ED50 of lidocaine for motor blockade using a fixed volume was 1.4% in control, and 0.9% in diabetic animals. The difference is significant, and similar in magnitude to differences in local anesthetic requirement as a result of, for example, pregnancy.[27] This indicates that diabetic neuropathic nerves are more sensitive to local anesthetics. This finding was corroborated by *in vitro* investigations of sodium channel currents which showed that the inhibitory effect of a given lidocaine concentration was much more pronounced in primarily sensory neurons harvested from diabetic as compared to control neurons. Diabetic DRGs are hyperexcitable as

reflected by the increased number of action potentials during depolarizing pulses compared to control DRGs (Figure 3), but these are also susceptible to silencing by local anesthetics (Figure 5). In addition, the action potential upstroke and the current density of total I_{Na} was significantly higher in DM DRGs, due to upregulation of both TTX-sensitive and TTX-resistant I_{Na} (Figure 3). These findings correspond well to previous literature [20] and tie in with evidence from neurological investigations demonstrating that nerve excitability is heightened in diabetic neuropathy.[28]

Pathological alterations seem particularly prominent in nodal regions.[29] All of this leads to a functional change in the axon which is reflected by a decrease in the strength-duration time constant, a measure of axonal membrane excitability, and an increase in rheobase, the minimal strength of a stimulus of indefinite duration to depolarize the axon.[28] The latter change may, at least in part, explain the increased threshold for peripheral nerve stimulation in diabetic neuropathy observed experimentally [30] and perioperatively.[31, 32] The net effect concerning nerve blockade seems to be that the axonal membrane of diabetic neuropathic nerves is less excitable by electrical stimulation than normal membranes, and that it is at the same time more sensitive to local anesthetics. Therefore, in diabetic neuropathy, a smaller dose of a local anesthetic may achieve the same result as a larger dose in a healthy nerve. Reduction of doses in diabetic neuropathic patients has been suggested [1] and tested in a small clinical trial [33] but until now, this has not been systematically investigated in clinical trials. Our experimental setup would support these contentions by showing that the *in vivo* MLAC was decreased by 35%, and the sensitivity to lidocaine during patch-clamp experiments was increased in diabetic neuropathy.

The blockade of Na^+ channels by lidocaine can be complex,[34] and various DM-induced changes in Na^+ channel properties may contribute to our observed increased lidocaine sensitivity. Lidocaine can block the sodium channels in inactivated and resting state, thereby resulting in phasic (or use-dependent) and tonic blockade, respectively.[34] Typically, the IC50 is lower for phasic lidocaine block compared to tonic blockade in both TTX-resistant [34] and TTX-sensitive [35] currents. Diabetes or high glucose levels result in slower recovery from inactivation, a negative shift in voltage-dependence of inactivation,[19, 21, 36, 37] all conditions which thus promote phasic lidocaine blockade and tonic block, when the membrane is at its resting potential, -60mV in sensory neuron soma. Firing rate during depolarizing current pulses is significantly increased in DM which will further promote use-dependent block by lidocaine. In addition, and as mentioned before, DM results in an increase of various TTX-sensitive and TTX-resistant Na^+ channels. TTX-sensitive Na^+ channels are

approximately five times more sensitive to lidocaine than TTX-resistant for tonic block [34, 38] and the changes in the various isoforms may thus affect the lidocaine sensitivity. Moreover, β-subunits of Na+ channels importantly modulate I_{Na} densities and gating properties, and it is well-known that they also affect lidocaine sensitivity, with a more pronounced block as β-subunits decrease.[39-41] DM increases the β3, but does not change the β1-subunit.[42] Due to the increase in α-subunits, the ratio between β1 and α-subunits becomes lower and we cannot exclude this as potential mechanism for the increased lidocaine sensitivity. Finally, DM results in multiple biochemical changes which may have an impact on lidocaine sensitivity. For example, DM increases PKC/cAMP in DRGs,[19] and cAMP lowers the IC50 for lidocaine in TTX-resistant channels.[43] Thus multiple mechanisms may be responsible for the observed increased lidocaine sensitivity.

Further research should determine detailed dose-response curves in diabetic versus control animals, specifically investigating whether these alterations are found across different neuronal subgroups, are particular to specific sodium currents, and are different with various local anesthetics.

Pharmacokinetics – Intraneural lidocaine

Another potential cause for the prolonged block duration may be impaired nerve blood flow in diabetic neuropathy.[44] This has been demonstrated for Type I DM [45] and similar findings have been obtained in models of Type II DM.[7] Further, blood flow is also reduced in autonomic and dorsal root ganglia.[44] The main pathogenic mechanisms is diabetes-induced vasa nervorum endotheliopathy,[44] and the net effect is a substantial decrease in axonal flow unit. Cameron and coworkers, for example, found a reduction in blood flow of approximately 40% when measured using microelectrode polarography and hydrogen clearance in STZ rats.[45] We demonstrated that the content of radiolabeled lidocaine was higher in the diabetic nerve than in control nerves at 60 minutes, which may at least contribute to the prolonged block duration in diabetic nerves. The timepoint at 60 minutes is the most important one in the measurement series, since it is the timepoint when functional deficits from motor block have typically recovered in healthy nerves, whereas most diabetic nerves are still blocked.[14]

Limitations

Our model is not directly comparable to some previous investigations by other authors since we used Type II DM animals, while most others used Type I DM animals.[13,

[46-48] However, we believe that our methodology better reflects the growing patient collective of Type II diabetics with neuropathy presenting for surgery.[49] We performed our experiments using the local anesthetic lidocaine, because this has been the most widely used drug when diabetic neuropathy was investigated. Lastly, we did not take active steps to blind experimenters to the experimental group allocation during *in vivo* experiments, as the diabetic animals are much more obese than control animals, and therefore group allocation is immediately visible. To counteract this potential bias, we randomized animals to group allocation whenever possible.

Conclusions

In a rodent model of regional anesthesia in animals with neuropathy secondary to Type 2 Diabetes, we have observed increased nerve block duration, as previously described. Further, dose-finding and electrophysiological experiments suggest that diabetic neuropathic neurons and nerves are blocked at lower concentrations of lidocaine than healthy nerves. Lastly, we report that at 60 minutes after nerve block, intraneural lidocaine is less in healthy than in diabetic nerves. Within the limitations of our preclinical model, our results support both pharmacodynamic and pharmacokinetic mechanisms to explain increased block duration with diabetic neuropathy.

To summarize, future research endeavors should focus on elucidating detailed dose-response curves in diabetic subjects. This research should delve into the nuances of sensitivity to local anesthetics, exploring potential variations across diverse neuronal subgroups. Furthermore, there is a need to determine whether this sensitivity exhibits specificity to particular sodium currents and varies in response to different local anesthetics. By addressing these specific aspects, researchers can enhance our understanding of the complex interactions between diabetes and local anesthetics, providing valuable insights that may contribute to improved clinical management and tailored interventions in diabetic individuals.

References

1. Lirk P, Birmingham B, Hogan Q. Regional anesthesia in patients with preexisting neuropathy. *Int Anesthesiol Clin* 2011;49:144-65
2. Blumenthal S, Borgeat A, Maurer K, Beck-Schimmer B, Kliesch U, Marquardt M, Urech J. Preexisting subclinical neuropathy as a risk factor for nerve injury after continuous ropivacaine administration through a femoral nerve catheter. *Anesthesiology* 2006;105:1053-6
3. Lirk P, Flatz M, Haller I, Hausott B, Blumenthal S, Stevens MF, Suzuki S, Klimaschewski L, Gerner P. In Zucker Diabetic Fatty Rats, Subclinical Diabetic Neuropathy Increases In Vivo Lidocaine Block Duration But Not In Vitro Neurotoxicity. *Reg Anesth Pain Med* 2012;37:601-6
4. Cuvillon P, Reubrecht V, Zoric L, Lemoine L, Belin M, Ducombs O, Birenbaum A, Riou B, Langeron O. Comparison of subgluteal sciatic nerve block duration in type 2 diabetic and non-diabetic patients. *Br J Anaesth* 2013;110:823-30
5. Craner MJ, Klein JP, Renganathan M, Black JA, Waxman SG. Changes of sodium channel expression in experimental painful diabetic neuropathy. *Ann Neurol* 2002;52:786-92
6. Meerupally R, Singh JN, Sharma SS. Diabetic-induced increased sodium channel activity attenuated by tetracaine in sensory neurons in vitro. *Biochem Biophys Res Commun* 2014;453:296-301
7. Williams BA. Toward a potential paradigm shift for the clinical care of diabetic patients requiring perineural analgesia: strategies for using the diabetic rodent model. *Reg Anesth Pain Med* 2010;35:329-32
8. Pop-Busui R, Marinescu V, Van Huysen C, Li F, Sullivan K, Greene DA, Larkin D, Stevens MJ. Dissection of metabolic, vascular, and nerve conduction interrelationships in experimental diabetic neuropathy by cyclooxygenase inhibition and acetyl-L-carnitine administration. *Diabetes* 2002;51:2619-28
9. Galley HF. Mice, men, and medicine. *Br J Anaesth* 2010;105:396-400
10. Brussee V, Guo G, Dong Y, Cheng C, Martinez JA, Smith D, Glazner GW, Fernyhough P, Zochodne DW. Distal degenerative sensory neuropathy in a long-term type 2 diabetes rat model. *Diabetes* 2008;57:1664-73
11. Oh SS, Hayes JM, Sims-Robinson C, Sullivan KA, Feldman EL. The effects of anesthesia on measures of nerve conduction velocity in male C57Bl6/J mice. *Neurosci Lett* 2010;483:127-31
12. Thalhammer JG, Vladimirova M, Bershadsky B, Strichartz GR. Neurologic evaluation of the rat during sciatic nerve block with lidocaine. *Anesthesiology* 1995;82:1013-25
13. Kroin JS, Buvanendran A, Williams DK, Wagenaar B, Moric M, Tuman KJ, Kerns JM. Local anesthetic sciatic nerve block and nerve fiber damage in diabetic rats. *Reg Anesth Pain Med* 2010;35:343-50
14. Lirk P, Verhamme C, Boeckh R, Stevens MF, ten Hoope W, Gerner P, Blumenthal S, de Girolami U, van Schaik IN, Hollmann MW, Picardi S. Effects of early and late diabetic neuropathy on sciatic nerve block duration and neurotoxicity in Zucker diabetic fatty rats. *Br J Anaesth* 2015;114:319-26
15. Verhamme C, King RH, ten Asbroek AL, Muddle JR, Nourallah M, Wolterman R, Baas F, van Schaik IN. Myelin and axon pathology in a long-term study of PMP22-overexpressing mice. *J Neuropathol Exp Neurol* 2011;70:386-98
16. Dixon WJ. Staircase bioassay: the up-and-down method. *Neurosci Biobehav Rev* 1991;15:47-50

17. Verkerk AO, den Ruijter HM, Bourier J, Boukens BJ, Brouwer IA, Wilders R, Coronel R. Dietary fish oil reduces pacemaker current and heart rate in rabbit. *Heart Rhythm* 2009;6:1485-92
18. Sinnott CJ, Cogswell IL, Johnson A, Strichartz GR. On the mechanism by which epinephrine potentiates lidocaine's peripheral nerve block. *Anesthesiology* 2003;98:181-8
19. Hayase F, Matsuura H, Sanada M, Kitada-Hamada K, Omatsu-Kanbe M, Maeda K, Kashiwagi A, Yasuda H. Inhibitory action of protein kinase Cbeta inhibitor on tetrodotoxin-resistant Na+ current in small dorsal root ganglion neurons in diabetic rats. *Neurosci Lett* 2007;417:90-4
20. Sun W, Miao B, Wang XC, Duan JH, Wang WT, Kuang F, Xie RG, Xing JL, Xu H, Song XJ, Luo C, Hu SJ. Reduced conduction failure of the main axon of polymodal nociceptive C-fibres contributes to painful diabetic neuropathy in rats. *Brain* 2012;135:359-75
21. Hong S, Wiley JW. Altered expression and function of sodium channels in large DRG neurons and myelinated A-fibers in early diabetic neuropathy in the rat. *Biochem Biophys Res Commun* 2006;339:652-60
22. Bierhaus A, Fleming T, Stoyanov S, Leffler A, Babes A, Neacsu C, Sauer SK, Eberhardt M, Schnolzer M, Lasischka F, Neuhuber WL, Kichko TI, Konrade I, Elvert R, Mier W, Pirags V, Lukic IK, Morcos M, Dehmer T, Rabbani N, Thornalley PJ, Edelstein D, Nau C, Forbes J, Humpert PM, Schwaninger M, Ziegler D, Stern DM, Cooper ME, Haberkorn U, Brownlee M, Reeh PW, Nawroth PP. Methylglyoxal modification of Na(v)1.8 facilitates nociceptive neuron firing and causes hyperalgesia in diabetic neuropathy. *Nat Med* 2012;18:1445
23. Hong S, Wiley JW. Early painful diabetic neuropathy is associated with differential changes in the expression and function of vanilloid receptor 1. *J Biol Chem* 2005;280:618-27
24. Feldman EL, Nave KA, Jensen TS, Bennett DL. New Horizons in Diabetic Neuropathy: Mechanisms, Bioenergetics, and Pain. *Neuron* 2017;93:1296-313
25. Said G, Baudoin D, Toyooka K. Sensory loss, pains, motor deficit and axonal regeneration in length-dependent diabetic polyneuropathy. *J Neurol* 2008;255:1693-702
26. Kwai NC, Arnold R, Wickremaarachchi C, Lin CS, Poynten AM, Kiernan MC, Krishnan AV. Effects of axonal ion channel dysfunction on quality of life in type 2 diabetes. *Diabetes Care* 2013;36:1272-7
27. Zhan Q, Huang S, Geng G, Xie Y. Comparison of relative potency of intrathecal bupivacaine for motor block in pregnant versus non-pregnant women. *Int J Obstet Anesth* 2011;20:219-23
28. Nodera H, Kaji R. Nerve excitability testing and its clinical application to neuromuscular diseases. *Clin Neurophysiol* 2006;117:1902-16
29. Zenker J, Ziegler D, Chrast R. Novel pathogenic pathways in diabetic neuropathy. *Trends Neurosci* 2013;36:439-49
30. Rigaud M, Filip P, Lirk P, Fuchs A, Gemes G, Hogan Q. Guidance of block needle insertion by electrical nerve stimulation: a pilot study of the resulting distribution of injected solution in dogs. *Anesthesiology* 2008;109:473-8
31. Keyl C, Held T, Albiez G, Schmack A, Wiesenack C. Increased electrical nerve stimulation threshold of the sciatic nerve in patients with diabetic foot gangrene: a prospective parallel cohort study. *Eur J Anaesthesiol* 2013;30:435-40
32. Heschl S, Hallmann B, Zilke T, Gemes G, Schoerghuber M, Auer-Grumbach RA, Quehenberger F, Lirk P, Hogan QH, Rigaud M. Diabetic neuropathy increases stimulation threshold during popliteal sciatic nerve block. *Br J Anaesth* 2015;in press

33. Kocum A, Turkoz A, Bozdogan N, Caliskan E, Eker EH, Arslan G. Femoral and sciatic nerve block with 0.25% bupivacaine for surgical management of diabetic foot syndrome: an anesthetic technique for high-risk patients with diabetic nephropathy. *J Clin Anesth* 2010;22:363-6
34. Scholz A, Kuboyama N, Hempelmann G, Vogel W. Complex blockade of TTX-resistant Na+ currents by lidocaine and bupivacaine reduce firing frequency in DRG neurons. *J Neurophysiol* 1998;79:1746-54
35. Hille B. The pH-dependent rate of action of local anesthetics on the node of Ranvier. *J Gen Physiol* 1977;69:475-96
36. Hirade M, Yasuda H, Omatsu-Kanbe M, Kikkawa R, Kitasato H. Tetrodotoxin-resistant sodium channels of dorsal root ganglion neurons are readily activated in diabetic rats. *Neuroscience* 1999;90:933-9
37. Kharatmal SB, Singh JN, Sharma SS. Comparative evaluation of in vitro and in vivo high glucose-induced alterations in voltage-gated tetrodotoxin-resistant sodium channel: Effects attenuated by sodium channel blockers. *Neuroscience* 2015;305:183-96
38. Chevrier P, Vijayaragavan K, Chahine M. Differential modulation of Nav1.7 and Nav1.8 peripheral nerve sodium channels by the local anesthetic lidocaine. *Br J Pharmacol* 2004;142:576-84
39. Makielski JC, Limberis JT, Chang SY, Fan Z, Kyle JW. Coexpression of beta 1 with cardiac sodium channel alpha subunits in oocytes decreases lidocaine block. *Mol Pharmacol* 1996;49:30-9
40. Balser JR, Nuss HB, Romashko DN, Marban E, Tomaselli GF. Functional consequences of lidocaine binding to slow-inactivated sodium channels. *J Gen Physiol* 1996;107:643-58
41. Lenkowski PW, Shah BS, Dinn AE, Lee K, Patel MK. Lidocaine block of neonatal Nav1.3 is differentially modulated by co-expression of beta1 and beta3 subunits. *Eur J Pharmacol* 2003;467:23-30
42. Shah BS, Gonzalez MI, Bramwell S, Pinnock RD, Lee K, Dixon AK. Beta3, a novel auxiliary subunit for the voltage gated sodium channel is upregulated in sensory neurones following streptozocin induced diabetic neuropathy in rat. *Neurosci Lett* 2001;309:1-4
43. Docherty RJ, Farrag KJ. The effect of dibutyryl cAMP on tetrodotoxin-sensitive and -resistant voltage-gated sodium currents in rat dorsal root ganglion neurons and the consequences for their sensitivity to lidocaine. *Neuropharmacology* 2006;51:1047-57
44. Sytze Van Dam P, Cotter MA, Bravenboer B, Cameron NE. Pathogenesis of diabetic neuropathy: focus on neurovascular mechanisms. *Eur J Pharmacol* 2013;719:180-6
45. Cameron NE, Cotter MA, Low PA. Nerve blood flow in early experimental diabetes in rats: relation to conduction deficits. *Am J Physiol* 1991;261:E1-8
46. Kroin JS, Buvanendran A, Tuman KJ, Kerns JM. Safety of Local Anesthetics Administered Intrathecally in Diabetic Rats. *Pain Med* 2012;13:802-7
47. Kroin JS, Buvanendran A, Tuman KJ, Kerns JM. Effect of Acute Versus Continuous Glycemic Control on Duration of Local Anesthetic Sciatic Nerve Block in Diabetic Rats. *Reg Anesth Pain Med* 2012;37:595-600
48. Kalichman MW, Calcutt NA. Local anesthetic-induced conduction block and nerve fiber injury in streptozotocin-diabetic rats. *Anesthesiology* 1992;77:941-7
49. Ibinson JW, Mangione MP, Williams BA. Local Anesthetics in Diabetic Rats (and Patients): Shifting From a Known Slippery Slope Toward a Potentially Better Multimodal Perineural Paradigm? *Reg Anesth Pain Med* 2012;37:574-6

Section 2

Translational research and regional anaesthesia

Chapter 4

Adductor canal block techniques do not lead to involvement of sciatic nerve branches: a radiological cadaveric study

Based on: Pascal S.H. Smulders, Werner ten Hoope, Holger M. Baumann, Jeroen Hermanides, Robert Hemke, Ludo F.M. Beenen, Roelof-Jan Oostra, Peter Marhofer, Philipp Lirk, Markus W. Hollmann
Reg Anesth Pain Med. 2023 Jun 29:rapm-2022-104227

Abstract

Introduction

Low and high-volume mid-thigh (i.e., distal femoral triangle) and distal adductor canal block approaches are frequently applied for knee surgical procedures. Although these techniques aim to contain the injectate within the adductor canal, spillage into the popliteal fossa has been reported. While in theory this could improve analgesia, it might also result in motor blockade due to coverage of motor branches of the sciatic nerve. This radiological cadaveric study therefore investigated the incidence of coverage of sciatic nerve divisions after various adductor canal block techniques.

Methods

Eighteen fresh, unfrozen and unembalmed human cadavers were randomized to receive ultrasound-guided distal femoral triangle or distal adductor canal injections, with 2 mL or 30 mL injectate volume, on both sides (36 blocks in total). The injectate was a 1:10 dilution of contrast medium in local anesthetic. Injectate spread was assessed using whole-body computed tomography with reconstructions in axial, sagittal and coronal planes.

Results

No coverage of the sciatic nerve or its main divisions was found. The contrast mixture spread to the popliteal fossa in three of 36 nerve blocks. Contrast reached the saphenous nerve after all injections, whereas the femoral nerve was always spared.

Conclusions

Adductor canal block techniques are unlikely, even when using larger volumes, to block the sciatic nerve, or its main branches. Further, injectate reached the popliteal fossa in a small minority of cases, yet if a clinical analgesic effect is achieved by this mechanism is still unknown.

What is already known on this topic

Adductor canal block techniques may lead to sciatic nerve involvement due to inferoposterior spread of the injectate to the popliteal fossa. Currently, however, our anatomical knowledge of distal injectate spread patterns is limited and it is unknown

how different variations of the adductor canal block compare regarding the incidence of sciatic nerve coverage.

What this study adds

This study investigated the effect of 2 mL and 30 mL mid-thigh (i.e., distal femoral triangle) and distal adductor canal block on involvement of the sciatic nerve and its main divisions. No coverage of the sciatic nerve, or its main branches, was found for any of the techniques. The contrast mixture spread to the popliteal fossa after three of 36 injections.

How this study might affect research, practice or policy

The presented data indicate that adductor canal block techniques are unlikely to involve the sciatic nerve or its main divisions, even when using larger injectate volumes. Future research should study the possible analgesic benefit of inferoposterior spread, as injectate was found to inconsistently reach the popliteal fossa.

Introduction

The incidence of total knee arthroplasty (TKA), a severely painful procedure, continues to increase, with an estimated 911,000 procedures performed in 2017 in the United States alone.[1, 2] Perioperative treatment pathways are being optimized to utilize multimodal analgesic strategies, resulting in improved pain relief and patient satisfaction, while expediting postoperative mobilization and decreasing reliance on opioids.[3] Central to these efforts is the incorporation of regional anesthesia techniques as an analgesic adjunct.[4, 5]

Previously, the nerve block preferred for TKA was the Femoral nerve block (FNB), however, variations (such as low and high volume mid-thigh and distal adductor canal (AC) approaches) of the adductor canal block (ACB) are thought to be a suitable substitute with reduced motor blockade.[6] Specifically, ACB has been shown to be superior to FNB in terms of quadriceps muscle strength, risk of postoperative falls, and functional recovery, whilst providing similar pain control.[7-9] The injection target for ACB, the AC, is a triangular neurovascular tunnel, roofed by the vastoadductor membrane, that stretches from the top of the femoral triangle (FT) to the adductor hiatus.[10, 11] The AC consistently contains the saphenous nerve (SN; the

primary target of ACB), whereas inclusion of the nerve to the vastus medialis and the anterior branch of the obturator nerve (ON) is reported to be inconsistent.[11-13]

Although ACB techniques aim to spread the injected local anesthetic (LA) within the AC, excessive injectate spread over its distal margins, towards the popliteal fossa (PF), has been reported.[14-20] In theory, this could improve analgesia for knee surgical procedures by involvement of the posterior branch of the ON and articular branches of the sacral plexus. However, it also poses the risk of coverage of the main motor branches of the sciatic nerve (SCN), as previously found in several clinical reports and dissection studies, and thereby adverse events (e.g., postoperative falls).[16-21] To date, however, our (anatomical) knowledge regarding distal injectate spread patterns remains limited. Concurrently, interpretation of the existing literature is complicated due to the focus of most reports on a single nerve block technique, whereas in clinical practice a wide range of techniques is performed.

This radiological cadaveric study therefore investigated the effect of various ACB techniques on coverage of the main SCN divisions, using low and high-volume mid-thigh and distal AC approaches.

Methods

The fresh, unfrozen and unembalmed cadavers of 18 adult humans were included in this study. All cadavers were bequeathed (during life) to the Amsterdam University Medical Centers (location AMC) for use in research and education, in keeping with the Dutch Burial and Cremation act (BWBR0005009). The Medical Ethical Committee of the Amsterdam University Medical Centers (location AMC) provided a waiver for approval of this study. The presented findings are reported according to the Anatomical Quality Assurance (AQUA) checklist.[22]

Injection technique

Injections in the adductor canal were placed on both sides, however, each leg was randomized separately. All (ultrasound-guided) procedures were performed by three experienced regional anesthesiologists (WH, HMB, PL). A 1:10 dilution of contrast medium (Visipaque™, GE Healthcare, Eindhoven, the Netherlands) in bupivacaine 5 mg/mL was used to enable whole-body computed tomography (CT) (Siemens SOMATOM Force, Siemens Healthineers, Forchheim, Germany; CT collimation 0.6 mm, dual energy 100/Sn150 kVp, 486/244 mA, pitch 0.6, slice thickness 1.0 mm, soft kernel)

documentation of injectate spread, 15 minutes after injection. Study proceedings were concluded within six hours of arrival at the hospital.

Four different versions of the ACB were tested here (Table 1). These techniques were chosen to enable presentation of data applicable to the entire range of clinically practiced techniques, and thus represent its outer limits in injection volume (i.e., 2 and 30 mL) and injection site (i.e., mid-thigh and distal AC). The classical mid-thigh approach, wherein the injection is placed midway between the anterior superior iliac spine and the patella, was performed using an injectate volume of 30 mL. Previously, it was shown that this approach targets the FT proximal to its apex, and as such this technique was recently renamed the 'subsartorial block at the level of the distal FT' or distal femoral triangle block (distal FTB).[23, 24] Alternatively, the SN was selectively targeted at the same injection site employing a 2 mL injectate volume.[25] Distal ACB was accomplished by injection of 30 mL into the AC, 2-3 cm proximal to the adductor hiatus.[26] Isolated SN block was performed at the distal AC using a 2 mL injectate volume.[25]

Table 1. Studied nerve block techniques

Injection technique	Injection site	Injection volume
Low volume distal FTB	Mid-thigh at the distal femoral triangle	2 mL
High volume distal FTB	Mid-thigh at the distal femoral triangle	30 mL
Low volume distal ACB	Proximal to the adductor hiatus at the distal adductor canal	2 mL
High volume distal ACB	Proximal to the adductor hiatus at the distal adductor canal	30 mL

Abbreviations: FTB, femoral triangle block; ACB, adductor canal block.

Outcome

The primary endpoint of this cadaver study was the incidence of SCN, tibial nerve (TN), and common peroneal nerve (PN) coverage. Spread to the PF, and involvement of the SN and FN were secondary outcome measures. Further, proximal to distal contrast spread was measured in coronal images from the femoral head, intercondylar notch or knee joint space.

A musculoskeletal radiologist blinded to the injection technique assessed the locoregional contrast medium spread using multiplanar reconstructions. Perineural presence of contrast mixture around the aforementioned structures, and within the PF, was assessed by inspection of the anatomical location of the relevant struc-

tures in coronal, axial and sagittal planes.[27] Additional reformatting was utilized when necessary. Data are presented descriptively or as median with interquartile range, where applicable.

Results

Specimens were found to be largely male (13 of 18, 72%). Other baseline characteristics were unavailable, due to the anonymized nature of the body donation program. Regarding the primary outcome, no involvement of the SCN, TN, or PN, was found in any of the cadavers, for any of the techniques. Table 2 details the median contrast spread characteristics per injection technique, while Figure 1 depicts typical injectate distribution after low and high volume distal ACB.

Spread of contrast to the PF, however, was detected in three (1x 30 mL distal FTB, 2x 30 mL distal ACB) of 36 cadaver sides. Contrast never spread outside of the AC or FT in any of the other 33 cases. Table 3 documents the depth of the contrast within the PF for the aforementioned three cases. Figure 2 illustrates the proximal-distal injectate spread of case 3 (30 mL distal ACB) using a volume rendering reconstruction, whereas Figure 3 shows extensive distal spread not reaching the PF in a cadaver limb treated with high volume distal FTB.

Efficacy of the injections in the adductor canal was high, as injectate was observed to involve the SN after every injection, whereas more proximally the FN was spared by every technique. The nerve to the vastus medialis could not be visualized due to its small caliber.

Table 2. Contrast spread characteristics per injection technique

	Distance between the proximal end of the contrast and the femoral head (IQR)	Total proximal to distal contrast spread (IQR)	Distance between the distal end of the contrast and the proximal end of the intercondylar notch (IQR)
2 mL Distal FTB	217 (197-245) mm	102 (72-113) mm	175 (141-190) mm
30 mL Distal FTB	123 (88-161) mm	251 (182-303) mm	107 (74-118) mm
2 mL Distal ACB	249 (193-263) mm	117 (93-129) mm	117 (97-173) mm
30 mL Distal ACB	102 (69-158) mm	265 (217-307) mm	75 (60-94) mm

Abbreviations: FTB, femoral triangle block; ACB, adductor canal block; IQR, interquartile range.

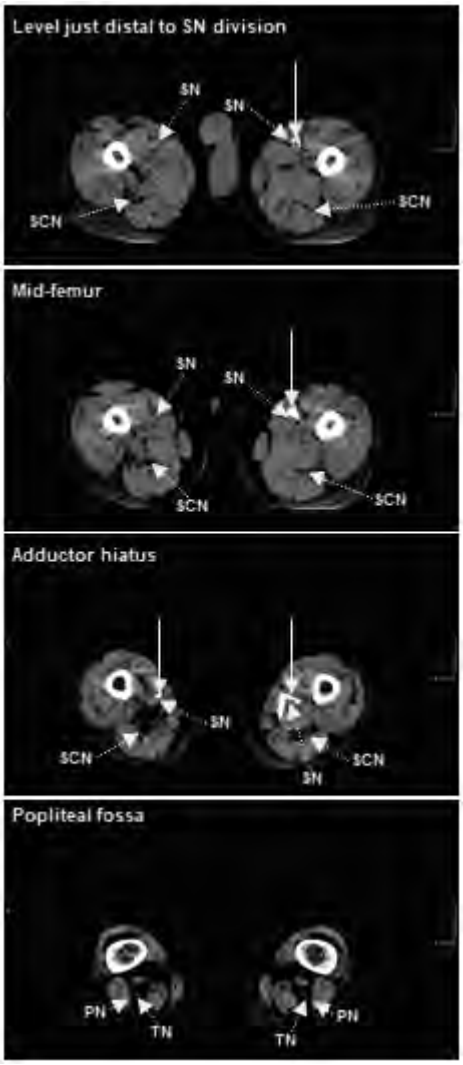

Figure 1. Axial CT imagery presenting typical injectate spread patterns after low (left) and high (right) volume distal adductor block. Solid arrows point to contrast, whereas dotted arrows indicate specific nerves.
Abbreviations: SN, saphenous nerve; SCN, sciatic nerve; PN, common peroneal nerve; TN, tibial nerve.

Table 3. *Contrast spread characteristics of the three cases with spread to the popliteal fossa*

	Distance between the proximal end of the contrast and the femoral head	Total proximal to distal contrast spread	Distance between the distal end of the contrast and the proximal end of the intercondylar notch	Distance between the distal end of the contrast and the knee joint space
Case 1: 30 mL Distal FTB	98 mm	296 mm	51 mm	73 mm
Case 2: 30 mL Distal ACB	150 mm	241 mm	54 mm	75 mm
Case 3: 30 mL Distal ACB	61 mm	371 mm	17 mm	55 mm

Abbreviations: FTB, femoral triangle block; ACB, adductor canal block; IQR, interquartile range.

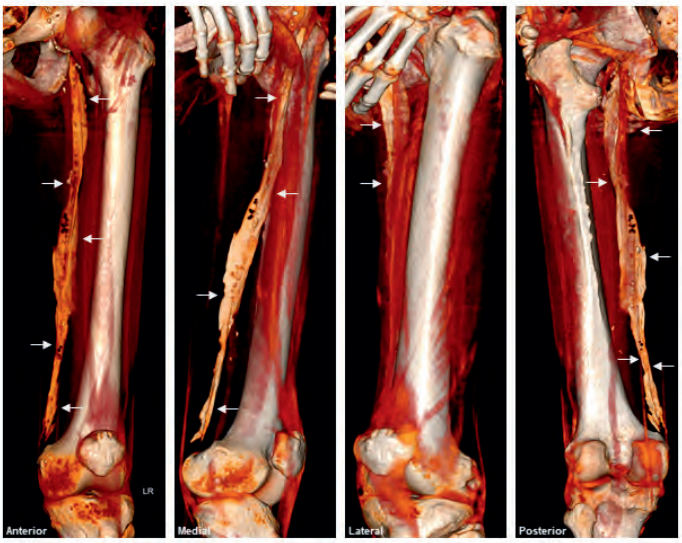

Figure 2. A 3D volume rendered reconstruction of CT-imaging detailing proximal-distal injectate spread after a high volume distal adductor canal block that reached the popliteal fossa. Arrows point to contrast.

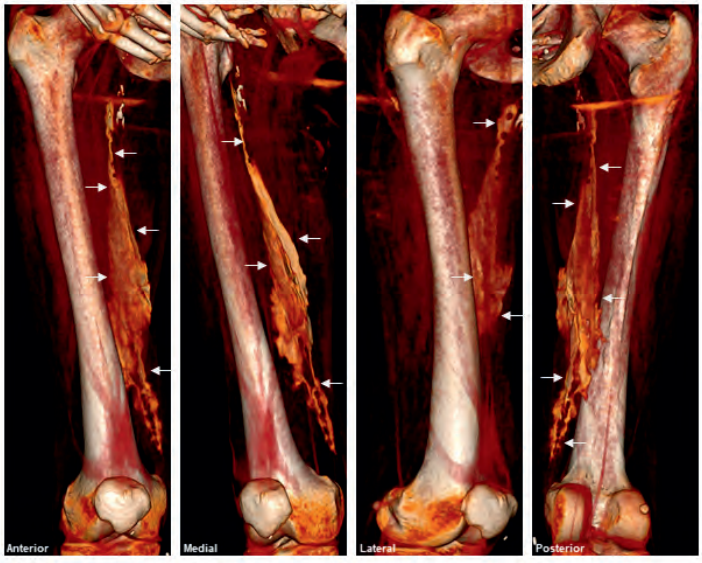

Figure 3. A 3D volume rendered reconstruction of CT-imaging showing proximal-distal injectate spread after a high volume distal femoral triangle block that led to extensive distal spread, yet did not reach the popliteal fossa. Arrows point to contrast.

Discussion

This radiological cadaveric investigation studied the effects of four ACB techniques regarding the incidence of coverage of SCN branches. Techniques were chosen to represent the outer limits of what is performed in clinical practice regarding injection volume (i.e., 2 and 30 mL) and injection site (i.e., mid-thigh and distal AC), in order to provide guidance to all anesthesiologists practicing injection techniques within this range. No involvement of the SCN, or its main divisions, was observed, whereas contrast spread to the PF in three of 36 cadaver sides. Further, the SN was covered by all injections, but neither low nor high volume techniques reached proximal enough to involve the FN.

Although the literature on involvement of the SCN (divisions) after ACB is heterogeneous regarding injection technique and study design, results can be compared when accounting for injection site and volume. Findings concerning the mid-thigh approach have been reported in three different publications. A dissection study that injected 5-10 mL of methylene blue in three cadaver sides found no SCN coverage, while investigators applying 25 mL, with or without a thigh tourniquet, found contrast close to the bifurcation in one (non-tourniquet) of 10 cadaver limbs.[17, 20] Lastly, a case-report described impaired sensory and motor function in regions innervated by the SCN after continuous distal FTB (and 20 mL bolus injection).[19] Meanwhile, a novel high volume (30-40 mL) technique description targeting the proximal AC showed ultrasound images with presence of LA around the SCN.[21] Distal ACB was investigated in a dissection study using a 10 mL injectate, resulting in SCN coverage in one out of 10 blocks.[20] Further, two articles describe 20 mL distal ACB and evidence of involvement of SCN branches in all 14 radiologically examined cases.[16, 18] Of these, Gautier *et al*. tested sensation in 15 patients and found that 41% and 61% had reduced sensation in areas innervated by the PN and TN, respectively, while motor function was unaffected.[18] Care should, however, be taken when interpreting findings of cutaneous sensation, as somatosensory distribution may vary widely between individuals. As such, it could potentially confound studies and demonstrates the importance of investigating the anatomical issues underlying regional anesthesia, as done in this study.

As the literature overview above shows, involvement of SCN branches is uncommon for mid-thigh (i.e., distal FT) and low volume ACB techniques, as supported by the current study. However, the data presented here are in contrast to previous studies demonstrating SCN coverage after 20 mL distal ACB, in spite of the large injectate

used in our study.[16, 18] Interestingly, both papers are from the same research group, suggesting that, although the same technique description was applied as used in this study, minor differences in injection technique (for example in injection pressure and speed) might be of influence.[16, 18] Nevertheless, the presented data suggest that ACB approaches are unlikely to result in adverse events (e.g., postoperative falls) caused by motor blockade due to SCN involvement.

Theoretically, the inconsistent spread patterns to the PF found in three cadaver limbs might have advantageous effects, as involvement of the posterior branch of the ON and articular branches from the sacral plexus may improve analgesia for knee surgical procedures. However, while most of the literature reports spread to the PF after ACB, depth of spread within the PF is rarely mentioned.[14-21] Thus, it remains uncertain whether the injectate consistently involves these nerves when it reaches the PF and what clinical analgesic effect is achieved. Additionally, as some studies present substantially higher incidence of PF spread than others, it also remains unknown what factors promote injectate spread to the PF. For example, Runge and colleagues demonstrated PF spread in 10 of 10 cadaver sides, yet applied the same distal ACB technique as used here, but with a smaller injectate volume of 10 mL.[20] Thereby, again suggesting that extensive distal injectate spread might be dependent on subtle differences in technique. As such, more research is needed regarding inferoposterior spread patterns after ACB.

This study has a number of limitations. First, the observed spread patterns might not be identical to that seen *in vivo* due to tissue deterioration after death and potential differences in flow characteristics between the injected contrast mixture and clinically used solutions. However, tissue quality was good as cadavers were used fresh, unfrozen and unembalmed, and SN capture rates were excellent. Second, although this study has a relatively large sample size when compared to other cadaver studies, results could be subject to sampling bias (e.g., due to anatomical variations). Third, although injection pressure and speed might influence injectate spread, neither was defined. Lastly, this study applied CT-imaging to assess the spread of a LA-based contrast mixture, as dissection studies might disrupt the integrity of fascial planes, yet as a consequence, the nerve to the vastus medialis and articular branches to the knee joint could not be examined.

Conclusions

In conclusion, ACB techniques are unlikely to involve the SCN, or its main branches. Further, injectate reached the PF in less than 10% of cases, yet if a clinical analgesic effect is achieved by this mechanism is unknown.

To Summarize: no evidence of sciatic nerve, tibial nerve, or profundal nerve involvement was observed in ACB techniques, even when larger volumes are administered. Future research should give precedence to establishing the consistency of sensory nerve engagement by the LA upon reaching the popliteal fossa and clarifying the consequent clinical analgesic effects.

References

1. Abdelaal MS, Restrepo C, Sharkey PF. Global Perspectives on Arthroplasty of Hip and Knee Joints. *Orthop Clin North Am*. 2020;51(2):169-76.
2. Gerbershagen HJ, Aduckathil S, van Wijck AJ, et al. Pain intensity on the first day after surgery: a prospective cohort study comparing 179 surgical procedures. *Anesthesiology*. 2013;118(4):934-44.
3. Moucha CS, Weiser MC, Levin EJ. Current Strategies in Anesthesia and Analgesia for Total Knee Arthroplasty. *J Am Acad Orthop Surg*. 2016;24(2):60-73.
4. Wick EC, Grant MC, Wu CL. Postoperative Multimodal Analgesia Pain Management With Nonopioid Analgesics and Techniques: A Review. *JAMA Surg*. 2017;152(7):691-7.
5. Lavand'homme PM, Kehlet H, Rawal N, et al. Pain management after total knee arthroplasty: PROcedure SPEcific Postoperative Pain ManagemenT recommendations. *Eur J Anaesthesiol*. 2022;39(9):743-57.
6. Vora MU, Nicholas TA, Kassel CA, et al. Adductor canal block for knee surgical procedures: review article. *J Clin Anesth*. 2016;35:295-303.
7. Gao F, Ma J, Sun W, et al. Adductor Canal Block Versus Femoral Nerve Block for Analgesia After Total Knee Arthroplasty: A Systematic Review and Meta-analysis. *Clin J Pain*. 2017;33(4):356-68.
8. Wang D, Yang Y, Li Q, et al. Adductor canal block versus femoral nerve block for total knee arthroplasty: a meta-analysis of randomized controlled trials. *Sci Rep*. 2017;7(1):40721.
9. Hussain N, Ferreri TG, Prusick PJ, et al. Adductor Canal Block Versus Femoral Canal Block for Total Knee Arthroplasty: A Meta-Analysis: What Does the Evidence Suggest? *Reg Anesth Pain Med*. 2016;41(3):314-20.
10. Tubbs RS, Loukas M, Shoja MM, et al. Anatomy and potential clinical significance of the vastoadductor membrane. *Surg Radiol Anat*. 2007;29(7):569-73.
11. Burckett-St Laurant D, Peng P, Giron Arango L, et al. The Nerves of the Adductor Canal and the Innervation of the Knee: An Anatomic Study. *Reg Anesth Pain Med*. 2016;41(3):321-7.
12. Horner G, Dellon AL. Innervation of the human knee joint and implications for surgery. *Clin Orthop Relat Res*. 1994(301):221-6.
13. Orduna Valls JM, Vallejo R, Lopez Pais P, et al. Anatomic and Ultrasonographic Evaluation of the Knee Sensory Innervation: A Cadaveric Study to Determine Anatomic Targets in the Treatment of Chronic Knee Pain. *Reg Anesth Pain Med*. 2017;42(1):90-8.
14. Tran J, Chan VWS, Peng PWH, et al. Evaluation of the proximal adductor canal block injectate spread: a cadaveric study. *Reg Anesth Pain Med*. 2019;45(2):124.
15. Andersen HL, Andersen SL, Tranum-Jensen J. The spread of injectate during saphenous nerve block at the adductor canal: a cadaver study. *Acta Anaesthesiol Scand*. 2015;59(2):238-45.
16. Goffin P, Lecoq JP, Ninane V, et al. Interfascial Spread of Injectate After Adductor Canal Injection in Fresh Human Cadavers. *Anesth Analg*. 2016;123(2):501-3.
17. Nair A, Dolan J, Tanner KE, et al. Ultrasound-guided adductor canal block: a cadaver study investigating the effect of a thigh tourniquet. *Br J Anaesth*. 2018;121(4):890-8.
18. Gautier PE, Hadzic A, Lecoq JP, et al. Distribution of Injectate and Sensory-Motor Blockade After Adductor Canal Block. *Anesth Analg*. 2016;122(1):279-82.

19. Gautier PE, Lecoq JP, Vandepitte C, et al. Impairment of sciatic nerve function during adductor canal block. *Reg Anesth Pain Med*. 2015;40(1):85-9.
20. Runge C, Moriggl B, Borglum J, et al. The Spread of Ultrasound-Guided Injectate From the Adductor Canal to the Genicular Branch of the Posterior Obturator Nerve and the Popliteal Plexus: A Cadaveric Study. *Reg Anesth Pain Med*. 2017;42(6):725-30.
21. Sonawane K, Dixit H, Mistry T, et al. A high-volume proximal adductor canal (Hi-PAC) block - an indirect anterior approach of the popliteal sciatic nerve block. *J Clin Anesth*. 2021;73:110348.
22. Tomaszewski KA, Henry BM, Kumar Ramakrishnan P, et al. Development of the Anatomical Quality Assurance (AQUA) checklist: Guidelines for reporting original anatomical studies. *Clin Anat*. 2017;30(1):14-20.
23. Lund J, Jenstrup MT, Jaeger P, et al. Continuous adductor-canal-blockade for adjuvant post-operative analgesia after major knee surgery: preliminary results. *Acta Anaesthesiol Scand*. 2011;55(1):14-9.
24. Wong WY, Bjorn S, Strid JM, et al. Defining the Location of the Adductor Canal Using Ultrasound. *Reg Anesth Pain Med*. 2017;42(2):241-5.
25. Ten Hoope W, Hollmann MW, Atchabahian A, et al. Minimum local anesthetic volumes for a selective saphenous nerve block: a dose-finding study. *Minerva Anestesiol*. 2017;83(2):183-90.
26. Manickam B, Perlas A, Duggan E, et al. Feasibility and efficacy of ultrasound-guided block of the saphenous nerve in the adductor canal. *Reg Anesth Pain Med*. 2009;34(6):578-80.
27. Moore KL, Dalley AF, Agur AMR. Clinically Oriented Anatomy. 8th ed. Philadelphia: Wolters Kluwer; 2017.

Chapter 5

A radiological cadaveric study of obturator nerve involvement and cranial injectate spread after different approaches to the fascia iliaca compartment block

Based on: Werner ten Hoope, Pascal S.H. Smulders, Holger M. Baumann, Jeroen Hermanides, Ludo F.M. Beenen, Roelof-Jan Oostra, Peter Marhofer, Philipp Lirk, Markus W. Hollmann
Sci Rep. 2023 Jul 26;13(1):12070

Abstract

Whether the fascia iliac compartment block (FICB) involves the obturator nerve (ON) remains controversial. Involvement may require that the injectate spreads deep in the cranial direction and might thus depend on the site of injection. Therefore, the effect of suprainguinal needle insertion with five centimeters of hydrodissection-mediated needle advancement (S-FICB-H) on ON involvement and cranial injectate spread was studied in this radiological cadaveric study. Results were compared with suprainguinal FICB without additional hydrodissection-mediated needle advancement (S-FICB), infrainguinal FICB (I-FICB), and femoral nerve block (FNB). Seventeen human cadavers were randomized to receive ultrasound-guided nerve block with a 40 mL solution of local anesthetic and contrast medium, on both sides. Injectate spread was objectified using computed tomography. The femoral and lateral femoral cutaneous nerves were consistently covered when S-FICB-H, S-FICB or FNB was applied, while the ON was involved in only one of the 34 nerve blocks. I-FICB failed to provide the same consistency of nerve involvement as S-FICB-H, S-FICB or FNB. Injectate reached most cranial in specimens treated with S-FICB-H. Our results demonstrate that even the technique with the most extensive cranial spread (S-FICB-H) does not lead to ON involvement and as such, the ON seems unrelated to FICB. Separate ON block should be considered when clinically indicated.

Introduction

Regional anesthesia (RA) techniques, such as fascial plane blocks and peripheral nerve blocks, have become a central component of multimodal analgesic strategies.[1] Benefits, in theory, include superior pain control, improved patient satisfaction, prevention of postoperative delirium, and reduced opioid consumption.[2-4] The use of RA is particularly relevant for (lower) extremity surgery due to its painful characteristics.[5] Numerous injection techniques targeting the hip, anterior thigh and knee have been developed, one of which is the fascia iliac compartment block (FICB).

The origins of FICB can be traced back to Winnie's three-in-one block, which targets the femoral nerve (FN), lateral femoral cutaneous nerve (LFCN) and obturator nerve (ON) through an anterior landmark approximation to the lumbar plexus.[6] Reports of inconsistent LFCN and ON blockade then led to studies that investigated the anatomical relations of the inguinal region, and local anesthetic distribution during 3-in-1 block.[7,8] These studies ultimately resulted in the establishment of a loss-of resistance technique, now known as FICB, targeting the fascia iliaca compartment (FIC).[8] Later modifications of the technique include the incorporation of ultrasound guidance and more recently, the growing popularity of suprainguinal (S-FICB) over infrainguinal (I-FICB) injection sites.[9-11] However, although S-FICB was developed to acquire more consistent results when compared to I-FICB, debate persists over clinical superiority regarding coverage of the ON.[12-20]

Similar to other fascial plane blocks, FICB provides analgesia on the assumption that an injectate can open the possible area between the fascia iliaca (FI) as the anterior border and the psoas major and iliacus muscles as the posterior border, and spread towards the nerves within by means of bulk flow and diffusion.[21] However, recent anatomical reports have shown that the ON does not transverse the FIC, but rather passes through the psoas, retro-psoas and retroperitoneal compartments (Figure 1).[12,13] Consequently, local anesthetic (LA) is required to spread outside of the FIC in order to involve this nerve. While these studies agree on the closure of the FIC on its posteromedial border, they offer conflicting views on the existence of a cranially located opening to the retroperitoneal compartment and ON.[12,13] If this cranial path indeed exists, successful blockade of the ON with FICB would likely mandate overflowing the FIC, or a cranial injection site within the FIC.

Therefore, we set up a radiological cadaveric study to determine the effect of a cranial injection deep under the FI using suprainguinal needle insertion with five centimeters of additional hydrodissection-mediated needle advancement (S-FICB-H) on

coverage of the ON. Further, we measured cranial injectate spread and involvement of the FN and LFCN. Results were compared with S-FICB without additional hydrodissection-mediated needle advancement, I-FICB, and femoral nerve block (FNB). We hypothesized that the injectate would reach most cranial for S-FICB-H, but that none of the nerve block techniques would result in reliable coverage of the ON.

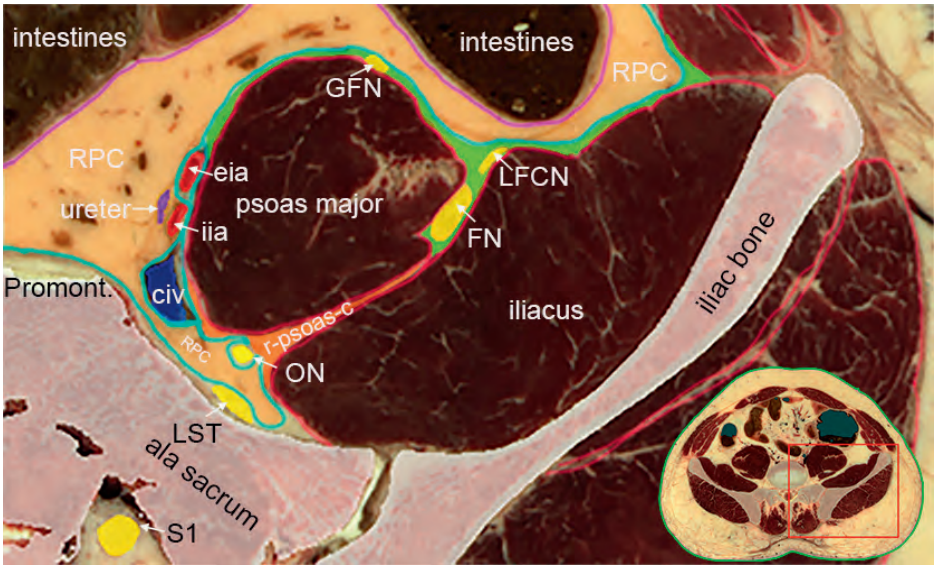

Figure 1: A cross-sectional image, cut at the level of the anterior superior iliac spine, explaining the anatomical location of the obturator nerve (ON). The ON originates from the anterior divisions of the 1st, 2nd and 4th lumbar spinal nerves in the psoas compartment. It then enters the retro-psoas compartment at the posteromedial border of the psoas major muscle, posterior to the iliac arteries and vein. Here, it is separated from the FIC (shown in green) by the psoas major and iliacus muscles, and the fascia transversalis (TF; shown in cyan). The parietal peritoneum is shown in purple. Subsequently, the ON enters the retroperitoneal compartment by invaginating the TF, and runs down the pelvis until it exits through the obturator canal. Thus, the FIC never encompasses the ON, but whether it has a cranial opening that offers a route to the retroperitoneal compartment and ON remains debated. The figure is reprinted with permission from Thomas Fichtner Bendtsen.[13]
Abbreviations: RPC, retroperitoneal compartment; GFN, genitofemoral nerve; LFCN, lateral femoral cutaneous nerve; FN, femoral nerve; eia, external iliac artery; iia, internal iliac artery; civ, common iliac vein; ON, obturator nerve; r-psoas-c, retro-psoas compartment; LST, lumbosacral trunk.

Methods

A convenience sample of 17 fresh, unfrozen and unembalmed adult human cadavers was included in this study. Cadavers were bequeathed to the Amsterdam University Medical Centers (location AMC) to serve research and educational purposes. Written informed consent for donation was given during life, in accordance with the Dutch Burial and Cremation act (BWBR0005009). The Medical Ethical Committee of the Amsterdam University Medical Centers (location AMC) provided a waiver for approval of this study. Further, experiments were performed according to relevant international and institutional regulations and ethics guidelines. The presented findings are reported according to the Anatomical Quality Assurance (AQUA) checklist.[22]

Nerve block technique

Nerve blocks were performed bilaterally, but each side was randomized individually. Thus, totaling eight or nine nerve blocks per injection technique (Table 1). The injectate was a mixture of 38 mL of LA and 2 mL of contrast medium (Visipaque™, GE Healthcare, Eindhoven, The Netherlands) for all techniques. This total volume was chosen as it reflects routine clinical practice, while previous research suggests that this volume may be able to reach the target nerves, including the ON.[17,23] Ultrasound guidance was used to visualize the different anatomical structures, to guide the needle tip to the correct plane, and to observe injectate spread. Nerve blocks were placed by two anesthesiologists specialized in regional anesthesia (WtH, HMB). Study procedures were completed within six hours of arrival at the Amsterdam University Medical Centers.

Table 1. A summary of nerve involvement after the different injection techniques.

	S-FICB-H (9 blocks)	S-FICB (8 blocks)	FNB (8 blocks)	I-FICB (9 blocks)
FN, n (%)	9 (100.0)	8 (100.0)	8 (100.0)	2 (22.2)
LFCN, n (%)	9 (100.0)	8 (100.0)	7 (87.5)	4 (44.4)
ON, n (%)	0 (0.0)	1 (12.5)	0 (0.0)	0 (0.0)

Abbreviations: FN, femoral nerve; LFCN, lateral femoral cutaneous nerve; ON, obturator nerve; S-FICB(-H), suprainguinal fascia iliaca compartment block with or without hydrodissection; FNB, femoral nerve block; I-FICB, infrainguinal fascia iliaca compartment block.

S-FICB was applied by puncturing the skin approximately one centimeter cranial to the inguinal ligament in caudal to cranial fashion.[9] In the S-FICB-H group, we subsequently advanced the needle tip an additional five centimeters under the FI (using hydrodissection) in order to achieve a pronounced cranial position not previously documented in the literature for a single-shot technique. I-FICB was performed at the lateral third of the line connecting the anterior superior iliac spine and the pubic tubercle, one centimeter caudal to the inguinal ligament.[10] The injection was placed at the inguinal crease, adjacent to the FN, in case of (ultrasound-guided) FNB.

Outcome parameters and data analysis

The primary outcome parameter of this study was ON coverage. Additionally, we measured cranial injectate spread as a function of the injectate's ability to migrate to the debated cranial opening (in the FIC) and ON.[12,13] Further, FN and LFCN coverage were other secondary outcome parameters.

Injectate spread was documented 15 minutes after injection using whole-body computed tomography (CT) (Siemens SOMATOM Force, Siemens Healthineers, Forchheim, Germany; CT collimation 0.6 mm, dual energy 100/Sn150 kVp, 486/244 mA, pitch 0.6, slice thickness 1.0 mm, soft kernel). A musculoskeletal radiologist blinded to the injection technique assessed the locoregional contrast medium spread. Perineural presence of contrast was assessed by visualization and inspection of the anatomical location of the relevant structures in axial, sagittal and coronal planes, with additional reformatting when deemed necessary. For example, the full path of the ON between its origin and exit through the obturator foramen was inspected. Cranial diffusion was measured in coronal reformatted images from the femoral head (in centimeters) and is also described in relation to the corresponding vertebra.

Data for cranial injectate spread was tested for normality using histograms and the Shapiro-Wilk test and is presented as mean ± standard deviation. Cranial injectate spread was subsequently compared across the study arms by applying one-way ANOVA and Tukey post-hoc testing. Other outcome measures were summarized as frequencies with percentages. A *P*-value smaller than 0.05 was deemed statistically significant. IBM SPSS Statistics, Version 28.0.1.0, was used for statistical analysis (IBM Corp., Armonk, NY, USA).

Results

Cadavers were predominantly male (12 of 17, 71%). Further baseline characteristics and details about prior medical history were unavailable, due to the anonymous nature of the body donation program.

Nerve involvement

The ON was involved in one (S-FICB) of 34 nerve blocks, while none reached the lumbar plexus. The nerve block that did reach the ON was found to involve this nerve in the retroperitoneal compartment, at a level corresponding to the first sacral vertebra (Figure 2). This was also the maximum height reached by the contrast for this block. Medial injectate spread was limited in other cases and did not reach the ON, as exemplified in Figure 3 after bilateral S-FICB-H.

The FN and LFCN were consistently involved in S-FICB-H, S-FICB and FNB, while these structures were considerably less often involved in I-FICB (22.2% and 44.4% of cases, respectively). Details of nerve involvement are summarized in Table 1. Figure 4 depicts a volume rendering reconstruction of a cadaver with typical injectate distribution patterns after bilateral S-FICB-H.

Figure 2: Coronal (A) and axial (B) CT imagery of the S-FICB case wherein the contrast mixture reached the ON (left side). The injectate was found to involve the ON in the retroperitoneal compartment at the level of the first sacral vertebra, which was also the maximum height that was reached. Dashed arrows point to the ON, while solid arrows point to contrast.

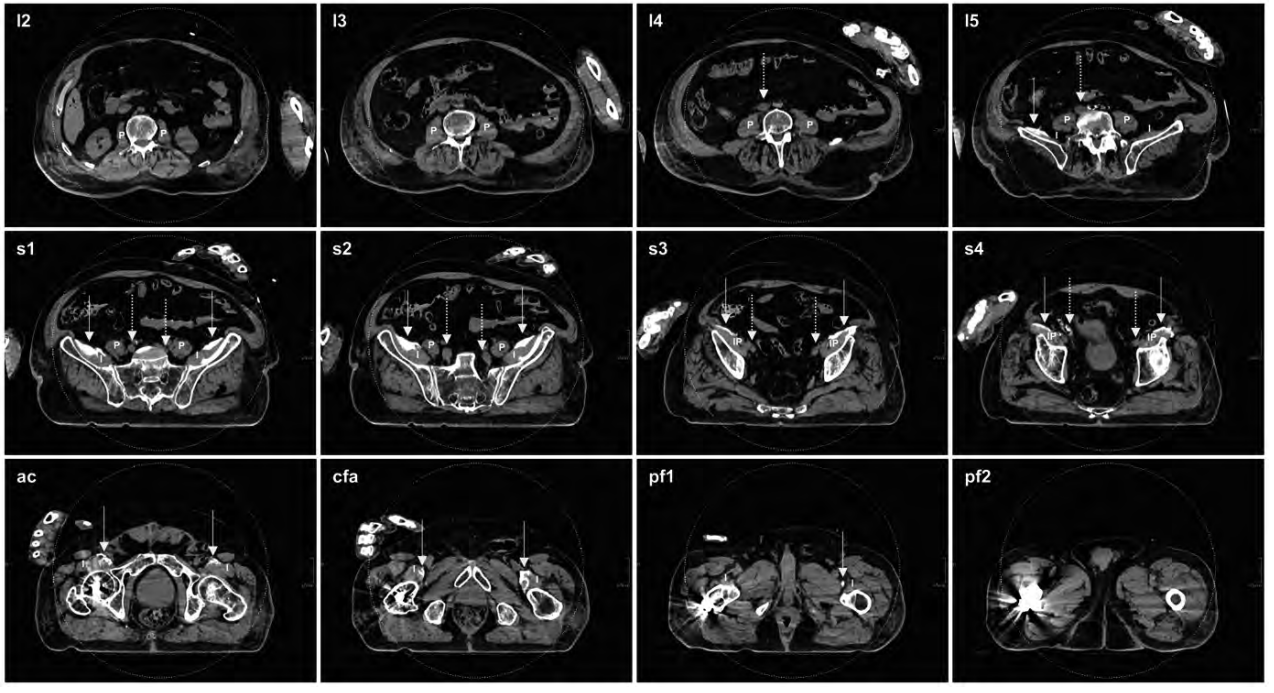

Figure 3: Axial CT slices detailing typical spread of injectate after (bilateral) S-FICB-H. The LA-based contrast mixture was determined to reach a maximum height corresponding to the 5th lumbar vertebra on the left side and the intervertebral disc of lumbar vertebrae four-five on the right side. Medial spread of contrast stayed anterior to the iliopsoas muscles and iliac arteries. As such, contrast remained removed of the location of the lumbar plexus and ON, both in the cranial and medial directions. Dotted arrows point to the iliac arteries, solid arrows point to the contrast.
Abbreviations: l, lumbar vertebra; s, sacral vertebra; ac, acetabulum; cfa, common femoral artery; pf, proximal femur; P, psoas muscle; I, iliacus muscle; IP, iliopsoas muscle.

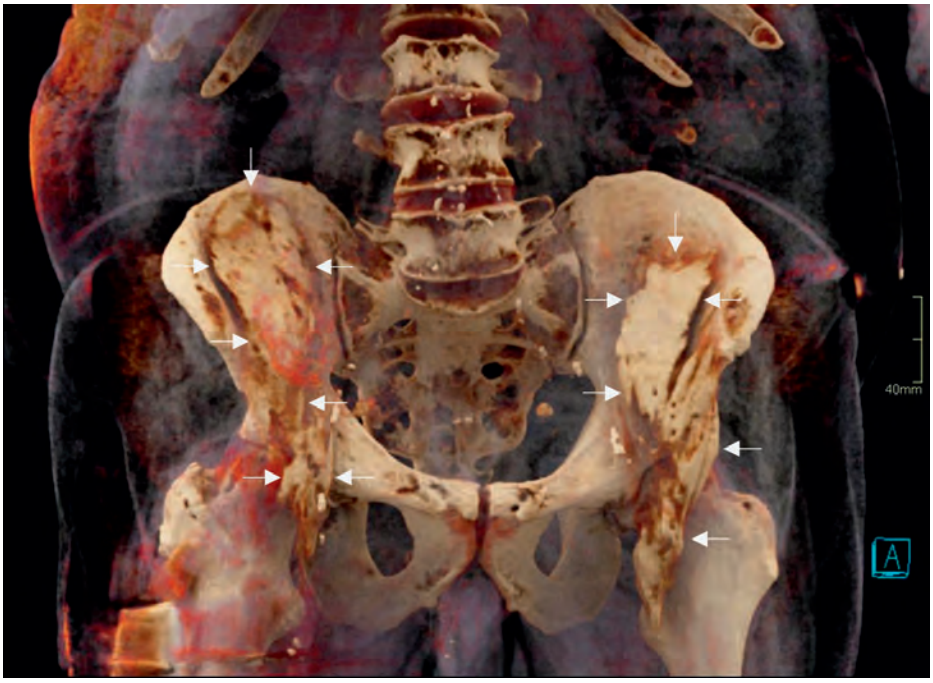

Figure 4: A 3D volume rendered reconstruction of CT-imaging of a specimen that was randomized to receive bilateral S-FICB-H. Contrast reached a maximum height equal to the level of the 5th lumbar vertebra on the left side and the intervertebral disc of lumbar vertebrae four-five on the right side. The arrows point to the contrast.

Cranial injectate spread

Spread of the injectate towards the lumbar plexus was measured in relation to the femoral head. Truncal spread was found in only two of nine (22%) I-FICBs and as such, I-FICB was excluded from statistical analysis. The mean cranial spread of S-FICB-H (14.00 ± 3.16 cm) was significantly more than that of S-FICB (10.28 ± 2.95 cm, $p = 0.046$), or FNB (5.30 ± 2.86 cm, $p = < 0.001$). Injectate reached higher for S-FICB than for FNB ($p = 0.008$). Similar distribution patterns were observed when cranial injectate spread was related to the vertebral column, as shown in Table 2, and demonstrated for S-FICB-H in Figure 3.

Table 2. *Cranial injectate spread related to the vertebral column.*

	S-FICB-H (9 blocks)	S-FICB (8 blocks)	FNB (8 blocks)	I-FICB (9 blocks)
L2, n (%)	1 (11.1)	-	-	-
…				
L4, n (%)	2 (22.2)	3 (37.5)	-	-
IVD L4-L5, n (%)	1 (11.1)	-	-	-
L5, n (%)	4 (44.5)	1 (12.5)	-	-
IVD L5-S1, n (%)	1 (11.1)	-	1 (12.5)	1 (11.1)
S1, n (%)	-	2 (25.0)	1 (12.5)	1 (11.1)
IVD S1-S2, n (%)	-	2 (25.0)	-	-
S2, n (%)	-	-	3 (37.5)	-
…				
Coccyges, n (%)	-	-	2 (25.0)	-
…				
Below the VC, n (%)	-	-	1 (12.5)	7 (77.8)

Abbreviations: L, lumbar vertebra; S, sacral vertebra; IVD, intervertebral disc; VC, vertebral column; S-FICB(-H), suprainguinal fascia iliaca compartment block with or without hydrodissection; FNB, femoral nerve block; I-FICB, infrainguinal fascia iliaca compartment block.

Discussion

This radiological cadaveric study supports the hypothesis that S-FICB-H leads to the most cranial injectate spread of the techniques targeting the FIC. Concurrently, however, our findings also demonstrate that pronounced cranial injectate spread will not result in reliable blockade of the ON. I-FICB resulted in less involvement of the FN and LFCN than S-FICB-H, S-FICB and FNB.

The ON is a mixed sensory and motor nerve that derives from the anterior divisions of the 2nd, 3rd and 4th lumbar spinal nerves. Its branches innervate the adductor muscles of the thigh, and the hip and knee joints. Further, the ON contributes, in some patients, to the sensory innervation of a section of the medial thigh. Therefore, inclusion of ON blockade in FICB would improve analgesia after lower extremity procedures, such as hip fracture surgery.

However, it is still debated whether the ON can indeed be covered during FICB. Clinical examination after FICB may be ambiguous due to the highly variable cutaneous innervation of the ON and co-innervation to the adductor muscles.[24] Mean-

while, (both primary and secondary) cadaveric dissection is prone to disrupt the integrity of fascial layers, and is therefore at risk of false positive research results. This study therefore applied CT-imaging of a LA-based contrast mixture, as it allowed for precise and objective (numerical) measurements of injectate spread. Additionally, CT-imaging allowed us to include 34 samples, a number which would have been unrealistic to obtain with dissection (or magnetic resonance imaging; MRI). Further, the advanced CT scanner used here provided us with similar information as would have been obtained with MRI.

The data presented here for S-FICB (both with and without additional needle advancement) deviates from previously reported success rates of ON involvement, but is closely aligned to reported rates of FN and LFCN blockade.[9,11,17] Literature details differing success rates for I-FICB.[8,10,17,25-30] Interestingly, our results are similar to that of authors who performed I-FICB based on the description that was also the foundation of the technique applied in this study.[17,28] The current study supports the conclusion that S-FICB leads to more cranial spread and better FN and LFCN involvement than I-FICB, yet our results indicate less cranial distribution patterns for conventional S-FICB and I-FICB than previously reported in a volunteer study.[17] The 40 mL injectate allowed FNB to behave as a field block, while the inguinal injection site might have facilitated more efficient migration towards the FN and LFCN than possible for I-FICB.

The ON's path between its origin and the obturator foramen is of importance as the aforementioned nerve block approaches are all based on the presumption that the ON can be reached by an injectate in the FIC.[6,8-11] However, anatomical reports have shown that the ON does not travel within the FIC and suggested an alternative mechanism of action: cranial diffusion from the FIC to the retroperitoneal compartment.[12,13] Assuming this path exists, lack of ON involvement can be hypothesized to be caused by either an inadequate injection volume and injection force, or a too distal injection site, placing the LA out of reach from the retroperitoneal compartment. This scenario could explain the unusually high – compared to the FIC's capacity of 23 mL – minimum effective volume of 62.5 mL found in a recent cadaver dissection study that applied a step-up, step-down algorithm to determine the optimal injectate volume.[12,14] However, it is as of yet unknown what effect a large injectate volume, or high injection pressure, has on fascial plane integrity (while concurrently the clinical relevance and utility of a nerve block approach that requires injection of a large number of ampoules can be debated). Similar to needle misplacement in the retroperitoneal compartment, disruption of the fascial compartment

could lead to creation of an artificial opening in the FI and diffusion towards the ON.[15] This, however, would not be a *true* fascial plane block and constitutes a different mechanism than sought after with a FICB. We speculate that this mechanism is the explanation for the case in which the ON was successfully involved in our study, and the underlying reason for the limited replicability of studies.

Alternatively, this investigation assessed whether advanced needle insertion into the cranial direction would result in ON involvement. The lack thereof shown here contradicts the existence of an easily accessible cranial route from the FIC to the retroperitoneal compartment. Further, as reported in other studies, posteromedial spread was limited and remained removed from the ON.[19,25] Thus, overall, achieving reliable ON blockade using a FIC approach seems not possible, as illustrated by the presented data, the considerable number of published methodological variations, and the differences in reported success rates between studies that applied the same injection technique.

A limitation of this study is the reliance on (human) cadavers as tissue quality might have deteriorated after death. However, specimens were fresh, unfrozen and unembalmed, allowing for near-normal block procedures as shown by the pattern of spread after nerve blocks.

Conclusion

In summary, neither S-FICB-H nor any other technique targeting the FIC leads to reliable ON involvement, and as such the ON seems to be unrelated to fascial plane blocks targeting the FIC. Addition of a separate ON block to S-FICB (or large volume FNB) should be considered when clinically indicated.

To summarize: the obturator nerve is not consistently affected by fascial plane blocks targeting the iliac facial plane. Future research endeavors should explore a dependable approach for achieving obturator nerve anesthesia within the retroperitoneal compartment.

References

1 Wick, E. C., Grant, M. C. & Wu, C. L. Postoperative Multimodal Analgesia Pain Management With Nonopioid Analgesics and Techniques: A Review. *JAMA Surg* **152**, 691-697, doi:10.1001/jamasurg.2017.0898 (2017).

2 Joshi, G., Gandhi, K., Shah, N., Gadsden, J. & Corman, S. L. Peripheral nerve blocks in the management of postoperative pain: challenges and opportunities. *J Clin Anesth* **35**, 524-529, doi:10.1016/j.jclinane.2016.08.041 (2016).

3 Mouzopoulos, G. *et al.* Fascia iliaca block prophylaxis for hip fracture patients at risk for delirium: a randomized placebo-controlled study. *J Orthop Traumatol* **10**, 127-133, doi:10.1007/s10195-009-0062-6 (2009).

4 Kim, C. H. *et al.* The effect of regional nerve block on perioperative delirium in hip fracture surgery for the elderly: A systematic review and meta-analysis of randomized controlled trials. *Orthop Traumatol Surg Res* **108**, 103151, doi:10.1016/j.otsr.2021.103151 (2022).

5 Gerbershagen, H. J. *et al.* Pain intensity on the first day after surgery: a prospective cohort study comparing 179 surgical procedures. *Anesthesiology* **118**, 934-944, doi:10.1097/ALN.0b013e31828866b3 (2013).

6 Winnie, A. P., Ramamurthy, S. & Durrani, Z. The inguinal paravascular technic of lumbar plexus anesthesia: the '3 in 1 block'. *Anesth Analg* **52**, 989-996 (1973).

7 Marhofer, P., Nasel, C., Sitzwohl, C. & Kapral, S. Magnetic resonance imaging of the distribution of local anesthetic during the three-in-one block. *Anesth Analg* **90**, 119-124, doi:10.1097/00000539-200001000-00027 (2000).

8 Dalens, B., Vanneuville, G. & Tanguy, A. Comparison of the fascia iliaca compartment block with the 3-in-1 block in children. *Anesth Analg* **69**, 705-713 (1989).

9 Desmet, M. *et al.* A Longitudinal Supra-Inguinal Fascia Iliaca Compartment Block Reduces Morphine Consumption After Total Hip Arthroplasty. *Reg Anesth Pain Med* **42**, 327-333, doi:10.1097/AAP.0000000000000543 (2017).

10 Dolan, J., Williams, A., Murney, E., Smith, M. & Kenny, G. N. Ultrasound guided fascia iliaca block: a comparison with the loss of resistance technique. *Reg Anesth Pain Med* **33**, 526-531, doi:10.1016/j.rapm.2008.03.008 (2008).

11 Hebbard, P., Ivanusic, J. & Sha, S. Ultrasound-guided supra-inguinal fascia iliaca block: a cadaveric evaluation of a novel approach. *Anaesthesia* **66**, 300-305, doi:10.1111/j.1365-2044.2011.06628.x (2011).

12 Xu, Z. *et al.* Fibrous configuration of the fascia iliaca compartment: An epoxy sheet plastination and confocal microscopy study. *Sci Rep* **10**, 1548, doi:10.1038/s41598-020-58519-0 (2020).

13 Bendtsen, T. F. *et al.* Anatomical considerations for obturator nerve block with fascia iliaca compartment block. *Reg Anesth Pain Med* **46**, 806-812, doi:10.1136/rapm-2021-102553 (2021).

14 Kantakam, P. *et al.* Cadaveric investigation of the minimum effective volume for ultrasound-guided suprainguinal fascia iliaca block. *Reg Anesth Pain Med* **46**, 757-762, doi:10.1136/rapm-2021-102563 (2021).

15 Bendtsen, T. F. *et al.* Suprainguinal fascia iliaca block: does it block the obturator nerve? *Reg Anesth Pain Med* **46**, 832, doi:10.1136/rapm-2021-102712 (2021).

16 Tran, Q. *et al.* Reply to Dr Bendtsen and colleagues. *Reg Anesth Pain Med* **46**, 832-833, doi:10.1136/rapm-2021-102782 (2021).
17 Vermeylen, K. *et al.* Supra-inguinal injection for fascia iliaca compartment block results in more consistent spread towards the lumbar plexus than an infra-inguinal injection: a volunteer study. *Reg Anesth Pain Med* **44**, 483, doi:10.1136/rapm-2018-100092 (2019).
18 Vermeylen, K., Leunen, I. & Desmet, M. Response to the letter to the editor by Bendtsen et al "Supra-inguinal injection for fascia iliaca compartment block results in more consistent spread towards the lumbar plexus than an infra-inguinal injection: a volunteer study". *Reg Anesth Pain Med* **45**, 243-244, doi:10.1136/rapm-2019-100725 (2020).
19 Bendtsen, T. F., Pedersen, E. M. & Peng, P. Course of the obturator nerve. *Reg Anesth Pain Med* **44**, 1039, doi:10.1136/rapm-2019-100655 (2019).
20 Tran, D. Q., Boezaart, A. P. & Neal, J. M. Reply to Dr Wilson. *Reg Anesth Pain Med* **43**, 564-565, doi:10.1097/AAP.0000000000000800 (2018).
21 Chin, K. J., Lirk, P., Hollmann, M. W. & Schwarz, S. K. W. Mechanisms of action of fascial plane blocks: a narrative review. *Reg Anesth Pain Med* **46**, 618-628, doi:10.1136/rapm-2020-102305 (2021).
22 Tomaszewski, K. A. *et al.* Development of the Anatomical Quality Assurance (AQUA) checklist: Guidelines for reporting original anatomical studies. *Clin Anat* **30**, 14-20, doi:10.1002/ca.22800 (2017).
23 Vermeylen, K. *et al.* The effect of the volume of supra-inguinal injected solution on the spread of the injectate under the fascia iliaca: a preliminary study. *J Anesth* **32**, 908-913, doi:10.1007/s00540-018-2558-9 (2018).
24 Bouaziz, H. *et al.* An evaluation of the cutaneous distribution after obturator nerve block. *Anesth Analg* **94**, 445-449, table of contents, doi:10.1097/00000539-200202000-00041 (2002).
25 Swenson, J. D. *et al.* Local anesthetic injection deep to the fascia iliaca at the level of the inguinal ligament: the pattern of distribution and effects on the obturator nerve. *J Clin Anesth* **27**, 652-657, doi:10.1016/j.jclinane.2015.07.001 (2015).
26 Capdevila, X. *et al.* Comparison of the three-in-one and fascia iliaca compartment blocks in adults: clinical and radiographic analysis. *Anesth Analg* **86**, 1039-1044, doi:10.1097/00000539-199805000-00025 (1998).
27 Morau, D. *et al.* Comparison of continuous 3-in-1 and fascia Iliaca compartment blocks for postoperative analgesia: feasibility, catheter migration, distribution of sensory block, and analgesic efficacy. *Reg Anesth Pain Med* **28**, 309-314, doi:10.1016/s1098-7339(03)00183-4 (2003).
28 Shariat, A. N. *et al.* Fascia Iliaca block for analgesia after hip arthroplasty: a randomized double-blind, placebo-controlled trial. *Reg Anesth Pain Med* **38**, 201-205, doi:10.1097/AAP.0b013e31828a3c7c (2013).
29 Foss, N. B. *et al.* Fascia iliaca compartment blockade for acute pain control in hip fracture patients: a randomized, placebo-controlled trial. *Anesthesiology* **106**, 773-778, doi:10.1097/01.anes.0000264764.56544.d2 (2007).
30 Lopez, S., Gros, T., Bernard, N., Plasse, C. & Capdevila, X. Fascia iliaca compartment block for femoral bone fractures in prehospital care. *Reg Anesth Pain Med* **28**, 203-207, doi:10.1053/rapm.2003.50134 (2003).

Section 3

Clinical research and regional anesthesia

Chapter 6

Minimum local anesthetic volumes for a selective saphenous nerve block: a dosefinding study

Based on: Werner ten Hoope, Markus W Hollmann, Arthur Atchabahian, Marcel Rigaud, Gino M Kerkhoffs, Philipp Lirk, Holger M Baumann
Minerva Anestesiol. 2017 Feb;83(2):183-190

Abstract

Background

Saphenous nerve block contributes to analgesia after knee and lower leg surgery. However, literature reports a wide range of volumes of local anaesthetic being used for this block.

Methods

A non-randomized controlled trial in a single university hospital in March 2015. Eighteen healthy volunteers (ASA 1 status, aged 27-43 years; male/female ratio 11 vs. 7) were needed to determine the minimum local anaesthetic volume (MLAV) of mepivacaine 2% using the Dixon up-and-down method to achieve a selective ultrasound-guided saphenous nerve block. The primary endpoint MLAV (ED50 and ED95) for an ultrasound-guided saphenous nerve block were determined. The secondary endpoints were the position of the saphenous nerve, block onset and duration of action, cutaneous spread of the block, and the occurrence of femoral nerve motor block.

Results

The measured MLAV dose that was effective in 50% of cases (ED50) for a complete saphenous nerve block was 1.5 mL; the calculated MLAV dose for 95% of cases (ED95) was 1.9 mL. The saphenous nerve was encountered in almost all cases on the anterior / anteromedial aspect of the femoral artery. We found no correlation between local anaesthetic volume and the onset or duration of the block. Cutaneous spread of the nerve block was observed on the anteromedial aspect of the lower leg, with considerable individual variation between individuals in the study. No femoral motor block was observed.

Conclusions

For a selective ultrasound-guided saphenous nerve block, the ED95 MLAV of mepivacaine 2% is 1.9 mL.

Introduction

The saphenous nerve, the sensory end branch of the femoral nerve, contributes to the innervation of the knee and lower leg.[1] Because it is purely sensory, it has recently been recognized as a potential target structure to achieve analgesia after knee and lower leg surgery, without loss of motor function.[2, 3]

The saphenous nerve runs distally in the adductor canal, a musculo-fibrous compartment bordered laterally by the vastus medialis muscle, posteriorly by the adductor longus muscle, and anteromedially by the vasto-adductor membrane.[1] The adductor canal includes the femoral artery and vein, saphenous nerve, and the femoral nerve branch to the vastus medialis muscle which comprises an articular branch.[1] Superficial to the vasto-adductor membrane lays the anterior branch of the obturator nerve, which innervates the medial thigh,[4, 5] while the posterior branch has an inconsistent articular branch which perforates the adductor magnus muscle, and travels in the distal adductor canal.[1] In theory, therefore, a high-volume adductor canal injection not only blocks the saphenous nerve, but also major sensory portions of the obturator nerve and the nerve to the vastus medialis.[1, 6]

An adductor canal block may be different to a selective saphenous nerve block. However, nobody has yet performed a structured assessment of the efficacy of selective saphenous nerve block, and thus the required minimum effective volume of local anaesthetic (MLAV) for this peripheral nerve block is unknown. For other nerve blocks, dose-finding studies have allowed clinicians to tailor the dose of local anaesthetic according to scientific evidenceSo the main objective of this study was to characterize ultrasound-guided selective saphenous nerve block by determining the MLAV of mepivacaine 2% effective in 50% of volunteers (ED50), and calculating the corresponding volume effective in 95% of healthy volunteers (ED95). The secondary aims were to evaluate block characteristics and anatomic relationships between the saphenous nerve and the surrounding structures.

Materials and Methods

Subjects

The present dose-finding study (trial registration EudraCT number: *2014-004672-38)* was performed in accordance with the Helsinki Declaration after approval (Protocol No. 2014_348) on January 5th, 2015 by the institutional review board; Medical Ethical

Committee AMC, Academic Medical Centre, Meibergdreef 9 Amsterdam The Netherlands, and was carried out in eighteen healthy volunteers. We obtained from all volunteers included in the study a written informed consent before participation. Exclusion criteria included allergy to local anaesthetics, ingestion of any pain medication within the previous 24 hours, pregnancy, or breastfeeding status.

Saphenous nerve block

Volunteers received a ultrasound-guided saphenous nerve block on their left leg as described by Manickam and colleagues.[11] Briefly, a high-frequency (13-6 MHz) linear ultrasound probe (SonoSite M Turbo; Secma, Amsterdam, The Netherlands) was used to locate the femoral artery over the medial aspect of the thigh (Figure 1). The artery was followed distally until it deviated posteriorly through the adductor hiatus. The block was performed 2 cm proximal to this location. The saphenous nerve was visualized in the short axis (transverse plane). The probe was covered using an Ecolab Probe cover kit (Microtek, Zutphen, The Netherlands) and we used SonoPlex NanoLine echogenic 21G / 10 cm needles (Pajunk, Geisingen, Germany). The volume of mepivacaine 20 mg/mL (BBraun, Melsungen, Germany) was dictated by the Dixon model.[13]

An experienced investigator (H.B.) who routinely performs this block in clinical practice performed all nerve blocks. An independent assessor performed qualitative and quantitative testing of the nerve block. The volunteers were blinded to the volume of local anaesthetic. All blocks were documented by ultrasound image capture at three time points: 1) before needle insertion to document anatomy, 2) with the needle inserted next to the nerve, and 3) after the injection of the local anaesthetic. We recorded variations in nerve localization and vessel anatomy, and the occurrence of fascial clicks.

Primary study endpoint

As a first step, the ED50 MLAV of mepivacaine 2% was determined using the Dixon model, with successful block (yes/no) defined as a loss of sensation to pinpricks at each of the following locations: 1) the skin above the tibial tuberosity, 2) the skin of the medial surface of the tibial plateau and 3) the skin above the medial ankle. This was scored on a 100-mm scale compared to the contralateral, non-anaesthetized side (0 = no difference between sides thus no block at all, 100 = complete loss of sensation to pinprick) 20 minutes after injection, analogous to a previous dose-finding study by Eichenberger *et al*.[14]

Figure 1 Probe and needle placement during eco-guided procedure.

Therefore, full sensory block (100 mm) at all three sites was considered a successful saphenous nerve block, whereas anything less than a full sensory block (<100 mm) at all three sites was considered a failed block. Starting with a volume of 10 mL, each volunteer's response determined the volume of mepivacaine 2% for the next volunteer. When successful saphenous nerve block was achieved, volume was decreased by 1 mL for the next patient; if the block was insufficient, a 1 mL increase of the volume was used; for volumes below 1 mL, the protocol stipulated additional steps with 0.2 mL increments. As described by Dixon,[13] the study would be terminated after three oscillations (up/down) around a given volume.

Secondary study endpoints

Secondary aims were to evaluate the influence of the volume used on block onset and block offset at 2, 4, 6, 8, 10, 15, 20, 25, and 30 minutes, and every 15 minutes thereafter until block resolution (defined as no difference compared to the contralateral non-anaesthetised side), the extent of motor block, the maximum spread of sensory block on the skin surface at 20 minutes and evaluation of anatomical

variations of the position of the saphenous nerve relative to the femoral artery, as well as potential double arteries and accessory veins.

Sensory mapping was performed by pinprick. The border of sensory block was marked on the skin, and the borders of the anaesthetized area drawn out and plotted onto a transparent foil to measure the surface area using Image J version 1.48 (open source by W. Rasband, Research Services Brand, National Institutes of Mental Health, Bethesda, MD). Next, we marked the tibial tuberosity, the ankle, and the anterior crest of the tibia in all volunteers, and photo-documented cutaneous sensory spread using digital photography in two dimensions (from the anterior and the medial side). For each anterior and medial photograph, we extracted the border of cutaneous spread, filled the border with a light grey shade, and scaled this to a "standard leg" using Adobe Photoshop version 2.2 (Adobe Systems Benelux, Amsterdam, The Netherlands). We superimposed these scaled shaded images such that the overlapping areas would become darker in colour with each added subject, to identify which cutaneous areas of the leg were most likely to be blocked by the saphenous nerve. This meant that a darker grey hue would indicate a more uniform block in this area across people in the test.

A standardized MRC scoring system (score 0-5) was used by an unblended investigator to determine muscle strength of the quadriceps muscle. The volunteers sat on a chair, with a 90-degree flexion at the hip and the knee. Muscle strength was assessed as: no contraction (0); muscle flicker, but no movement (1); movement possible, but not against gravity (by testing the joint in a horizontal plane) (2); movement possible against gravity, but not against resistance by the examiner (3); movement possible against some resistance by the examiner (4); normal strength (5).

Finally, demographic parameters (ASA status, sex, age, height and weight of test persons) were recorded.

Statistics

The average dose required to achieve successful nerve blockade in patients, subsequently followed by three failed nerve blocks in these same patients, was used to determine the volume of mepivacaine 2% required to achieve successful nerve blockade in 50% of patients (ED50).The dose at which an adequate block would be expected in 95% of patients (ED95) was estimated by a logistic regression with a probit link function; for this analysis the log10 dose was linked to a successful block using the maximum likelihood. It is assumed that the number of successful blocks

has a normal distribution. The dose for an adequate block was correlated using the Spearman's rho test as described previously.[14]

The number of volunteers are dictated by the model described by Dixon,[13] the inclusion of volunteers would be terminated after three oscillations (up/down) around a given volume.

SPSS statistics version 22 (IBM, Amsterdam, The Netherlands) was used for statistical analysis. Baseline characteristics are presented using descriptive statistics. Continuous data are reported as means and standard deviation if normally distributed, and otherwise as medians and interquartile range. Categorical data are reported as numbers and percentages per group.

Results

Demographics and Anatomy

After eighteen consecutive volunteers, the conditions were met to complete the Dixon model and determine the ED50 MLAV for saphenous nerve block. In seventeen of the eighteen volunteers, the saphenous nerve was adequately visualized by ultrasonography. In one volunteer, this was not achieved, and subsequently, block failure was observed. Volunteer characteristics and demographics are presented in Table 1 and Table 2. In one volunteer who received 8 mL, we initially scored a block failure because the sensory area at the tibial tuberosity was smaller than in the two preceding test subjects. However, as the trial progressed, we observed substantial variability of the cutaneous innervation provided by the saphenous nerve, explaining the slight change in sensory area observed in this volunteer. This subject was excluded from further calculations of ED50/95.

Table 1. Demographics of volunteers

Male / Female	11 / 7
ASA classification	I (18)
Age (years)	35 ± 5.0
Height (cm)	178.4 ± 9.9
Weight (kg)	77 ± 14

Demographics. Values are in means (±SD).

Table 2. Results per volunteer

Volunteer number	Block Y/N	Volume of LA (mL)	MRC	Onset time (minutes)	Duration (minutes)	Block surface (cm^2)
1	Y	10	5	10	105	672
2	Y	9	5	6	150	806
3	N *	8	5	6	195	554
4	Y	9	5	8	195	588
5	Y	8	5	4	195	540
6	Y	7	5	2	180	693
7	Y	6	3	2	270	575
8	Y	5	5	2	310	538
9	Y	4	5	4	240	770
10	Y	3	5	2	180	669
11	Y	2	5	2	150	349
12	N	1	5	10	240	508
13	Y	2	5	4	135	652
14	N	1	5	2	240	405
15	Y	2	5	2	210	566
16	N	1	5	2	150	203
17	N **	2	5	-	-	-
18	Y	2	5	2	210	716

*Saphenous nerve block characteristics per volunteer. * Initially scored as negative block (no complete sensory block of all three areas) due to slight change in sensory area observed. This subject was excluded from further calculations. ** Block failure; no sensory block.*
LA: local anesthetic, MRC: Medical Research Council (MRC) Scale for Muscle Strength.

Dose finding

The measured MLAV doses that were effective in 50% (ED50) and calculated MLAV effective dose in 95% (ED95) for a complete saphenous nerve block were 1.5 and 1.9 mL, respectively. The up and down dose-finding sequence is illustrated in Figure 2.

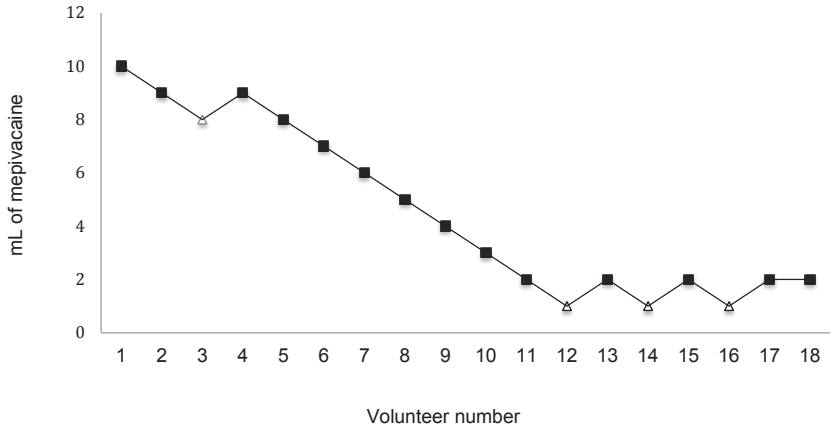

Figure 2. Up-and-down sequence for saphenous nerve block. A solid mark represents a successful block, and a hollow mark represents a failed block (no complete sensory block of all three areas: tibial tuberosity, medial leg and ankle).

Block characteristics

The time to block onset varied between two and twenty minutes (mean 9 ± 7 min). In our small sample, we found no correlation between volume of local anesthetic and block onset time or sensory spread. We found no correlation between local anesthetic volume and block duration either. The mean block duration was 195 ± 54 min (range 105 – 310) with a mean sensory spread of 621 ± 116 cm^2 (range 349 – 806). Neither duration (ρ = -0.03, P = 0.93) nor spread (ρ = 0.51, P = 0.33) was correlated to the dose of local anesthetic. The cutaneous distribution of sensory block is illustrated in Figure 3. In three patients, we found cutaneous sensory block in the region traditionally ascribed to the obturator nerve. The failed blocks were characterized by patchy distribution of sensory block, a failure of block both proximally at the tuberosity and distally at the medial malleolus, and a substantially smaller area of block at the tibia. No occurrence of femoral motor block was observed, but one volunteer who received 6 mL of local anesthetic experienced a transient and incomplete motor block (MRC 3) of the peroneal nerve.

Figure 3 Frontal (A) and medial (B) view of cutaneous distribution on the left leg. Darker grey hue indicates overlap between sensory areas of individual volunteers.

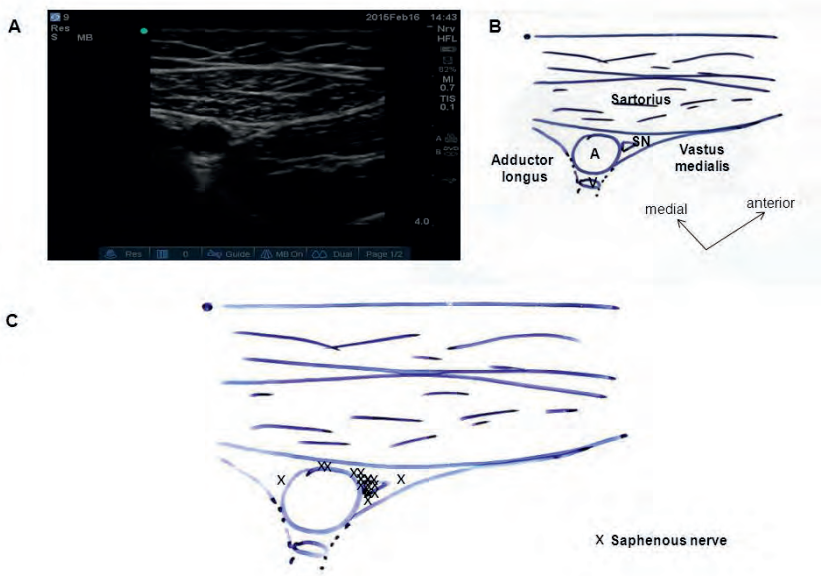

Figure 4. Ultrasound picture (A) with legend (B) of a typical volunteer undergoing saphenous nerve block, with variations in the position of the saphenous nerve (C).
A: femoral artery; V: femoral vein; SN: saphenous nerve.

Anatomy

In sixteen of the seventeen volunteers with positive nerve visualization, the saphenous nerve was located in close proximity to the femoral artery; one nerve was situated slightly more anteriorly in a fascial plane between the sartorius and the vastus medialis muscle. The nerve was located anteriorly, or slightly anterolaterally in the majority of cases, and anteromedially in only a minority of cases (Figure 4). In the case of double vessels or accessory veins, the saphenous nerve was in close relation to with the more superficial artery. When placing the needle, a fascial click was consistently observed as the vasto-adductor membrane was pierced.

Discussion

We investigated the MLAV for ultrasound-guided block of the saphenous nerve using mepivacaine 2%. The measured MLAV ED50 and calculated MLAV ED95 for a saphenous nerve block are 1.5 and 1.9 mL, respectively.

Dose finding

The minimal block volume reported here is, relatively, different from previous investigations in other nerves. Assuming a diameter of the saphenous nerve of 3 mm (see Figure 1), the cross-sectional area of the nerve is approximately 7 mm^2 and the adapted ED95 volume in our study would be 0.27 mL/mm^2. This is higher than the 0.1 mL/mm^2 described for the ulnar nerve,[14] and higher than the sciatic ED99 volume of 0.1 mL/mm^2 reported by Latzke *et al.*,[15] but substantially lower than the sciatic ED95 of 2 mL/mm^2 described by Jeong *et al.* for the sciatic nerve.[16] Several factors may account for this discrepancy. We think that the major difference is the different definition of block success from previous investigators. We chose to evaluate nerve block 20 minutes after injection, as compared to 30 minutes in the study by Jeong [16] and 45 minutes in the study by Latzke on the sciatic nerve.[15] However, one could argue that the sciatic nerve is larger and this would in itself necessitate a longer evaluation period. So, the present investigation may compare better to the study by Eichenberger *et al.* on the ulnar nerve, which is more similar to the saphenous nerve in size and structure. In contrast to the study by Eichenberger, we evaluated several areas of innervation (tibial tuberosity, medial leg and ankle) and we defined block success as complete sensory block of all three areas. The block failures described here still had detectable block at the anteromedial side of the leg, but failure around

the tibial tuberosity and the medial malleolus. Had we defined block success "only" as block at the medial leg, our determined MLAV might have been substantially lower. Our data was not sufficient to determine the ED95 directly, therefore a probit regression analysis was used as a theoretical and mathematical approach. We believe that 2 mL is a realistic and clinically meaningful volume, and the findings from our study can directly be transferred to clinical practice for selective block of the saphenous nerve.

Block characteristics

We note that overall, the sensory area of the successful saphenous nerve blocks did not vary with the dose administered, but the failed blocks had a substantially smaller area of block and were characterized by a failure of block both proximally and distally. This is understandable since the saphenous nerve is a small nerve with a well-defined, albeit variable, cutaneous innervation. The small diameter of the nerve is likely to promote fast penetration, so the sensory onset time was unaffected by the volume of the local anesthetic. The cutaneous distribution observed in this study (Figure 2) confirms previous reports of a high inter-individual variability. In particular, the innervation of the medial malleolus is highly inconstant, and shared to a variable degree with the sural and tibial nerves.[17] Our results also agree with a recent study by Lopez et al. who demonstrated that saphenous nerve block resulted in a sensory block on the medial leg and about 5-6 cm distal of the medial malleolus, again with a high variability between individuals.[18]

We were surprised, however, to find no relationship between volume and block duration. In previous investigations, high-volume injections at other nerves typically produced longer block durations than low-volume blocks.[19] For example, following interscalene block using ropivacaine 0.375%, increasing the volume four-fold led to a 50% increase in block duration.[20] A moderate correlation was observed between block duration and local anesthetic dose in the sciatic nerve study by Latzke et al.[15] The block duration we observed corresponds largely to the expected duration of a single shot block using mepivacaine. We note that in the present study, increasing the volume of medium-acting local anesthetics did not lead to a substantial prolongation of saphenous nerve block.

One purported advantage of saphenous nerve block is the avoidance of quadriceps motor block because more proximal motor fibers are theoretically spared. Some evidence supports this. For example, when 15 mL of dye were injected into the adductor canal of cadavers, proximal spread of injectate was observed

reaching the apex of the femoral triangle, and distal spread reached the adductor hiatus.[21] However, clinically, excessive proximal spread with consecutive motor block of the femoral nerve using a volume of 20 mL has been reported,[22] and another case report illustrated the possibility of distal spread with consecutive popliteal sciatic nerve block.[23] In our study, using relatively small volumes of injection, no volunteer experienced motor block of the femoral nerve, but one volunteer, at a volume of 6 mL, experienced a transient and incomplete popliteal sciatic nerve block. The volume of 2 mL for selective block of the saphenous nerve reported here as the MLAV ED 95 should realistically avoid discernible motor block.

Anatomy

We note that at the level of the Manickam approach, the saphenous nerve is about to change position relative to the femoral artery. Whereas the saphenous (and femoral) nerve is lateral to the artery at the inguinal crease, it is found anterior to the femoral artery at the entry into the adductor canal,[12] and exits the canal by piercing the vastoadductor membrane.[24] The majority of saphenous nerves were anterior or slightly anterolateral in position, while only a small number were found medially. This is in slight conflict with the previous description by Manickam that the nerve was most constantly found slightly anteromedial to the femoral artery.[11] In our study, correct identification of the saphenous nerve was confirmed by successful block even with a very localized spread of local anesthetic and a small volume. Thus, the anatomy of the saphenous nerve proximal to the adductor hiatus is variable, and anatomical studies detailing the variability in position of the saphenous nerve for different approaches should be undertaken.

The exact nomenclature of saphenous nerve or adductor canal blocks has been the subject of recent discussion.[8] The adductor canal contains the saphenous nerve, the femoral nerve branch to the vastus medialis muscle, and the posterior branch of the obturator nerve. The focus of the present investigation was on the selective block of the saphenous nerve alone.

Limitations

Finally, we would like to address potential limitations of the present study. First, findings considering block duration have to be interpreted with caution, as the sample size was small and block duration varied considerably. Second, the most important limitation is that this study was performed in volunteers and not in the perioperative setting, so adequate pain relief after lower leg surgery can only be inferred on the

basis of this study. However, the efficacy of saphenous nerve block has been previously demonstrated,[2] and we believe that by defining block success as full block in three areas (tibial tuberosity, medial tibial surface, medial malleolus), we can safely assume clinically effective full block of the saphenous nerve.

To summarize: We conclude that a clinically meaningful volume to block the distal saphenous nerve under ultrasound guidance is 2 mL. Significant individual variability was observed in the cutaneous spread of the selective nerve block, particularly in relation to the innervation of the dorsal and medial foot. Notably, no distinct correlation was identified between the administered volume of local anesthetic and the onset or duration of the selective saphenous nerve block. These findings underscore the complexity and individualized nature of the response to local anesthesia in the context of saphenous nerve blocks.

References

1. Gray H. Gray's Anatomy, 40th Edition: Bartleby; 2009.
2. Andersen HL, Gyrn J, Moller L, Christensen B, Zaric D. Continuous Saphenous Nerve Block as Supplement to Single-Dose Local Infiltration Analgesia for Postoperative Pain Management After Total Knee Arthroplasty. Reg Anesth Pain Med. 2013 Dec 7;38(2):106-11.
3. Borglum J, Johansen K, Christensen MD, Lenz K, Bendtsen TF, Tanggaard K, et al. Ultrasound-guided single-penetration dual-injection block for leg and foot surgery: a prospective, randomized, double-blind study. Regional anesthesia and pain medicine. 2014 Jan-Feb;39(1):18-25.
4. Horner G, Dellon AL. Innervation of the human knee joint and implications for surgery. Clin Orthop Relat Res. 1994 Apr(301):221-6.
5. Bouaziz H, Vial F, Jochum D, Macalou D, Heck M, Meuret P, et al. An evaluation of the cutaneous distribution after obturator nerve block. Anesthesia and analgesia. 2002 Feb;94(2):445-9.
6. Lund J, Jenstrup MT, Jaeger P, Sorensen AM, Dahl JB. Continuous adductor-canal-blockade for adjuvant post-operative analgesia after major knee surgery: preliminary results. Acta anaesthesiologica Scandinavica. 2011 Jan;55(1):14-9.
7. Andersen HL, Zaric D. Adductor canal block or midthigh saphenous nerve block: same same but different name! Regional anesthesia and pain medicine. 2014 May-Jun;39(3):256-7.
8. Bendtsen TF, Moriggl B, Chan V, Pedersen EM, Borglum J. Redefining the adductor canal block. Reg Anesth Pain Med. 2014 Sep-Oct;39(5):442-3.
9. Benzon HT, Sharma S, Calimaran A. Comparison of the different approaches to saphenous nerve block. Anesthesiology. 2005 Mar;102(3):633-8.
10. Jaeger P, Zaric D, Fomsgaard JS, Hilsted KL, Bjerregaard J, Gyrn J, et al. Adductor canal block versus femoral nerve block for analgesia after total knee arthroplasty: a randomized, double-blind study. Reg Anesth Pain Med. 2013 Nov-Dec;38(6):526-32.
11. Manickam B, Perlas A, Duggan E, Brull R, Chan VW, Ramlogan R. Feasibility and efficacy of ultrasound-guided block of the saphenous nerve in the adductor canal. Reg Anesth Pain Med. 2009 Nov-Dec;34(6):578-80.
12. Sirang H. [Saphenous nerve: origin, course and branches]. Anat Anz. 1972;130(1):158-69. PubMed PMID: 5026254. Epub 1972/01/01. Ursprung, Verlauf und Aste des N. saphenus.
13. Dixon WJ. Staircase bioassay: the up-and-down method. Neurosci Biobehav Rev. 1991 Spring;15(1):47-50.
14. Eichenberger U, Huber G, Stockli S, Marhofer P, Willimann P, Kettner SC, et al. Minimal local anesthetic volume for peripheral nerve block: a new ultrasound-guided, nerve dimension-based method. Regional anesthesia and pain medicine. 2009 May-Jun;34(3):242-6.
15. Latzke D, Marhofer P, Zeitlinger M, Machata A, Neumann F, Lackner E, et al. Minimal local anaesthetic volumes for sciatic nerve block: evaluation of ED 99 in volunteers. Br J Anaesth. 2010 Feb;104(2):239-44.
16. Jeong JS, Shim JC, Jeong MA, Lee BC, Sung IH. Minimum effective anaesthetic volume of 0.5% ropivacaine for ultrasound-guided popliteal sciatic nerve block in patients undergoing foot and ankle surgery: determination of ED50 and ED95. Anaesth Intensive Care. 2015 Jan;43(1):92-7.

17. Aszmann OC, Ebmer JM, Dellon AL. Cutaneous innervation of the medial ankle: an anatomic study of the saphenous, sural, and tibial nerves and their clinical significance. Foot Ankle Int. 1998 Nov;19(11):753-6.
18. Lopez AM, Sala-Blanch X, Magaldi M, Poggio D, Asuncion J, Franco CD. Ultrasound-guided ankle block for forefoot surgery: the contribution of the saphenous nerve. Regional anesthesia and pain medicine. 2012 Sep-Oct;37(5):554-7.
19. Fredrickson MJ, White R, Danesh-Clough TK. Low-volume ultrasound-guided nerve block provides inferior postoperative analgesia compared to a higher-volume landmark technique. Reg Anesth Pain Med. 2011 Jul-Aug;36(4):393-8.
20. Fredrickson MJ, Abeysekera A, White R. Randomized study of the effect of local anesthetic volume and concentration on the duration of peripheral nerve blockade. Reg Anesth Pain Med. 2012 Sep-Oct;37(5):495-501.
21. Andersen HL, Andersen SL, Tranum-Jensen J. The spread of injectate during saphenous nerve block at the adductor canal: a cadaver study. Acta Anaesthesiol Scand. 2015 Feb;59(2):238-45.
22. Chen J, Lesser JB, Hadzic A, Reiss W, Resta-Flarer F. Adductor canal block can result in motor block of the quadriceps muscle. Reg Anesth Pain Med. 2014 Mar-Apr;39(2):170-1.
23. Gautier PE, Lecoq JP, Vandepitte C, Harstein G, Brichant JF. Impairment of sciatic nerve function during adductor canal block. Reg Anesth Pain Med. 2015 Jan-Feb;40(1):85-9.
24. Lumsden DB, Kalenak A. The saphenous nerve: an external method for identifying its exit from the adductor canal. Orthop Rev. 1993 Apr;22(4):451-5.
25. Kardash K, Hickey D, Tessler MJ, Payne S, Zukor D, Velly AM. Obturator versus femoral nerve block for analgesia after total knee arthroplasty. Anesth Analg. 2007 Sep;105(3):853-8.
26. Macalou D, Trueck S, Meuret P, Heck M, Vial F, Ouologuem S, et al. Postoperative analgesia after total knee replacement: the effect of an obturator nerve block added to the femoral 3-in-1 nerve block. Anesth Analg. 2004 Jul;99(1):251-4.
27. Sato K, Sai S, Shirai N, Adachi T. Ultrasound guided obturator versus sciatic nerve block in addition to continuous femoral nerve block for analgesia after total knee arthroplasty. Jpn Clin Med. 2011;2:29-34. PubMed PMID: 23885188.

Chapter 7

The effectiveness of adductor canal block compared to femoral nerve block on readiness for discharge in patients undergoing outpatient anterior cruciate ligament surgery reconstruction: a multi-center randomized clinical trial

Based on: Werner ten Hoope, Manouk Admiraal, Jeroen Hermanides, Henning Hermanns, Markus W. Hollmann, Philipp Lirk MD, Gino M.M.W. Kerkhoffs, Jeroen Steens and Rienk van Beek
J Clin Med. 2023 Sep 17;12(18):6019

Abstract

This study evaluated the effect of adductor canal block (ACB) versus femoral nerve block (FNB) on readiness for discharge in patients undergoing outpatient anterior cruciate ligament (ACL) reconstruction. We hypothesized that ACB would provide sufficient pain relief while maintaining motor strength and safety, thus allowing for earlier discharge. Randomized, multi-center, superiority trial. From March 2014 to July 2017, patients undergoing ACL-reconstruction were enrolled. Primary outcome was difference in readiness for discharge, defined as Post-Anesthetic Discharge Scoring System score ≥ 9. Twenty-six patients were allocated to FNB and 27 to ACB. No difference in readiness for discharge was found (FNB median 1.8 (95% CI 1.0 to 3.5) vs. ACB 2.9 (1.5 to 4.7) hours, p = 0.3). Motor blocks and (near) falls were more frequently reported in patients with FNB vs. ACB (20 (76.9%) vs. 1 (3.7%), p < 0.001, and 7 (29.2%) vs. 1 (4.0%), p = 0.023. However, less opioids were consumed in the post-anesthesia care unit for FNB (median 3 [0, 21] vs. 15 [12, 42.5] oral morphine milligram equivalents, p = 0.004) for ACB. Between patients with FNB or ACB, no difference concerning readiness for discharge was found. Despite a slight reduction in opioid consumption immediately after surgery, FNB demonstrates a less favorable safety profile compared to ACB, with more motor blocks and (near) falls.

Introduction

The number of patients undergoing anterior cruciate ligament (ACL) reconstruction has risen over the past decade [1]. This procedure is typically performed in an outpatient setting, due to satisfactory functional and cost-effective outcomes [2]. For outpatient surgery, adequate pain management is crucial for timely discharge of patients. Regional anesthesia, particularly peripheral nerve blocks, have become increasingly important in optimizing postoperative pain management and expediting discharge.

Nonetheless, guidance in this matter continues to exhibit variability. The Society for Ambulatory Anesthesia advocates for the utilization of local installation analgesia as the primary approach, suggesting the adoption of adductor canal block or femoral nerve block only when local installation is not a feasible option [3]. In contrast, a recent published network analysis, suggests the consideration of a single injection femoral nerve block combined with a sciatic nerve block, or local infiltration analgesia [4].

While femoral nerve blocks (FNB) have been associated with less pain and reduced analgesic consumption [5], there is an increased risk of motor weakness of the quadriceps muscles, and accidental falls as compared to placebo [6]. Besides short-term effects, a decreased quadriceps strength has also been observed six weeks after ACL-reconstruction in patients who had received a FNB [7]. Adductor canal block (ACB) has been proposed as a safe alternative preserving motor function [8]. Several studies have reported similar pain relief and a reduction in loss of quadriceps motor strength in favor of ACB compared to FNB [8-12].However, other studies have reported more pain after ACB [13, 14], or similar quadriceps muscle function between both groups [15-17].

Most of these studies base their conclusions on quadriceps motor strength on very specific outcome measurements, such as surface electromyography, maximal voluntary isometric contractions, the time to up and go-, or the straight leg raise test. It is unclear how these parameters translate into clinical practice. In the context of outpatient surgery, readiness for discharge is an important general outcome, including various factors such as pain management, associated side effects, mobility, vital parameters, and presence of any surgical complications such as bleeding [18]. We compared the impact of ACB versus FNB on readiness for discharge in patients undergoing outpatient ACL reconstruction. We hypothesized that ACB would lead to

adequate pain control with preserved motor strength and a favorable safety profile thereby facilitating earlier readiness for discharge.

Materials and Methods

Study design

This multi-center, pragmatic, single-blinded, parallel-grouping superiority trial was conducted at a tertiary referral center (University Medical Center Amsterdam) and a secondary referral center (Dijklander hospital, Hoorn) in the Netherlands. The study was approved by the Dutch Medical Ethics Committee (#46184 on January 20, 2014) and adhered to the Declaration of Helsinki (Fortaleza, Brazil, 2013), as well as Good Clinical Practice guidelines and the General Data Protection Regulations. The study was registered before the inclusion of the first subject (ClinicalTrails.gov, NCT02071433, first posted: February 25, 2014).

Patients

Adult patients, American Society of Anesthesiologists (ASA) classification I-III scheduled for elective outpatient ACL reconstruction were assessed for eligibility. Exclusion criteria were BMI > 35, an infection at the site of injection, coagulopathies, allergy to local anesthetics, pre-existing diagnosed neuropathy of the operated leg, chronic opioid use, pregnancy or breastfeeding status, any history of significant cardiovascular disease (myocardial infarction, cerebrovascular accident, peripheral vascular disease), and inability to provide oral and written informed consent.

Randomization and masking

Patients were randomly allocated in a 1:1 ratio to either the FNB or ACB group employing an online computer-based system with block randomization (size of four). As per study's nature, neither the patient, nor the anesthesiologist performing the block were blinded. Nevertheless, the outcome observer, who conducted sensory block testing, was blinded, and data were collected on a separate case report form to maintain the research assistant's blindness to study group allocation.

Procedures

All patients were administered premedication with paracetamol (2 g p.o.) and diclofenac (100 mg p.o.), unless contraindicated. An intravenous cannula was inserted

in the forearm and infusion of Sterofundin® ISO or Ringer-lactate (B. Braun, Oss, Netherlands) was initiated at a rate of 3 ml/kg/hour. Both groups underwent ultrasound-guided nerve blockade prior to induction of general anesthesia. Nerve block was performed by an experienced anesthesiologist. The spread of local anesthetic was recorded employing ultrasound. All patients received general anesthesia, using a laryngeal mask airway and propofol target controlled infusion (effect site concentration between 2.5-3.5 µg/ml, approximately 6-9 mg/kg/hr) and remifentanil infusion (15-23 mcg/kg/hr). Subsequently, all patients underwent arthroscopic all-inside ACL reconstruction with a hamstring or quadriceps tendon autograft. A tourniquet was used in all patients. As for the consistency of performing the surgical procedure, two orthopedic surgeons, fellowship trained in traumatology and sports-medicine performed all procedures. During surgery, a morphine bolus of 0.1 mg/kg was administered, and all patients received dexamethasone in a dose of 4 mg intravenously. After surgery, patients were transferred to the post anesthesia care unit (PACU). Morphine (2 mg i.v.) was titrated until patient-reported pain levels were ≤ 4 on the numeric rating scale (NRS). Postoperative pain management consisted of paracetamol (1000 mg orally every 6 hour) and diclofenac (50 mg orally every 8 hours) for both groups. Upon discharge, patients were provided with prescriptions for paracetamol (1000 mg orally every 6 hour), diclofenac (50 mg orally every 8 hours), and oxycodone (5 mg orally every 6 hours), as required.

Femoral nerve block (control). The femoral nerve was identified lateral to the femoral artery and superficial to the iliopsoas muscle as described before[19]. The block was initiated with 15 ml levobupivacaine 0.5% (Astra Zeneca BV, The Hague, The Netherlands), after needle placement using an in-plane technique.

Adductor canal block (intervention). The transducer is transversely placed over the medial part of the mid-thigh and is sliding distally to identify the femoral artery and vein subsartorially. The border of the sartorius (anterolateral) and adductor longus muscle (posterior) can be identified. From this point proximally limits the apex of the femoral triangle. The injection target is distally from the femoral triangle in the beginning of the adductor canal. Using a 50-80 mm gauge echogenic needle 15 ml of levobupivacaine 0.5% (Astra Zeneca BV, The Hague, The Netherlands) was administered using an in-plane technique.

Outcome

The primary outcome was the difference between groups in readiness for discharge, as measured by the Post-Anesthetic Discharge Scoring System (PADSS). The PADSS is a valid and reliable scoring system that assesses various aspects of safe discharge, including vital signs, ambulation, nausea/vomiting, pain, bleeding and urinating (Online Supplementary Material A)[18]. Each item was graded from 0 (worst) to 2 (best) and then summed up. A score of ≥ 9 indicates that the patient is ready for discharge home.

Secondary outcomes included between group differences in short term outcome measures i.e. the incidence of motor block, as measured by the Medical Research Council (MRC) scale,[20] the incidence of (near) falls, time to mobilization, assessment of sensory block one hour after surgery, the Overall Benefit of Analgesia (OBAS)-score on postoperative day (POD) 0 and 1, total postoperative opioid consumption at the PACU and on POD 1 at home, and NRS scores during hospitalization. Furthermore, long-term outcomes at six and 12 weeks were (near) falls, neurology of the knee assessed by the orthopedic surgeon, the Medical Outcomes General Health Survey (SF-36), and Knee Injury and Osteoarthritis Outcome Score (KOOS).

Measurements

The PADSS score was evaluated every 30 minutes after surgery. The incidence of motor block was measured one hour after surgery by the Medical Research Council (MRC) scale, which ranges from zero to five, with scores below four indicating motor block[20]. The frequency of falls, including both actual falls and near-falls, that occurred during inpatient active mobilization was recorded prior to discharge. Furthermore, during a follow-up call on POD 1, the outcome assessor inquired specifically about the occurrence of any falls or near-falls within the past 24 hours. A near fall was defined as an occurrence of stumbling or experiencing a momentary loss of balance, which would lead to an actual fall if the necessary recovery mechanisms were not activated.[21] We defined a fall according to the definition of Lach et al.: "an unexpected loss of balance resulting in coming to rest on the floor, the ground, or an object below knee level [22]." Sensory block area was assessed one hour after surgery at both lateral and medial sides of the ankle and knee. Opioid consumption was measured in oral milligram morphine equivalents (MME) (appendix A). The OBAS-score is a validated patient-reported outcome measure of pain that besides pain intensity includes opioid side effects and patient satisfaction [23]. It ranges from 0 (best) to 28 (worst) and was measured on POD 0 and POD 1. The NRS score

was used to assess pain every 30 minutes during hospitalization until maximum 10 hours after surgery.

The SF-36 questionnaire was used to assess generic health status before surgery and at six and 12 weeks after surgery. It includes eight subscales: physical functioning, role limitation physical, role limitation emotional, energy/ fatigue, emotional well-being, social functioning, pain, and general health [24]. Each subscale was individually calculated and transformed by subtracting the minimum score from the raw score, and dividing this by the subscale range, multiplied by 100. This calculation results in a score between 0 (extreme problems) and 100 (no problems) [25].

The KOOS-questionnaire, another reliable and valid outcome measure that assesses patient relevant outcomes after knee injury was taken before surgery, six and 12 weeks after surgery. Five subscales were evaluated including pain, symptoms, activities of daily living, sport and recreation function and knee-related quality of life [26]. Each subscale was individually calculated and transformed by dividing the raw score by the maximum score and multiplied by 100. This number was subtracted from 100 what resulted in a score between 0 (extreme knee problems) and 100 (no knee problems).

Statistical analysis

Sample size.
To detect a reduction in readiness for discharge of at least one hour (using 1.2 hours in our calculation), estimating a standard deviation of 1.5 hours with a power of 80% and a 2-sided alpha of 0.05, we needed 26 patients per group.

Continuous data were described as median and interquartile ranges or mean with standard deviations depending on the distribution of the data, which was assessed by visual inspection. Categorical data were described with number and percentages. According to the intention to treat principle, among all randomized patients, Kaplan-Meier survival curves were used to analyze the time to readiness for discharge. A log-rank test was performed to test for differences between groups[27]. To assess differences between groups in the incidence of motor blocks, sensory blocks or (near) falls, we used the Fisher's exact test. Differences in opioid consumption and OBAS score were analyzed using the Wilcoxon Rank test. To analyze NRS scores over time, we used a mixed effects model. First, a baseline linear model was fitted with NRS as the dependent variable and time and randomization group as the fixed effect

with a random intercept and slope. Thereafter, an interaction term (time*randomization) was added to the model. Pairwise deletion was used to analyze patient-reported outcome measures (PROMs) to maximize all data available. The SF-36 and KOOS scores were analyzed using a Student's T test. A two-sided p-value < .05 was considered statistically significant. All statistical analyses were performed using R studio (Affero General Public License V3).

Table 1. Patient baseline characteristics

	FNB (n = 26)	ACB (n = 27)
Female sex	9 (34.6%)	10 (37.0%)
Age, yearsa	27.0 [21.3, 40]	25.0 [21, 36]
BMI, kg.m-1a	25.2 [22.5, 27.0]	23.8 [21.7, 26,7]
Smoking	5 (19.2%)	13 (48.1%)
Pain intensity before surgery		
NRS score at restb	0 [0, 0]	0 [0, 0]
NRS score on movementb	1 [0, 4]	0 [0, 3]
Surgical details		
Length of surgery, in minutesa	56.5 [47.5, 65.0]	59.0 [53.5, 72.5]
Choice of graft		
Hamstring tendon autograft	24 (92.3%)	23 (85.2%)
Quadriceps tendon autograft	0	2 (7.4%)
Unknown	2 (7.7%)	2 (7.4%)

Variable distributions were reported as number and percentage unless specified otherwise.
a = Median [IQR]
b = Mean (SD)
Abbreviations: FNB = femoral nerve block, ACB = adductor canal block, BMI = body mass index, NRS = numeric rating scale

Results

From March 2014 to July 2017, 61 patients were screened for participation in this trial. Fifty-three patients provided written informed consent. Of these, 26 patients were randomly allocated to receive a FNB, and 27 to receive an ACB. The time to PADSS score indicating readiness for discharge was available for 52 (98.1%) patients, with 43 (81.1%) patients available at six weeks follow-up and 40 (75.5%) completing the 12-week follow-up (Figure 1).

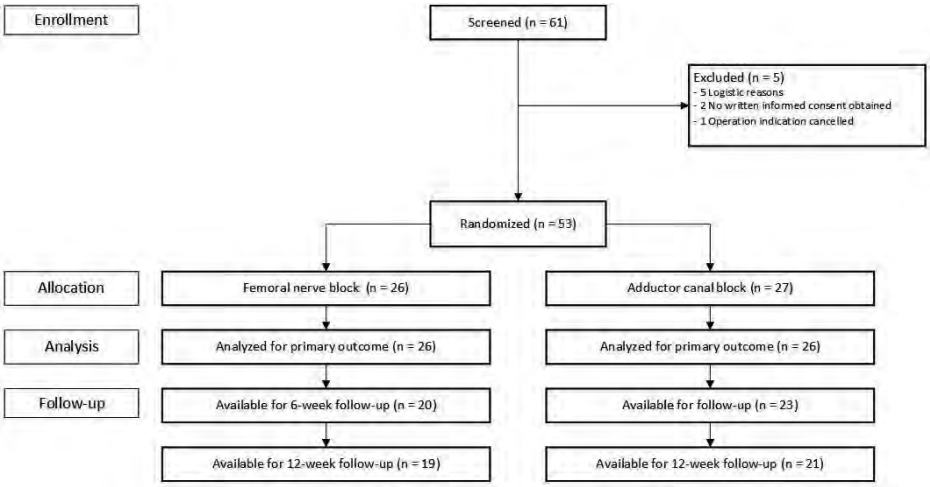

Figure 1. Flow diagram. A minority of patients was female (35.8%) and the median age of patients was 27 [IQR 21, 37]. The median NRS score before surgery was 0 [0, 0] in rest and 0.5 [0, 4] during movement. Patient characteristics were shown in groups, Table 1.

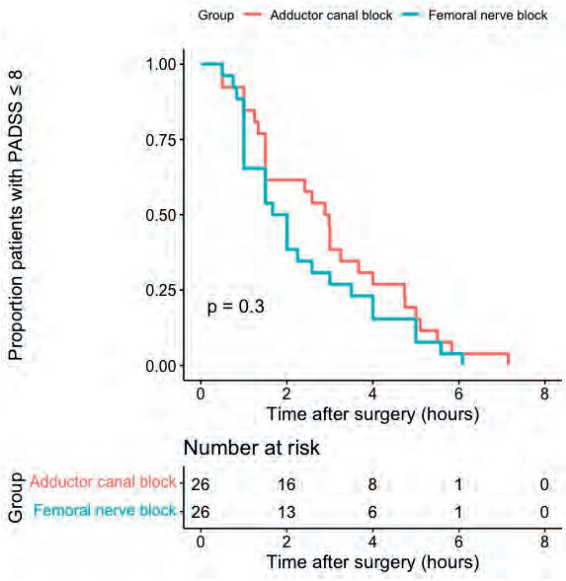

Figure 2. Between group differences in readiness to home discharge estimated by Kaplan-Meier method. Kaplan-Meier curves displaying the estimated proportion of patients ready for discharge (i.e. PADSS ≥ 9) for patients allocated to the adduct or canal block or femoral nerve block. Each vertical step in the curve indicates a patient ready for discharge. The log-rank test indicates no difference between the survival curves. Abbreviations: PADSS = Post Anesthetic Discharge Scoring System

Primary outcome

No between group difference in readiness for discharge was found (FNB median 1.8 (95% CI 1.0 to 3.5) hours vs. ACB 2.9 (1.5 to 4.7) hours, p = 0.3, (Figure 2).

Secondary outcomes

In 20 (76.9%) patients with FNB vs. 1 (3.7%) patient with ACB, a motor block (MRC < 4) was recorded, (p < 0.001, Table 2). A (near) fall was reported in seven (29.2%) patients with FNB compared to 1 (4%) patient with ACB, (p = 0.023). The majority of patients with FNB (84%), compared to all patients with ACB (100%) were able to mobilize within 24 hours, (p = 0.112). Time to first mobilization was similar between groups (p = 0.1). Distribution of sensory block was similar between groups (Online Supplementary Material B).

Patients with FNB consumed less opioids in the PACU compared to patients allocated to ACB (median 3 [0, 21] vs. 15 [12, 42.5] oral MME, p = 0.004). However, on postoperative day 1, opioid consumption was similar between groups (median 2.5 [2, 4.8] vs. 2 [1, 4] oral MME, p = 0.527. The OBAS score was comparable between groups on POD 0 and POD 1. No difference between groups was found in postoperative NRS scores over time (p = 0.124, Online Supplementary Material C). No differences were found at six, and 12- week follow-up regarding (near) falls, and neurology of the knee assessed by the orthopedic surgeon. Long-term patient-reported outcome measurements did not differ between groups, (Table 3).

Table 2 Secondary outcomes

	Available for	FNB (n = 26)	ACB (n = 27)	p-value
Incidence of a motor block, 1 hour after surgerya	48 (90.6%)	20 (76.9%)	1 (3.7%)	< 0.001***
The incidence of (near) falls first 24 hour	49 (92.5%)	7 (29.2%)	1 (4%)	0.023*
Mobilization				
Able to walk first 24 hour	49 (92.5%)	22 (84.6%)	23 (100%)	0.112
Time to first mobilization, hours	36 (67.9%)	19.0 (7.8, 23.1)	19.0 (17.4, 26.66)	0.100
Opioid consumption				
Total on PACU, in oral MMEc	53 (100%)	3.0 [0, 21.]	15.0 [12.0, 42.5]	0.004**
Total POD 1, in oral MMEcd	51 (96.2%)	0 [0, 7.5]	0 [0, 7.5]	0.527
OBASc				
Day of surgery	52 (98.1%)	3.0 [1.0, 6.5]	4.0 [2.0, 5.8]	0.402
Postoperative day 1	53 (100%)	2.5 [2.0, 4.8]	2.0 [1.0, 4.0]	0.220
Week 6				
(Near) falls	40 (75.5%)	2 (10.5%)	-	
Global intact neurology kneee	43 (81.1%)	11 (55%)	11 (47.8%)	0.763
Sensations of neuropraxiae	40 (75.5%)	10 (50%)	13 (65%)	0.197
Week 12				
(Near) falls	38 (71.7%)	1 (5.3%)	-	
Global intact neurology kneee	40 (75.5%)	10 (52.6%)	6 (28.6%)	0.523
Sensations of neuropraxiae	39 (74.6%)	8 (42.1%)	11 (55%)	0.527

Variable distributions were reported as number and percentage unless specified otherwise, Fisher exact test

a: The incidence of a motor block as defined as Medical Research Council scale score < 5.

b: Median (95% confidence limit), logrank test

c: Median [IQR], Wilcoxon Rank Sum

d: Measured until 16:00 on POD 1

e: Assessed by the orthopedic surgeon

Abbreviations: FNB = femoral nerve block, ACB = adductor canal block, PACU = post anaesthesia care unit, MME = milligram morphine equivalent, OBAS = Overall benefit of Analgesic score

Table 3. Patient-reported outcome measurements

	Available for	FNB (n = 26)	ACB (n = 27)	p-value
Baseline				
SF-36				
Physical functioning		73.4 (17.1)	76.6 (20.6)	
Role limitations due to physical health		44 (39.7)	68 (37.2)	
Role limitations due to emotional problems		78.7 (34.5)	86.7 (27.2)	
Energy, fatigue		70.4 (16.1)	78 (13.8)	
Emotional well-being		77.6 (18.3)	83.7 (13.5)	
Social functioning		72.5 (23.1)	85.0 (18.8)	
Pain		66.4 (20.5)	76.1 (22.8)	
General Health		81.5 (17.0)	84 (15.3)	
KOOS				
Symptoms		64.0 (19.7)	75.4 (17.0)	
Pain		72.2 (20.7)	86.1 (20.9)	
Function in daily life		79.6 (18.0)	87.8 (13.4)	
Function in spare time and sport activities		41.5 (29.1)	45 (28.7)	
Knee-associated quality of life		39.8 (21.3)	53.9 (23.4)	
Week 6				
SF-36				
Physical functioning	41 (77.4%)	54.5 (22.5)	66.8 (14.4)	0.049*
Role limitations due to physical health	40 (75.5%)	12.5 (15.5)	19.3 (31.7)	0.382
Role limitations due to emotional problems	41 (77.4%)	84.2 (34.0)	72.7 (42.0)	0.339
Energy, fatigue	41 (77.4%)	70.8 (14.9)	67.3 (16.2)	0.475
Emotional well-being	39 (73.6%)	84.9 (10.8)	77.3 (14.7)	0.072
Social functioning	41 (77.4%)	69.7 (22.6)	65.9 (21.2)	0.581
Pain	39 (73.6%)	58.9 (30.5)	67.4 (25.5)	0.358

Table 3. Patient-reported outcome measurements *(continued)*

	Available for	FNB (n = 26)	ACB (n = 27)	p-value
General Health	41 (77.4%)	79.2 (13.9)	80.5 (14.2)	0.779
KOOS				
Symptoms	41 (77.4%)	59.6 (20.3)	69.2 (14.5)	0.092
Pain	41 (77.4%)	74.3 (22.0)	78.2 (18)	0.542
Function in daily life	38 (71.7%)	77.9 (19.9)	73.9 (22.9)	0.568
Function in spare time and sport activities	34 (64.2%)	33.1 (30.9)	34.4 (17.1)	0.881
Knee-associated quality of life	35 (66.0%)	47.9 (20.0)	59.9 (26.9)	0.146
Week 12				
SF-36				
Physical functioning	36 (67.9%)	77.6 (18.7)	78.2 (17.9)	0.921
Role limitations due to physical health	37 (69.8%)	63.2 (45.2)	48.6 (41.5)	0.315
Role limitations due to emotional problems	37 (69.8%)	94.7 (22.9)	87.0 (32.6)	0.415
Energy, fatigue	35 (66.0%)	76.7 (16.2)	68.8 (14.0)	0.134
Emotional well-being	34 (64.2%)	86.6 (7.7)	83.8 (15.5)	0.509
Social functioning	36 (67.9%)	88.8 (16.1)	87.5 (16.5)	0.811
Pain	37 (69.8%)	78.6 (20.5)	77.9 (15.2)	0.915
General Health	34 (64.2%)	78.6 (12.9)	79.1 (16.0)	0.929
KOOS				
Symptoms	36 (67.9%)	75.2 (17.5)	73.8 (11.9)	0.783
Pain	39 (74.6%)	85.0 (19.7)	87.0 (10.6)	0.695
Function in daily life	38 (71.7%)	87.2 (20.0)	86.1 (13.4)	0.835
Function in spare time and sport activities	37 (69.8%)	58.7 (27.8)	55.8 (22.3)	0.732
Knee-associated quality of life	38 (71.7%)	62.5 (19.3)	64.2 (22.2)	0.800

Variable distributions were reported as mean (SD), student's t-test

Abbreviations: FNB = femoral nerve block, ACB = adductor canal block, SF = Short Form Health Survey, KOOS = Knee Injury and Osteoarthritis Outcome Score

Discussion

In this RCT evaluating the effectiveness of ACB as compared to FNB in patients undergoing ACL-reconstruction, we detected no significant difference in readiness for discharge between ACB over FNB. Our findings did suggest that FNB may provide superior pain relief on the day of surgery. Conversely, motor block was more prevalent in patients receiving FNB, which was accompanied by an increased risk of potential falls. No differences in long-term outcomes were observed.

Varying outcomes have been reported on readiness for discharge between ACB and FNB in patients undergoing ACL-reconstruction. In agreement with our study, Seanglueulur et al. reported comparable ability to discharge between groups [14], whereas Abdallah et al. found a shorter time to discharge by 18 minutes in patients with ADC compared to FNB [8]. The authors attribute this finding to the earlier achievement of ambulation criteria, as assessed by the Aldrete score. Although Abdallah's results show a statistical difference, one may wonder if this difference is also clinically relevant.

We observed a higher incidence of both motor blocks and potential falls in patients receiving FNB compared to ACB. Literature presents varying finding regarding the impact of the nerve block on quadriceps strength. Several studies have reported reduced quadriceps strength, or a higher risk of falls in patients with FNB compared to ACB [8-12]. However, three RCT involving 197 patients did not find any statistically significant differences in quadriceps strength, or recovery of knee function [15-17]. Studies investigating functional recovery, show substantial heterogeneity in the utilized outcome parameters and the timing of measurement. This heterogeneity complicates direct comparison between studies. Nevertheless, it appears evident that ACD provides superior motor sparing effects across various outcomes compared to FNB.

In our study, patients with FNB consumed less opioids during their PACU stay compared to patients with ACB. This contrasts from the findings of Sullivan, et al., who reported similar opioid consumption during PACU phase in 86 patients undergoing ACL-reconstruction allocated to FNB or ACB [10]. Similar opioid administration during the PACU period aligns with the conclusion drawn in the Cochrane review conducted by Schnabel et. al., which involved a meta-analysis of five trials comprising 305 patients undergoing knee surgery [28]. It is important to note that in our study, the decrease in opioid usage in the FNB-group did not persists beyond PACU stay. Furthermore, the increase in morphine consumption among ACB patients did

not result in a deterioration in OBAS score on the day of surgery. Both of these findings necessitate a critical evaluation of the clinical relevance of this slight decrease in morphine consumption in patients with FNB within the context of our study.

We were surprised by the relatively frequent occurrence of sensory block in the lateral ankle. Since we assessed sensory perception immediately after surgery in the PACU, our hypothesis was that the tourniquet application may have induced altered sensory experiences in the patients.

This study has some limitations. Patients were recruited at a slower than anticipated rate over a period of three years, primarily due to logistical challenges. Furthermore, we encountered a relatively high rate of missing data (70-75% available) for PROMs at six-, and 12 week follow up. We did not impute missing data. We acknowledge that this lack of imputation will decrease statistical power, however, PROMS are part of our secondary outcome and should be interpreted as exploratory in nature. Another potential limitation is that both the treating physicians and patients were not blinded to group allocation, which could introduce bias. However, we took measures to mitigate bias by ensuring that the outcome assessor remained blinded throughout the study. Finally, we acknowledge the time gap between the surgical procedures and the dissemination of findings. It is important to realize that medical knowledge and surgical techniques could have changed during this period. Accordingly, when interpreting the findings within their contextual framework, this publication retains the capacity to furnish valuable insights.

Strengths of this study include the multicenter, randomized trial design. Instead of focusing on a specific traditional outcome such as pain score, we chose for comprehensive outcomes such as readiness for discharge and PROMs. Additionally, we have studied long-term outcomes, an aspect that is tends to be insufficiently explored in these types of studies

To summarize: ACB did not shorten time to readiness for discharge as compared to FNB in patients undergoing ACL-reconstruction. While both techniques are comparable in terms of discharge readiness and pain management, FNB exhibits a less favorable safety profile characterized by increased motor blocks and (near) falls when contrasted with ACB.

References

1. Sanders, T.L., et al., *Incidence of Anterior Cruciate Ligament Tears and Reconstruction: A 21-Year Population-Based Study.* Am J Sports Med, 2016. **44**(6): p. 1502-7.
2. Ferrari, D., et al., *Outpatient versus inpatient anterior cruciate ligament reconstruction: A systematic review with meta-analysis.* The Knee, 2017. **24**(2): p. 197-206.
3. Abdallah, F.W., R. Brull, and G.P. Joshi, *Pain Management for Ambulatory Arthroscopic Anterior Cruciate Ligament Reconstruction: Evidence-Based Recommendations From the Society for Ambulatory Anesthesia.* Anesth Analg, 2019. **128**(4): p. 631-640.
4. Hussain, N., et al., *Network meta-analysis of the analgesic effectiveness of regional anaesthesia techniques for anterior cruciate ligament reconstruction.* Anaesthesia, 2023. **78**(2): p. 207-224.
5. Faunø, P., et al., *Analgesic effect of hamstring block after anterior cruciate ligament reconstruction compared with placebo: a prospective randomized trial.* Arthroscopy, 2015. **31**(1): p. 63-8.
6. Guirro, U.B., E.M. Tambara, and F.R. Munhoz, *Femoral nerve block: Assessment of postoperative analgesia in arthroscopic anterior cruciate ligament reconstruction.* Braz J Anesthesiol, 2013. **63**(6): p. 483-91.
7. Magnussen, R.A., et al., *Femoral Nerve Block after Anterior Cruciate Ligament Reconstruction.* J Knee Surg, 2017. **30**(4): p. 323-328.
8. Abdallah, F.W., et al., *Adductor Canal Block Provides Noninferior Analgesia and Superior Quadriceps Strength Compared with Femoral Nerve Block in Anterior Cruciate Ligament Reconstruction.* Anesthesiology, 2016. **124**(5): p. 1053-64.
9. Ghodki, P.S., P.S. Shalu, and S.P. Sardesai, *Ultrasound-guided adductor canal block versus femoral nerve block for arthroscopic anterior cruciate ligament repair under general anesthesia.* J Anaesthesiol Clin Pharmacol, 2018. **34**(2): p. 242-246.
10. Sullivan, J.P., *In ACL Reconstruction with Patellar Tendon Autograft, Adductor Canal Nerve Blockade Reduced Quadriceps Function Deficits Compared with Femoral Nerve Blockade, but Did Not Differ for Postoperative Pain.* J Bone Joint Surg Am, 2019. **101**(22): p. 2061.
11. Faiaz, A. and S. Kamath, *Randomised Controlled Trial between Ultrasound Guided Femoral Nerve Block and Adductor Canal Block for Postoperative Pain and Functional Outcome in Anterior Cruciate Ligament Reconstruction.* Journal of Clinical and Diagnostic Research, 2019. **13**: p. 11-14.
12. Bailey, L., et al., *Adductor Canal Nerve Versus Femoral Nerve Blockade for Pain Control and Quadriceps Function Following Anterior Cruciate Ligament Reconstruction With Patellar Tendon Autograft: A Prospective Randomized Trial.* Arthroscopy, 2019. **35**(3): p. 921-929.
13. El Ahl, M.S., *Femoral nerve block versus adductor canal block for postoperative pain control after anterior cruciate ligament reconstruction: A randomized controlled double blind study.* Saudi J Anaesth, 2015. **9**(3): p. 279-82.
14. Seangleulur A, M.S., Chernchujit B, Worathongchai S, Sorin T. , *Comparison of Post-Operative Analgesia between Adductor Canal Block and Femoral Nerve Block after Arthroscopic Anterior Cruciate Ligament Reconstruction: A Randomized Controlled Trial.* J Med Assoc Thai 2019;102:335-42.

15. Lynch, J.R., et al., *Adductor Canal Block Versus Femoral Nerve Block for Pain Control After Anterior Cruciate Ligament Reconstruction: A Prospective Randomized Trial.* Am J Sports Med, 2019. **47**(2): p. 355-363.
16. Ogura, T., et al., *Femoral nerve versus adductor canal block for early postoperative pain control and knee function after anterior cruciate ligament reconstruction with hamstring autografts: a prospective single-blind randomised controlled trial.* Arch Orthop Trauma Surg, 2021. **141**(11): p. 1927-1934.
17. Runner, R.P., et al., *Quadriceps Strength Deficits After a Femoral Nerve Block Versus Adductor Canal Block for Anterior Cruciate Ligament Reconstruction: A Prospective, Single-Blinded, Randomized Trial.* Orthop J Sports Med, 2018. **6**(9): p. 2325967118797990.
18. Chung, F., V.W. Chan, and D. Ong, *A post-anesthetic discharge scoring system for home readiness after ambulatory surgery.* J Clin Anesth, 1995. **7**(6): p. 500-6.
19. Marhofer, P., et al., *Ultrasonographic guidance improves sensory block and onset time of three-in-one blocks.* Anesth Analg, 1997. **85**(4): p. 854-7.
20. Council., M.R., *Aids to examination of the peripheral nervous system.* . 1976: Memorandum no. 45. London: Her Majesty's Stationary Office;.
21. Maidan, I., et al., *Introducing a new definition of a near fall: intra-rater and inter-rater reliability.* Gait Posture, 2014. **39**(1): p. 645-7.
22. Lach, H.W., et al., *Falls in the elderly: reliability of a classification system.* J Am Geriatr Soc, 1991. **39**(2): p. 197-202.
23. Lehmann, N., et al., *Development and longitudinal validation of the overall benefit of analgesia score: a simple multi-dimensional quality assessment instrument.* Br J Anaesth, 2010. **105**(4): p. 511-8.
24. Busija, L., et al., *Magnitude and meaningfulness of change in SF-36 scores in four types of orthopedic surgery.* Health Qual Life Outcomes, 2008. **6**: p. 55.
25. van der Zee KI, S.R., *Het meten van de algemene gezondheidstoestand met de RAND-36, een handleiding. Groningen: Rijksuniversiteit Groningen, Noordelijk Centrum voor Gezondheidsvraagstukken; 1992*.
26. Roos, E.M., et al., *Knee Injury and Osteoarthritis Outcome Score (KOOS)--development of a self-administered outcome measure.* J Orthop Sports Phys Ther, 1998. **28**(2): p. 88-96.
27. Schober, P. and T.R. Vetter, *Survival Analysis and Interpretation of Time-to-Event Data: The Tortoise and the Hare.* Anesth Analg, 2018. **127**(3): p. 792-798.
28. Schnabel, A., et al., *Adductor canal blocks for postoperative pain treatment in adults undergoing knee surgery.* Cochrane Database Syst Rev, 2019. **2019**(10).

Supplementary material A

Post Anesthetic Discharge Scoring System [18]

Vital Signs
2 = within 20% of preoperative value
1 = 20%-40% of preoperative value
0 = > 40% preoperative value

Activity and mental status
2 = Oriented × 3 AND has a steady gait
1 = Oriented × 3 OR has a steady gait
0 = Neither

Pain, nausea and/or vomiting
2 = Minimal
1 = Moderate, having required treatment
0 = Severe, requiring treatment

Surgical bleeding
2 = Minimal
1 = Moderate
0 = Severe

Intake and output
2 = has had PO fluids AND voided
1 = has had PO fluids OR voided
0 = Neither

*Total PADS score is 10; Score ≥ 9 considered fit for home discharge;
**PO = oral administration.

Supplementary material B

Assessment sensory block

	FNB(n=26)	ACB(n=27
Medial knee		
No sensory block	6 (23.1%)	8 (29.6%)
Sensory block	19 (73.1%)	18 (66.7%)
Unknown	1 (3.8%)	1 (3.7%)
Lateral knee		
No sensory block	16 (61.5%)	12 (44.4%)
Sensory block	9 (34.6%)	14 (51.9%)
Unknown	1 (3.8%)	1 (3.7%)
Medial ankle		
No sensory block	8 (30.8%)	7 (25.9%)
Sensory block	17 (65.4%)	20 (74.1%)
Unknown	1 (3.8%)	-
Lateral ankle		
No sensory block	10 (38.5%)	16 (59.3%)
Sensory block	6 (23.1%)	6 (22.2%)
Unknown	10 (38.5%)	5 (18.5%)

Variable distributions were reported as number and percentage unless specified otherwise. Abbreviations: FNB = femoral nerve block, ACB = adductor canal block.

Supplementary material C

postoperative NRS scores over time

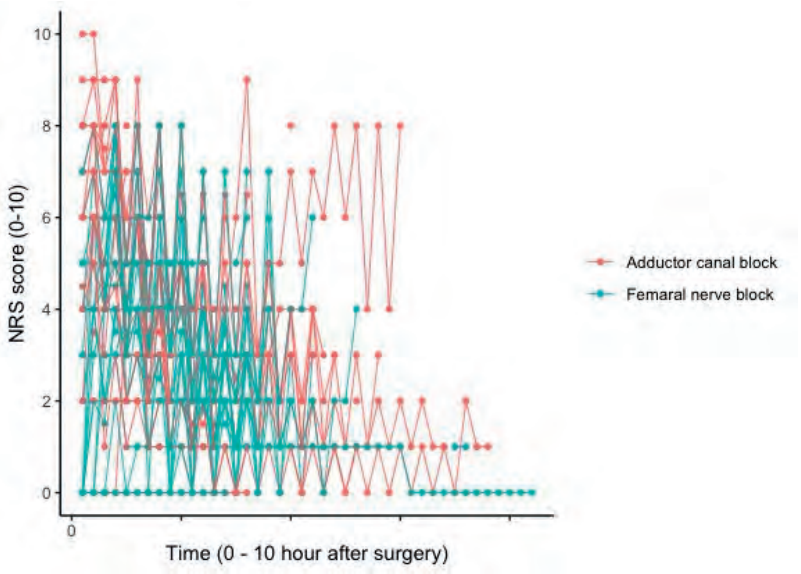

Section 4

Research prospectives: Role for stem cells in regional anesthesia

Chapter 8

Investigating peripheral regional anaesthesia using induced pluripotent stem cell technology: exploring novel terrain

Based on:Pascal S.H. Smulders, Mark L. van Zuylen, Jeroen Hermanides, Markus W. Hollmann, Nina C. Weber & Werner ten Hoope* (*These authors contributed equally) Anesth Analg. 2022 Sep 1;135(3):659-662*

In vitro research on peripheral regional anesthesia (RA) has historically been performed using animal cell types due to the challenges of obtaining human adult or fetal dorsal root ganglion (DRG) neurons. However, translation of results from animal studies is often problematic because of genetic differences between animals and humans. The discovery of human induced pluripotent stem cells (iPSC) now offers an opportunity to circumvent the obstacles of acquiring human neuronal tissue, as it allows conventional human cells to be reprogrammed to nociceptive DRG neurons. Here, we explain iPSC technology and focus on how it could facilitate drug research and personalized medicine for RA.

Progress in Induced Pluripotent Stem Cell Technology

The narrative of iPSC technology starts with landmark experiments in which tadpoles were generated from terminally differentiated intestinal epithelial nuclei. These studies demonstrated that specialized cells retain a full retinue of genes, and inspired the concept of reprogramming.[1] The development of pre-implantation embryo-derived cell lines, now known as embryonic stem cells (ESC), then led to cell fusion experiments that suggested the existence of transcription factor genes involved in reprogramming.[2] These reports ultimately culminated in the seminal discovery of iPSCs.[3] This man-made stem cell class possesses similar differentiation potential as ESCs, but is not burdened by the ethical and regulatory issues that makes handling of ESCs impractical.[4]

First described in 2006, iPSC production involves the forced introduction of transcription factors into a somatic host cell.[3] The somatic cell subsequently regresses to a pluripotent state, reacquiring the ability to differentiate into any cell type of the body (pluripotency) and to divide indefinitely, forming unaltered daughter cells (self-renewal) (Figure 1). The obtained iPSCs can then be differentiated into the cell type of interest using growth factors and small molecules. Neural cell types can thus be generated from easily obtainable cells, such as skin fibroblasts and umbilical cord blood cells, and expanded unlimitedly, placing previously unattainable human cell models within reach. Recent breakthroughs in stem cell biology further improved the quality of iPSC technology and paved the way for its utilization in disease modelling and drug discovery in non-specialized (anesthesiology) laboratories.[4,5]

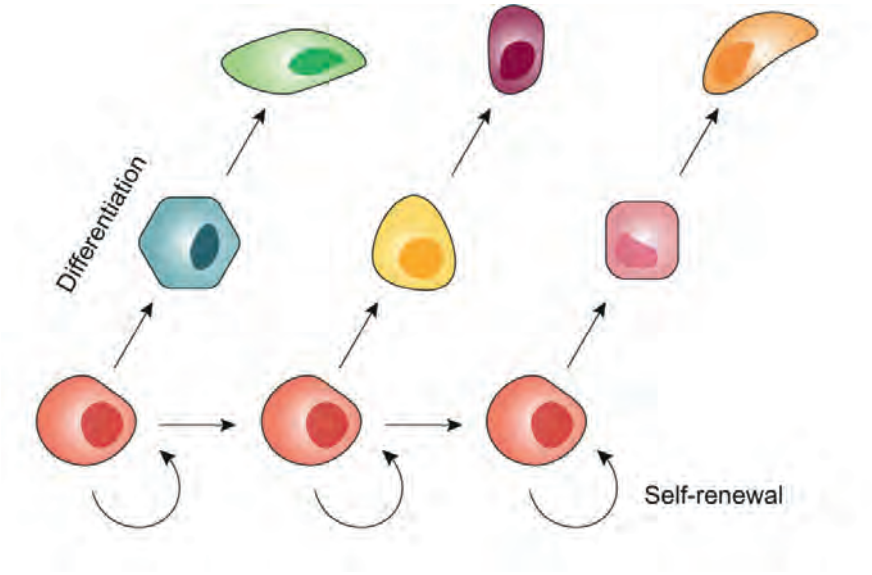

Figure 1. iPSCs are capable of differentiation into cell types from all three germ layers of the human body (pluripotency; depicted on the vertical axis by the different cellular shapes and colors), and indefinite division that creates unaltered daughter cells (self-renewal; illustrated on the horizontal axis by a circular arrow, for the first daughter cell, and the formation of an identical second daughter cell). Adapted from Kolios et al.[18]
iPSC: Induced pluripotent stem cell.

Differentiating Dorsal Root Ganglion Neurons from Induced Pluripotent Stem Cells

Neural induction is the first step in the development of the nervous system. Blockade of Smad phosphorylation (amongst other pathways) prevents the differentiation of ectodermal cells towards an epidermal fate, resulting in the columnar neuroepithelial cells that form the neural plate. Subsequent elongation, folding and closing of the neural plate forms the neural tube during neurulation. The neural tube then evolves into the brain and spinal cord, while the peripheral nervous system differentiates (except for neurons innervating the face) from neural crest cells (NCC) that delaminate from the dorsal section of the rudimentary neural tube. Next, part of the truncal NCCs aggregate into segmental clusters lining the spinal cord which, following terminal differentiation, form the DRG. Interestingly, the most common approach to nociceptive DRG neuron conversion leads iPSCs through stages strongly resembling the aforementioned embryological steps.

The substantial contributions made by Chambers *et al.* form the foundation of lineage-based DRG nociceptor reprogramming (Figure 2).[6,7] The process starts with the induction of pluripotency in the host cell through transient ectopic expression of reprogramming factors, which is continued until endogenous genes maintain pluripotency. Neural differentiation is later started by application of drugs inhibiting Smad signaling, resulting in colonies of columnar epithelial cells (or neural rosettes) that resemble the developing neural tube.[7,8] Subsequent parallel treatment with three small molecule inhibitors then settles differentiation from a NCC subphase to a DRG nociceptor fate.[6] The obtained early nociceptors are then matured using a cocktail of neurotrophins to acquire functionally mature nociceptive neurons that secrete the neurotransmitter substance P, which (in vivo) transmits information to second-order neurons.[6] Similar to in vivo DRG neurons, iPSC-derived nociceptors are electrically active and coalesce into ganglion-like structures.

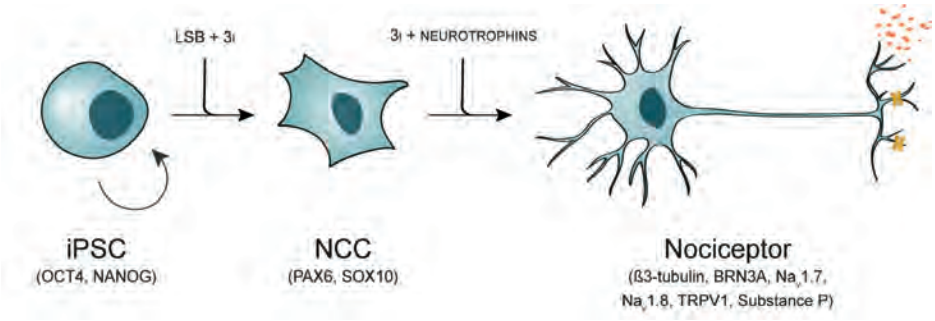

Figure 2. Lineage-based reprogramming follows steps comparable to embryological development. Conversion starts with an iPSC that is pluripotent and self-renewable in nature. Subsequent Smad-inhibition (depicted using the abbreviation 'LSB' for the compounds LDN-193189 and SB431542) and application of three small molecule inhibitors (3i) directs differentiation towards a NCC identity. Parallel treatment with a mixture of 3i and neurotrophins settles the DRG nociceptor fate. Correct differentiation can be determined using standard laboratory techniques, as differentiating cells possess markers corresponding to their (current) state. Mature nociceptive neurons, for example, will express neural cytoskeleton marker β3-tubulin, voltage-gated sodium channels (e.g. $Na_v1.7$) and transient receptor potential channels (e.g. TRPV1), and excrete Substance P, as shown here.
iPSC: Induced pluripotent stem cell, LSB: LDN-193189 and SB431542, 3i: three small molecule inhibitors, NCC: neural crest cell, DRG: dorsal root ganglion, $Na_v1.7/8$: voltage-gated sodium channel isoform 1.7/8, TRPV1: transient receptor potential vanilloid 1.

Central to successful iPSC modelling is correct differentiation and stepwise quality control. DRG nociceptors lose and gain expression of genes corresponding to the different developmental stages during differentiation. For example, iPSCs will lose expression of pluripotency markers (e.g. OCT4 and NANOG), while transiently expressing neuroectoderm PAX6 and NCC marker SOX10. Cells then gain a nociceptive neuron profile co-expressing neural β3-tubulin, sensory neuron-specific BRN3A and nociceptive markers, such as voltage-gated sodium channels (Na_v) and transient receptor potential channels. Transition through these formative steps can be confirmed with immunofluorescence imaging applications that detect the aforementioned antigens using fluorescent-labeled antibodies. In addition, optical microscopy can visualize the morphological changes that occur as the initially rounded iPSCs elongate, grow neurites and group into ganglion-like clusters during nociceptor conversion.

Electrophysiological assays are considered the gold standard for functional analysis of iPSC-derived nociceptors. Microelectrode array (MEA) enables extracellular recording of action potentials by coupling neuronal activity to electronic circuitry in a non-invasive manner. Therefore, MEA can affirm nociceptive neuron identity by detailing electrical activity of neuronal networks cultured over electrodes embedded within the culture plate. For example, treatment with capsaicin, an agonist of transient receptor potential vanilloid 1 (TRPV1), would trigger noxious signaling in the form of ionic current changes measurable as action potentials, while application of tetrodotoxin (TTX) could attest to the presence of TTX-reactive Na_vs. Whereas MEA enables high-throughput screening by extracellular measurements, patch clamping provides detailed intracellular recordings of an individual cell. In patch clamping, a high resistance seal is formed between the cell membrane and a micropipette, giving the experimenter access to the interior of the cell. Patch clamping therefore allows for mechanistic studies that evaluate ionic currents and membrane channel properties, thus complementing MEA.

Opportunities for Peripheral Regional Anesthesia

RA has evolved significantly over the last decades and has become an important component of balanced anesthesia.[9] Yet, the field could benefit from a research model that better reflects the human neurobiological intricacies of pain signaling than the currently available animal models.

Pain-related research results obtained from animal studies are often difficult to translate to the human situation due to heritable neural interspecies differences.

For example, the expression patterns and electrophysiological properties of TRPV1 and Na_v 1.7 and 1.8, canonical markers of pain signaling, differ significantly between humans and rodents.[10,11] Genetic differences could thus help explain the faltering discovery of novel anesthetic medication and nerve block strategies, supporting the need of a human cell model of RA. As described above, the progress in iPSC technology now allows reliable differentiation of human DRG neurons for use in preclinical research. Human iPSC-derived RA models could thus accommodate progressive drug testing and personalized medicine.

iPSC technology holds great potential for pharmaceutical research as it provides a non-invasive method of obtaining scalable quantities of (difficult to access) human cells that can be used for both functional analysis and (neuro)toxicity testing. As such, one of the main applications of the technique coincides with a major goal of RA: to find a selective long-lasting anesthetic agent that outlasts surgical pain and has minimal adverse effects.[12,13] To date, no such drug has been found, leading clinicians to seek an alternative in additives (e.g. α_2 agonists and dexamethasone) to local anesthetics. Although some of these combinations appear to result in prolongation of nerve blockade, additives fail to deliver the steerable and lasting effect that is sought for. Furthermore, the effect size and mechanism of action are often unknown, while data on neurotoxicity is unavailable due to off-label usage. Within this context, a human iPSC-derived RA model would enable the testing of novel drugs without the interference of other cell types or organ systems. Researchers could first screen for the presence of a nociceptor-mediated effect of a compound using MEA and subsequently perform patch clamping measurements to determine the exact result on ionic membrane currents. Toxicity assays would then complete a comprehensive preclinical screening of a potential analgesic. Similar methods could be used to investigate the properties of established additives and other relevant drugs. When adapted, the described system would also offer chances for research into treatment of chronic pain and painful neuropathies (e.g. by inducing a neuropathic phenotype through application of chemotherapeutics). Although iPSC technology is increasingly used for drug discovery in other specialties, it remains underutilized in anesthesiology and pain medicine.

The reprogramming process preserves the genetic code of the original somatic cell, including all (disease-related) mutations and variations. Single donor iPSC lines are therefore representative of the donor and offer the opportunity to perform experiments on patient-specific cells that were previously unavailable. iPSC technology thus enables a more personalized approach to RA (research); iPSCs can provide a

'trial in a dish' for underrepresented patient categories, complementing large clinical studies. RA-relevant genetic mutations (e.g. channelopathies) and diseases (e.g. neuropathies) can be reproduced and studied to provide directly translatable results, where this was previously impossible or impractical. In addition, a patient with a previously unexplained complication of RA, or a positive family history of such, could donate cells for reprogramming that may reveal an altered response to medication relevant to a planned surgical procedure.

iPSC reprogramming is a still evolving technique that has limitations. Currently, reprogramming efficiency is still relatively low, making iPSC culture expensive compared to other cell culture systems.[14] Contributing to the costs are the long culture time required for terminal differentiation and the associated labor-intensive nature of the sensitive cells.[15] Another factor to consider is the maturation status of the differentiated cells. Although the converted cells are morphologically and functionally similar to their in vivo counterparts, the differentiated cells might not be epigenetically identical.[16,17] New protocols and methods are constantly being developed and it is expected that these issues will be resolved in the coming years.

Although new to anesthesiology, human iPSCs provide a translatable platform that is directly applicable to RA. iPSC technology thus provides a method for performing progressive human disease modelling and drug discovery. As such, it is an opportunity to further elevate the status of RA and could contribute to the future of anesthesiology as a perioperative specialty.

References

1. Gurdon JB. The Developmental Capacity of Nuclei taken from Intestinal Epithelium Cells of Feeding Tadpoles. *Development.* 1962;10(4):622-640.
2. Tada M, Takahama Y, Abe K, Nakatsuji N, Tada T. Nuclear reprogramming of somatic cells by in vitro hybridization with ES cells. *Curr Biol.* 2001;11(19):1553-1558.
3. Takahashi K, Yamanaka S. Induction of pluripotent stem cells from mouse embryonic and adult fibroblast cultures by defined factors. *Cell.* 2006;126(4):663-676.
4. Omole AE, Fakoya AOJ. Ten years of progress and promise of induced pluripotent stem cells: historical origins, characteristics, mechanisms, limitations, and potential applications. *PeerJ.* 2018;6:e4370.
5. Takahashi K, Yamanaka S. A decade of transcription factor-mediated reprogramming to pluripotency. *Nat Rev Mol Cell Biol.* 2016;17(3):183-193.
6. Chambers SM, Qi Y, Mica Y, et al. Combined small-molecule inhibition accelerates developmental timing and converts human pluripotent stem cells into nociceptors. *Nat Biotechnol.* 2012;30(7):715-720.
7. Chambers SM, Fasano CA, Papapetrou EP, Tomishima M, Sadelain M, Studer L. Highly efficient neural conversion of human ES and iPS cells by dual inhibition of SMAD signaling. *Nat Biotechnol.* 2009;27(3):275-280.
8. Wilson PG, Stice SS. Development and differentiation of neural rosettes derived from human embryonic stem cells. *Stem Cell Rev.* 2006;2(1):67-77.
9. Mulroy M. A History of Regional Anesthesia. In: Eger Ii EI, Saidman LJ, Westhorpe RN, eds. *The Wondrous Story of Anesthesia.* New York, NY: Springer New York; 2014:859-870.
10. Rostock C, Schrenk-Siemens K, Pohle J, Siemens J. Human vs. Mouse Nociceptors – Similarities and Differences. *Neuroscience.* 2018;387:13-27.
11. Han C, Estacion M, Huang J, et al. Human Nav1.8: enhanced persistent and ramp currents contribute to distinct firing properties of human DRG neurons. *Journal of Neurophysiology.* 2015;113(9):3172-3185.
12. Jablonski S, Lirk P. Future in regional anesthesia and pain medicine: the pharmacological view. *Minerva Anestesiol.* 2021;87(3):351-357.
13. Boezaart AP, Zasimovich Y, Parvataneni HK. Long-acting local anesthetic agents and additives: snake oil, voodoo, or the real deal? *Pain Med.* 2015;16(1):13-17.
14. Malik N, Rao MS. A review of the methods for human iPSC derivation. *Methods Mol Biol.* 2013;997:23-33.
15. Lampert A, Bennett DL, McDermott LA, et al. Human sensory neurons derived from pluripotent stem cells for disease modelling and personalized medicine. *Neurobiology of Pain.* 2020:100055.
16. Bilic J, Izpisua Belmonte JC. Concise review: Induced pluripotent stem cells versus embryonic stem cells: close enough or yet too far apart? *Stem Cells.* 2012;30(1):33-41.
17. Karagiannis P, Takahashi K, Saito M, et al. Induced Pluripotent Stem Cells and Their Use in Human Models of Disease and Development. *Physiol Rev.* 2019;99(1):79-114.
18. Kolios G, Moodley Y. Introduction to stem cells and regenerative medicine. *Respiration.* 2013;85(1):3-10.

Chapter 9

Use of a human induced pluripotent stem cell-derived dorsal root ganglion neuron model to study analgesics in vitro: proof of principle using lidocaine

Based on: Pascal S.H. Smulders, Werner ten Hoope, Carmen Bernardino Morcillo, Jeroen Hermanides, Markus W. Hollmann, Nina C. Weber
Br J Anaesth. 2022 Dec;129(6):e172-e175

A translatable non-animal *in vitro* model that is applicable to peripheral regional anesthesia (RA) and can be utilized for pharmacological research is missing. This is problematic, because while RA has become central to perioperative multimodal analgesic treatment, development of novel analgesics is minimal.[1] Furthermore, questions addressing the mechanism of action and neurotoxicity of various analgesic drugs remain unresolved. Scientists currently rely on animal models to investigate these issues due to the ethical, practical and regulatory problems in acquiring human neuronal tissue. However, translation of research results is hampered by the (neurobiological) differences in pain signaling between humans and animals.[2,3] As we have reviewed recently, human induced pluripotent stem cells (iPSCs) now provide the opportunity to employ *in vitro* models of RA constructed from human neurones.[4]

iPSCs form a man-made stem cell class, created by forced regression of a conventional somatic cell, that has similar pluripotency (the ability to differentiate into cell types from all germ layers) and self-renewable (the ability to divide indefinitely by creating unaltered daughter cells) capabilities as embryonic stem cells.[5] Therefore, iPSC technology provides a method to obtain difficult-to-access human cells, such as nociceptive dorsal root ganglion (DRG) neurons, for use in model development and pharmacological research. We here showcase the applicability of a human iPSC derived nociceptive DRG neuron model for RA by means of a case study of lidocaine.

iPSC-derived DRG nociceptors were differentiated from commercial Human iPSC-Derived Sensory Neuron Progenitors (Axol Bioscience, Roslin, UK, ax0055) using a version of the conversion protocol of Chambers and colleagues.[6] This approach directs iPSCs through phases closely resembling embryological development, i.e. from a beginning that resembles the developing neural tube, to a neural crest subphase and finally a nociceptive DRG neuron state (Figure 1a).

In brief, cells were seeded in 10 mM Y-27632 supplemented Neural Plating Medium at a density of 100,000 cells per cm^2 (for immunofluorescence and toxicity assays) or 130,000 cells per 5 µL drop (for microelectrode array; MEA) on 80 µg/mL Matrigel GFR coated glass coverslips or cell culture plates. Cells were thereafter maintained in Sensory Neuron Maintenance Medium supplemented with 1 X Sensory Neuron Maturation Maximizer, 1 µg/mL laminin, 25 ng/mL human glial-derived neurotrophic factor, 25 ng/mL human nerve growth factor, 10 ng/mL human brain-derived neurotrophic factor and 10 ng/mL human neurotrophin-3. On day 3, cells were treated with 2.5 µg/mL Mitomycin C for 2 hours to eliminate any dividing non-neuronal cells. Medium was changed every 2 to 3 days until assay readiness. Cells were incubated at 37°C, 5% CO_2. Supplementary Table S1 shows further details on cell culture materials.

Different microscopy techniques were used to inspect cells for correct differentiation and maturation. During culture, cells were routinely subjected to bright field microscopy when changing media. The initially rounded cells were seen to elongate, grow long neurites that created an intricate network and migrate to form ganglion-like clusters, as nociceptor reprogramming progressed (Figure 1b). At 21 days post-seeding, samples were prepared for immunofluorescence confocal laser microscopy (see Supplementary Methods S1 and Supplementary Table S2; $n = 3$), targeting markers of the (nociceptive) nervous system. Positive immunostainings for β3-tubulin and BRN3A confirmed the peripheral sensory neuronal identity of the cells. Furthermore, neurons were found to express all expected markers of nociception, i.e. voltage-gated sodium channels 1.7 and 1.8, transient receptor potential cation channels ankyrin 1 (TRPA1) and vanilloid 1 (TRPV1), and neurotransmitter substance P (Figure 1c and Supplementary Figure S1). Thus, the differentiated cells were found to match human *in vivo* DRG nociceptive neuron morphology and were deemed mature for downstream assays.[7]

After confirming correct differentiation, the effect of lidocaine (Fresenius Kabi, Huis Ter Heide, The Netherlands, RVG 51673) on electrical activity, and its potential cytotoxicity was investigated. First, the minimal effective *in vitro* concentration of lidocaine was determined using MEA (configurations were set according to the manufacturer's instructions; Axion BioSystems, Atlanta, USA, Maestro Edge). This technique enables the extracellular measurement of action potentials of neuronal networks differentiated over electrodes embedded within the culture plate. Lidocaine was applied while the 24-day-old mature neurons were electrically stimulated (400 µs pulse of 700 mV 50 mA, every 10 s), in order to mimic noxious signaling. MEA showed an almost complete blockade of electrical activity ($p < 0.001$, paired T-test, $n = 3$) after application of 100 µM lidocaine (figure 1d). Neurotoxicity was then measured by detection of lactate dehydrogenase (LDH) (Cytotoxicity Detection Kit, performed according to the manufacturer's directions; Roche, Basel, Switzerland, 11644793001), released from the cytosol of damaged neurons. Incubation with the aforementioned concentration for 12 hrs. resulted in a 0.14% median increase in LDH, relative to untreated control and maximum available LDH (Supplementary Figure S2; $n = 3$).

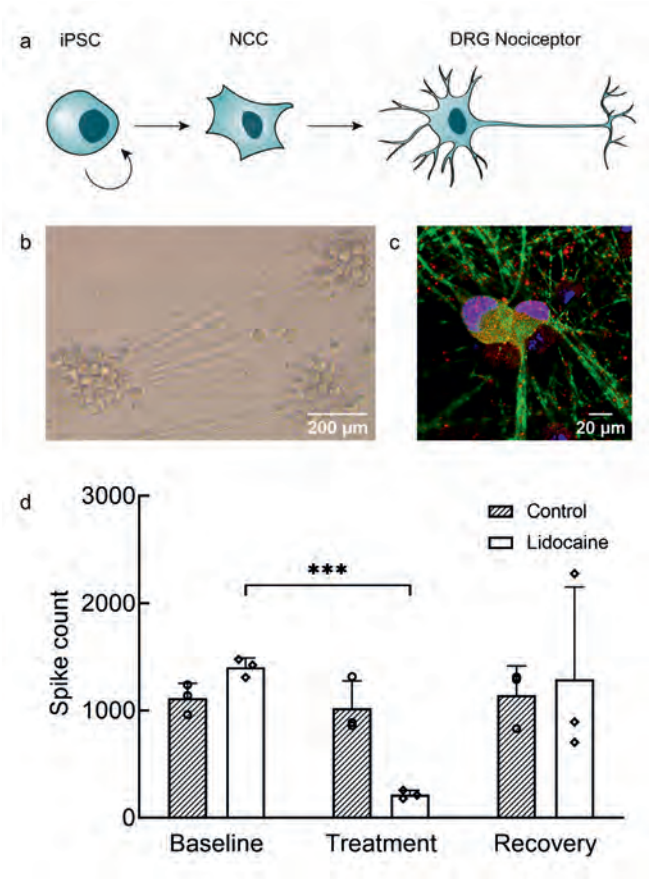

Figure 1: Human induced pluripotent stem cells (iPSCs) allow development of a translatable *in vitro* model of peripheral regional anesthesia.

(a) iPSCs can be differentiated into virtually all cell types of the body (pluripotency) and can divide into unaltered daughter cells (self-renewal; circled arrow). Therefore, iPSCs can be reprogrammed into nociceptive dorsal root ganglion (DRG) neurons, with lineage-based reprogramming closely resembling embryological development. iPSCs first pass a stage that mimics the developing neural tube, followed by a phase in which cells resemble neural crest cells (NCCs), and then terminally differentiate to form DRG nociceptors. These changes were visualized using microscopy techniques. (b) Cells were seen to elongate, grow a network of neurites and form ganglion-like clusters using bright field microscopy (scale bar is 200 µm). (c) Immunofluorescence imaging showed expression of nociception marker voltage-gated sodium channel 1.7 (red; blue: Hoechst; green: β3-tubulin) (other markers are depicted in Supplementary Figure S1) in the terminally differentiated neurons (scale bar is 20 µm; n = 3). (d) Electrical activity of the neurons was measured using microelectrode array over a period of 10 min. Application of 100 µM lidocaine resulted in a significant blockade of spikes (or action potentials) (p <0.001, paired T-test, n = 3).

As shown, human iPSC derived DRG nociceptors morphologically, molecularly and functionally resemble their *in vivo* counterparts. Applicability of this model to RA research was further demonstrated by detailing its susceptibility to the effects of the classical local anesthetic lidocaine. As such, this proof-of-concept study offers a first hint at the versatility of the model. For example, experimental procedures can be easily adapted to include additional functional (e.g. patch clamping or calcium imaging) and toxicological (e.g. detection of caspase enzyme activation) assays for a complete preclinical investigation of novel or established analgesics. The platform can also be used for disease modelling of (chronic) pain conditions, and potentially enables a more personalized approach to RA, as the genetic code (including mutations and variations) of the donor is preserved during iPSC reprogramming.[8-10] However, iPSC reprogramming also has limitations. The extended time needed for differentiation and low iPSC reprogramming efficiency makes iPSC culture labor-intensive and expensive, compared to conventional cell culture systems. Further, iPSCs may possess pre-existing or *de novo* mutations that could impact genetic stability and differentiation efficiency, while incomplete reprogramming might result in an impaired epigenetic status and accompanying deviations in gene expression and function (when compared to human *in vivo* and embryonic stem cell-derived DRG neurons).[11, 12] To conclude, human iPSC technology poses a valuable addition to the RA research portfolio.

To summarize: a functional examination is introduced utilizing iPSC derived DRG nociceptors. The findings showcase the responsiveness of these cells to lidocaine, providing valuable insights into their potential application as a model for comprehensive preclinical investigations of analgesics. This approach offers a promising avenue for advancing our understanding of pain mechanisms and evaluating the efficacy of various analgesic compounds before clinical trials.

References

1. Kissin I. The development of new analgesics over the past 50 years: a lack of real breakthrough drugs. *Anesth Analg* 2010; **110**: 780-9
2. Mao J. Current challenges in translational pain research. *Trends Pharmacol Sci* 2012; **33**: 568-73
3. Rostock C, Schrenk-Siemens K, Pohle J, Siemens J. Human vs. Mouse Nociceptors - Similarities and Differences. *Neuroscience* 2018; **387**: 13-27
4. Smulders PSH, van Zuylen ML, Hermanides J, Hollmann MW, Ten Hoope W, Weber NC. Investigating Peripheral Regional Anesthesia Using Induced Pluripotent Stem Cell Technology: Exploring Novel Terrain. *Anesth Analg* 2022; **135**: 659-62
5. Takahashi K, Yamanaka S. A decade of transcription factor-mediated reprogramming to pluripotency. *Nat Rev Mol Cell Biol* 2016; **17**: 183-93
6. Chambers SM, Qi Y, Mica Y, et al. Combined small-molecule inhibition accelerates developmental timing and converts human pluripotent stem cells into nociceptors. *Nat Biotechnol* 2012; **30**: 715-20
7. Haberberger RV, Barry C, Dominguez N, Matusica D. Human Dorsal Root Ganglia. *Front Cell Neurosci* 2019; **13**: 271
8. Lampert A, Bennett DL, McDermott LA, et al. Human sensory neurons derived from pluripotent stem cells for disease modelling and personalized medicine. *Neurobiol Pain* 2020; **8**: 100055
9. Middleton SJ, Barry AM, Comini M, et al. Studying human nociceptors: from fundamentals to clinic. *Brain* 2021; **144**: 1312-35
10. Obal D, Wu JC. Induced pluripotent stem cells as a platform to understand patient-specific responses to opioids and anaesthetics. *Br J Pharmacol* 2020; **177**: 4581-94
11. Poetsch MS, Strano A, Guan K. Human Induced Pluripotent Stem Cells: From Cell Origin, Genomic Stability, and Epigenetic Memory to Translational Medicine. *Stem Cells* 2022; **40**: 546-55
12. Bilic J, Izpisua Belmonte JC. Concise review: Induced pluripotent stem cells versus embryonic stem cells: close enough or yet too far apart? *Stem Cells* 2012; **30**: 33-41

Appendices

Supplementary Table S1: Cell culture materials
Supplementary Methods S1: Sample preparation for immunofluorescence imaging
Supplementary Table S2: Immunofluorescence antibodies
Supplementary Figure S1: Immunofluorescence imaging of (nociceptive) peripheral nervous system markers
Supplementary Figure S2: Lactate dehydrogenase release after treatment with lidocaine

Supplementary Table S1 – Cell culture materials

	Manufacturer	Catalogue number
Y-27632 dihydrochloride	Focus Biomolecules, Plymouth Meeting, USA	10-2301
Neural Plating Medium	Axol Bioscience, Roslin, UK	ax0033
Matrigel GFR	Corning Life Sciences, Corning, USA	354230
CytoView MEA 24	Axion BioSystems, Atlanta, USA	M384-tMEA-24W
µClear 96-well flat bottom	Greiner Bio-One, Frickenhausen, Germany	655090
Sensory Neuron Maintenance Medium	Axol Bioscience, Roslin, UK	ax0060
Sensory Neuron Maturation Maximizer	Axol Bioscience, Roslin, UK	ax0058
Laminin	Sigma-Aldrich, St. Louis, USA	L2020
Recombinant Human Glial-Derived Neurotrophic Factor	Axol Bioscience, Roslin, UK	ax139855
Recombinant Human Nerve Growth Factor	Axol Bioscience, Roslin, UK	ax139789
Recombinant Human Brain-Derived Neurotrophic Factor	Axol Bioscience, Roslin, UK	ax139800
Recombinant Human Neurotrophin-3	Axol Bioscience, Roslin, UK	ax139811
Mitomycin C	Substipharm, Paris, France	RVG 109336

Supplementary Methods S1

Sample preparation for immunofluorescence imaging

Cells were fixated using 2% paraformaldehyde in PBS (pH 7.4) for 10 min. The samples were subsequently permeabilized with 0.01% Triton X-100 in PBS for 5 min and then blocked by application of blocking buffer (PBS containing 5% goat serum) for 1 hr. Primary antibodies were incubated with the samples for 1 hr, while secondary antibodies were incubated for 30 min (in the dark). The samples were then mounted to increase photostability (Invitrogen ProLong Gold Antifade Mountant without DAPI; Thermo Fisher Scientific, Waltham, USA, P10144). Samples were washed with PBS in between steps and all steps were performed at room temperature. Finally, the samples were imaged using a confocal laser scanning microscope (Leica TCS SP8(X); Leica Microsystems, Wetzlar, Germany). Antibodies were diluted in blocking buffer. A complete list of antibodies and dilutions can be found in Supplementary Table S2.

Supplementary Table S2 – Immunofluorescence antibodies

	Dilution	Manufacturer	Catalogue number
Primary Antibodies			
Mouse anti-Human β3-tubulin	1:200	Elabscience, Houston, USA	E-AB-20093
Rabbit anti-Human BRN3A	1:100	Bioss Antibodies, Woburn, USA	BS-3669R
Rabbit anti-Human Na_v 1.7	1:200	Abcam, Cambridge, UK	ab65167
Rabbit anti-Human Na_v 1.8	1:200	Abcam, Cambridge, UK	ab66743
Rabbit anti-Human TRPV1	1:100	Abcam, Cambridge, UK	ab3487
Rabbit anti-Human TRPA1	1:100	Thermo Fisher Scientific, Waltham, USA	PA5-88615
Rabbit anti-Human Substance P	1:100	Thermo Fisher Scientific, Waltham, USA	PA5-106934
Secondary Antibodies			
Goat anti-Mouse Alexa Fluor 488	1:400	Thermo Fisher Scientific, Waltham, USA	A28175
Goat anti-Rabbit Alexa Fluor 647	1:200	Thermo Fisher Scientific, Waltham, USA	A27040
Nuclear Dye			
Hoechst 33342	1:5000	Thermo Fisher Scientific, Waltham, USA	H3570

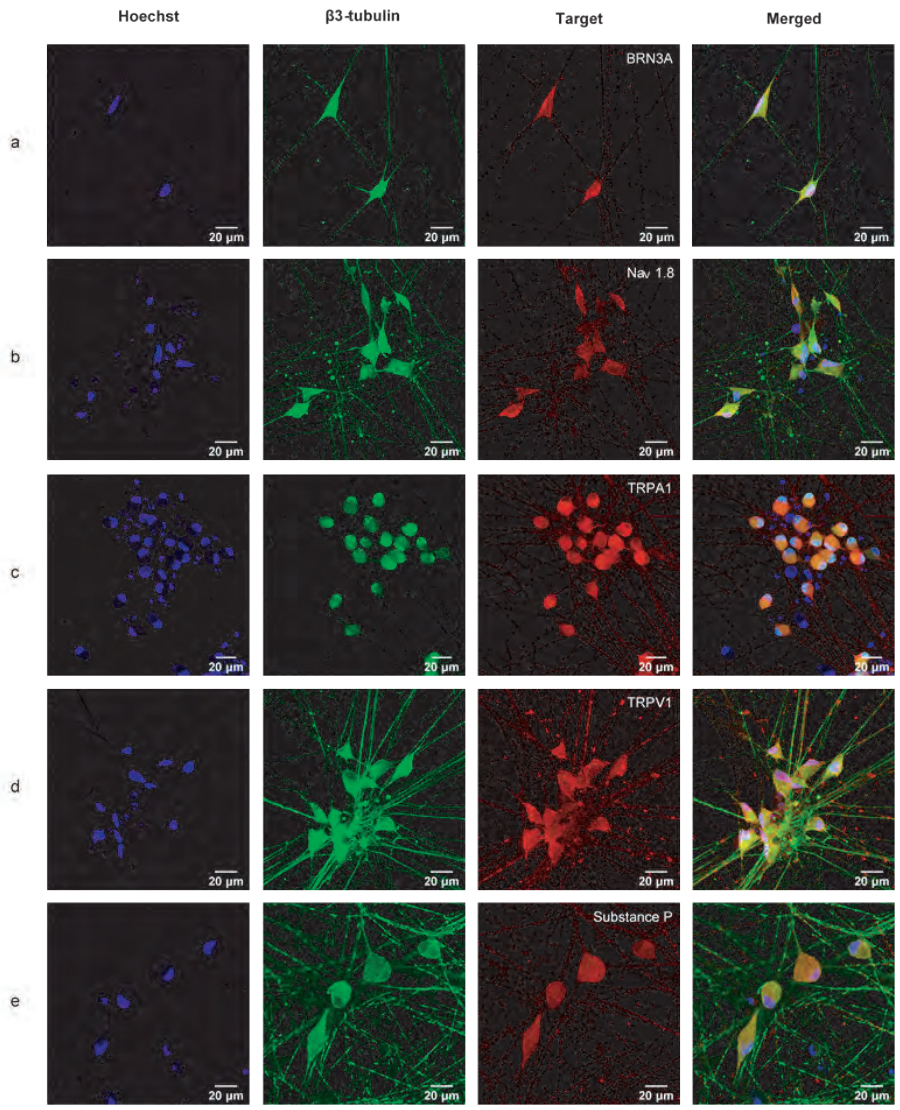

Supplementary Figure S1 – Immunofluorescence imaging of (nociceptive) peripheral nervous system markers

Representative confocal laser scanning microscopy images detailing presence of neuronal markers (n = 3). Expression of β3-tubulin (second column) and BRN3A (a) demonstrated the peripheral sensory neuronal identity of the cells. Additionally, positive immunostainings for voltage-gated sodium channel (Na_v) 1.8 (b), transient receptor potential channels ankyrin 1 (TRPA1) (c) and vanilloid 1 (TRPV1) (d), and substance P (e) confirmed their nociceptive profile. Samples were prepared as described in Supplementary Methods S1. Images were taken using 63x (a, b, d, e) or 40x (c) magnification. The scale bar is 20 µm.

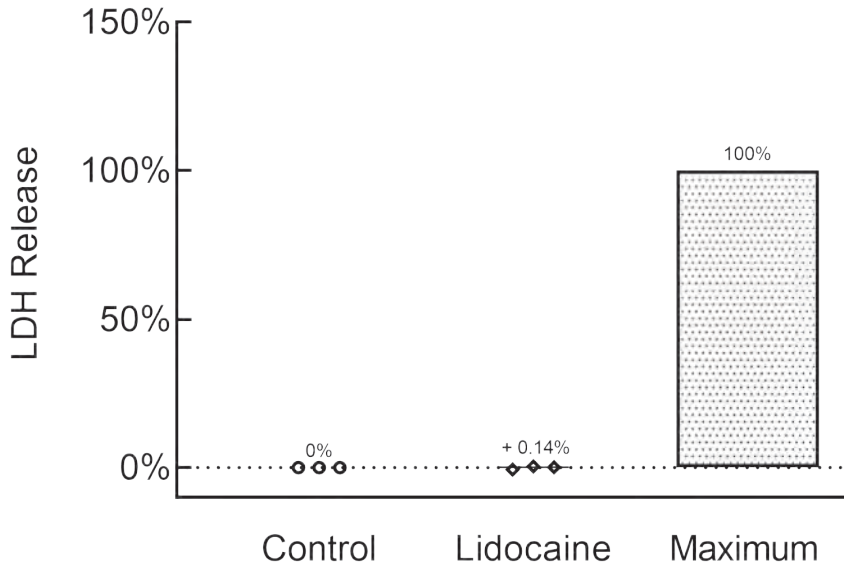

Supplementary Figure S2 – Lactate dehydrogenase release after treatment with lidocaine
Neurotoxicity of 100 µM lidocaine was investigated by measurement of lactate dehydrogenase (LDH) in the cell culture medium (*n* = 3). Compared to untreated control and maximum available LDH, 12 hrs incubation resulted in a 0.14% median increase in LDH.

Chapter 10

Thesis summary and future perspectives

Summary

This thesis aimed to answers the following research questions:

- Is diabetes mellitus (DM) a relevant co-morbidity to consider when applying regional anesthesia?
- Can the obturator nerve be effectively blocked during a fascia iliac compartment block?
- Can the branches of the sciatic nerve be reached in a saphenous block?
- What is a sufficient volume of local anesthetic for a saphenous nerve block? And is the saphenous block a viable analgesic alternative to a femoral nerve block for the treatment of postoperative pain following cruciate ligament surgery?
- What role can stem cells play in studying regional anesthesia?

In **Section 1** of this thesis, we delved into the clinical relevance of diabetes mellitus (DM) for regional anesthesia. In **Section 2**, we studied nerve anatomy to understand analgesic distribution for two regional anesthetic techniques in hip and knee surgery. Having examined the saphenous nerve in the preceding section, **Section 3** is dedicated to establishing the minimum volume dosage required for a saphenous nerve block in vivo, along with exploring the clinical significance of this analgesic block in knee surgery. A novel approach into research in regional anesthesia using stem cell technique is discussed in **section 4** of this thesis.

In Section 1. regional anesthesia was discussed in the context of diabetes mellitus. We discussed In **Chapter 2** recent relevant literature regarding regional anesthesia in the patient with DM and formulated recommendations for clinical practice. The pathophysiologic mechanisms of diabetic peripheral polyneuropathy (DPN) are multifactorial and primary based on inflammation, oxidative stress and mitochondrial dysfunction induced by long-standing hyperglycemia. This eventually leads to altered nerve excitability, due to changed sodium currents and microvascular damage. In patients with DPN, regional anesthesia differs in several aspects. The nerve's electric stimulation threshold is significantly increased, potentially elevating the risk of needle trauma in stimulator-guided nerve blocks. This elevated threshold could not be predicted accurately from anamnesis, or even detailed neurological testing. Additionally, in diabetic nerves the onset of block duration is longer, and the block regression time seems substantially longer in poorly controlled diabetes. The reasons

for the prolonged block duration have not been clarified, but both pharmacodynamic (sodium currents are more sensitive) and pharmacokinetic (decreased nerve blood flow leads to prolonged residence time of local anesthetics in the nerve) mechanisms have been conjectured. While there is speculation about local anesthetics being more toxic in diabetic neuropathy, the evidence is inconclusive and should not be a reason to withhold regional anesthesia from patients with a valid indication. It is important to note that when peripheral nerve catheters are employed, diabetes is an independent risk factor for catheter related infection.

Both the pharmacodynamic and -kinetic hypotheses described in **Chapter 2**, were studied in **Chapter 3.** We conducted sciatic nerve block experiments involving Zucker Diabetic Fatty (ZDF) rats. The minimum local anesthetic concentration (MLAC) of lidocaine for a sciatic nerve block was determined in vivo, where the motor block duration was significantly extended in the diabetic ZDF rats, as compared to the control group. Diabetic animals showed significant reduction in minimum local anesthetic dose (ED50) for a lidocaine-induced motor block (0,9%), compared to the control animals (1,4%) ($P < 0.05$ CI 0.58 to 0.57). This observation was supported by in vitro patch clamp examinations of sodium channel currents, indicating that the inhibitory impact of a specific lidocaine concentration was significantly more pronounced in primarily sensory neurons obtained from diabetic rats compared to those from the control group. Diabetic dorsal root ganglia (DRGs) exhibit hyperexcitability, as evidenced by a higher number of action potentials during depolarizing pulses compared to control DRGs. However, they are also susceptible to suppression by local anesthetics: single cell measurements showed a lower inhibitory concentration of lidocaine for blocking sodium currents in neuropathic neurons, as compared to control neurons. To study the pharmacokinetics, intraneural radiolabeled 14C-lidocaine was applied in the sciatic nerve block in 24 control and 25 diabetic rats and monitored over time. We observed that at 60 minutes the neural radiolabeled lidocaine content in nerves of control animals was (mean log) 5.4 *versus* 7.1 in diabetic animals ($P = 0.005$, CI −2.88 to 0.52). We illustrated heightened responsiveness of the diabetic neuropathic nerve to local anesthetics, as well as prolonged retention of local anesthetics in the diabetic neuropathic nerve. Thus, in this rodent model of neuropathy, both pharmacodynamic and pharmacokinetic mechanisms played a role in extending the duration of nerve block.

Diabetic peripheral neuropathy is a frequent complication of both type 1 and type 2 DM, and the most prevalent neuropathy in the Western world. Diabetes patients undergo surgery more often than patients without diabetes, and several surgical procedures for typical complications of long- standing DM, for example, creation of arteriovenous fistula in patients with end-stage renal disease, might be preferably performed under regional anesthesia. Anesthetists encounter patients with diabetic peripheral neuropathy daily, yet there remains a lack of comprehensive understanding regarding both prevention and treatment. We note that the pharmacodynamics and pharmacokinetics of local anesthetics exert an influence on regional nerve blockades in diabetic neuropathy. Future research is needed to delineate detailed dose-response curves in diabetic versus control animals. Specifically, this inquiry should investigate whether sensitivity to local anesthetics manifests across diverse neuronal subgroups, exhibits specificity to sodium currents, and varies with different local anesthetics.

Section 2 studied applied anatomy of the saphenous and the obturator nerve for nerve blocks in hip and knee areas.
In **Chapter 4** we performed a radiological cadaveric study to investigate the incidence of sciatic nerve involvement after various adductor canal block techniques, clinically used for knee and lower extremity surgery. Eighteen non-preserved human cadavers, in a fresh and unfrozen state, were randomly assigned to undergo ultrasound-guided injections in either the distal femoral triangle or distal adductor canal with two different injectate volumes. No involvement of the sciatic nerve, the tibial nerve, or the profundal nerve was found in any of the cadavers. Spread of contrast to the popliteal fossa was detected in three of 36 cadaver sides. Thus, adductor canal block techniques are unlikely to block the sciatic nerve or its main branches, even when larger volumes are used. Moreover, injectate reached the popliteal fossa in a minority of cases, and it remains uncertain whether a clinical analgesic effect is attained through this mechanism. A saphenous nerve block can thus safely be performed when no muscle weakness is preferred after surgery.

Whether the fascia iliac compartment block affects the obturator nerve (ON), is a contentious issue in anesthesia, particularly in the context of procedures such as hip surgery. The extent of involvement may hinge on the injectate spreading to the cranial direction. Hence, in **chapter 5** we studied the impact of a suprainguinal needle approach with hydrodissection-mediated needle advancement on obtura-

tor nerve involvement and cranial injectate spread. Seventeen fresh, unfrozen and unembalmed adult human cadavers were included to perform a total of 34 blocks, which were randomized to a suprainguinal or an infrainguinal technique. Neither the suprainguinal needle approach with hydrodissection, nor any other technique targeting the iliac facial compartment led to reliable obturator nerve involvement, and as such the obturator nerve seems to be unrelated to fascial plane blocks targeting the iliac facial compartment. The addition of a separate obturator nerve block or iliac facial compartment block (or large volume FNB) should be considered when clinically indicated.

Applied anatomical scientific research with a clinical outcome measure in regional anesthesia is challenging due to substantial anatomical variation. The translation from neuroanatomy in cadavers to the degree of clinical analgesia is often not a straightforward one-to-one correlation. Illustratively, in the cadaver study of an adductor canal nerve block in Chapter 4, the sciatic nerve is not implicated. However, in Chapter 6, clinical involvement is an incidental finding. Literature commonly describes the spread to the popliteal fossa after an adductor canal block (ACB), but specific details regarding the depth of spread within this fossa are seldom addressed. Subsequent investigations should prioritize determining whether the injectate consistently engages sensory nerves upon reaching the popliteal fossa and elucidate the resulting clinical analgesic effects. With respect to the obturator nerve, forthcoming studies should investigate a reliable method for achieving anesthesia of the obturator nerve within the retroperitoneal compartment.

Section 3 determined the minimal volume for saphenous nerve block, and the effectivity of a saphenous nerve block in day care anterior cruciate ligament surgery. In **Chapter 6**, we examined saphenous nerve blocks in healthy volunteers to delineate the altered distribution of skin sensation and determine the minimum dose of local anesthetic (MlaV) required to achieve proficient sensory block. Following the Dixon dosing model; the measured MlaV effective in 50% (eD50) of the volunteers and the calculated corresponding effective volume in 95% (eD95) of volunteers for a complete saphenous nerve block were 1.5 ml and 1.9 ml, respectively. The cutaneous spread of the selective nerve block exhibits substantial individual variability, particularly concerning the innervation of the dorsal and medial foot. There was no clear correlation between the volume of local anesthetic and the initiation or duration of the selective saphenous nerve block.

In **Chapter 7** we randomized 53 patients in a multi-center superiority trial undergoing surgery for outpatient anterior cruciate ligament reconstruction. Patients were randomly assigned in a 1:1 ratio to either the femoral nerve block group or the adductor canal block group. Both groups underwent ultrasound-guided nerve blockade before the induction of general anesthesia. There was no significant difference between the two nerve block groups in terms of readiness for discharge (FNB median 1.8 hours, 95% CI 1.0 to 3.5 hours, vs. ACB 2.9 hours, 1.5 to 4.7 hours; p = 0.3). However, motor blocks and instances of (near) falls were more frequently reported in patients with a femoral nerve block, compared to those with an adductor canal block. There were no discernible differences between the groups in postoperative Numeric Rating Scale scores over time. Similarly, no distinctions were observed at the six-week and 12-week follow-up assessments with respect to occurrences of (near) falls and the orthopedic surgeon's evaluation of knee neurology. Additionally, long-term patient-reported outcome measurements did not show between group differences. Hence, a femoral nerve block has a less favorable safety profile than an adductor canal block, characterized by more motor blocks and (near) falls.

Further investigation is necessary to determine whether a correlation exists between the administered dose of local anesthetic in the adductor canal and the duration of postoperative analgesia, as this poses a more clinically relevant question. From a clinical perspective, we acknowledge that the patient population undergoing cruciate ligament reconstructions is highly heterogeneous. For future endeavors, it is essential to investigate predefined criteria to better characterize which category of patients who would profit most from this intervention.

Section 4 Introduced stem cells

This section is essentially the part of the thesis that should fuel the discussion where research in regional anesthesia should be heading. Making the transition from animal studies to the area of stem cells is a thrilling endeavor; to comprehend the principles of stem cells and develop a functional model applicable into anesthesiology.

Chapter 8 provides an overview of how induced pluripotent stem cells (iPSCs) position themselves within the context of useful stem cell models. We describe the process of how iPSC production involves regression to a pluripotent state of somatic cells, such as skin fibroblasts, regaining the capacity to differentiate into any cell

type in the body (pluripotency) and producing unaltered daughter cells (self-renewal). The neural induction of the pluripotent stem cell is described and the steps of differentiation to a peripheral neuron. These iPSC-derived nociceptors are functionally mature nociceptive neurons that secrete the neurotransmitter substance P, are electrically active, and merge into ganglion-like structures. The field could gain from a research model that more accurately mirrors the complex aspects of pain signaling in humans compared to the existing animal models and holds great potential for pharmaceutical research.

Finally, **Chapter 9** illustrated a functional study where we differentiated iPSC-derived DRG nociceptors from commercial Human iPSC-Derived Sensory Neuron Progenitors. iPSCs differentiation follows stages that closely mimic embryological development: progressing from an initial stage resembling the developing neural tube, to a subsequent neural crest subphase, and ultimately reaching a state resembling nociceptive dorsal root ganglion (DRG) neurons within 21-28 days. The use of immunofluorescence confirmed the peripheral sensory neuronal identity for β3-tubulin and BRN3A. Additionally, neurons were found to express all expected markers of nociception, including voltage-gated sodium channels 1.7 and 1.8, transient receptor potential cation channels ankyrin 1 (TRPA1) and vanilloid 1 (TRPV1), and the neurotransmitter substance P. Thereafter we studied the impact of lidocaine on electrical activity and its potential cytotoxicity. Using MEA, results demonstrated an almost complete blockade of electrical activity following the application of lidocaine, with in an increase in LDH to untreated control group. Hence, we introduce a model of human iPSC derived DRG nociceptors that exhibits morphological, molecular and functional characteristics resembling it's *in vivo* counterparts.

We validated our model by showcasing its responsiveness to the effects of the frequently used local anesthetic lidocaine. In future studies, experimental procedures can be tailored to include supplementary functional techniques, such as patch clamping or calcium imaging, and toxicological assays, such as the detection of caspase enzyme activation. This would facilitate a comprehensive preclinical investigation of both novel and established analgesics. The platform can also be utilized for disease modeling of (chronic) pain conditions and potentially allows for a more personalized approach to regional anesthesia, as the donor's genetic code (including mutations and variations) is preserved during iPSC reprogramming.

In conclusion, this thesis has addressed relevant questions in the realm of regional anesthesia, spanning diverse topics from diabetes mellitus as a co-morbidity to the application of stem cells in this field. We focused on the clinical relevance of diabetes mellitus, revealing altered responses to regional anesthesia in diabetic rodents. Pharmacodynamic and pharmacokinetic aspects were investigated of sciatic nerve blocks in diabetic rats, shedding light on heightened responsiveness and prolonged retention of local anesthetics in diabetic neuropathic nerves.

Findings of applied anatomy of the saphenous and obturator nerves for nerve blocks provided valuable insights into negligible involvement of both nerves in the corresponding blocks. The minimal volume local anesthetic required for a for a saphenous nerve block was determined, while we compared the femoral nerve blocks and adductor canal block in anterior cruciate ligament surgery. The results favored the latter due to a more favorable safety profile. The final part of this thesis introduced stem cells to regional anesthesia research. The potential of induced pluripotent stem cells (iPSCs) was discussed as a model for pain signaling, emphasizing their role in pharmaceutical research. We presented a functional study with iPSC derived DRG nociceptors, demonstrating their responsiveness to lidocaine and proposing a model for comprehensive preclinical investigations of analgesics.

Thus, in addition to addressing specific research questions, I also hope to have contributed to future perspectives in regional anesthesia. The integration of stem cell research opens new avenues for understanding pain mechanisms and developing innovative approaches for this medical domain.

Samenvatting

In **sectie 1** van deze thesis onderzochten we de klinische relevantie van diabetes mellitus (DM) voor regionale anesthesie. In **sectie 2** bestudeerden we radiologisch het verloop van de saphenus en obturatorius zenuw om de verdeling van analgesie te begrijpen voor twee regionale technieken bij heup- en kniechirurgie. Na de studie van de saphenus zenuw in het voorgaande hoofdstuk, is **sectie 3** gewijd aan het vaststellen van de minimale dosis vereist voor een saphenusblok *in vivo*, en het verkennen van de klinische relevantie van deze analgetisch blokkade bij kruisbandchirurgie van de knie. Een nieuwe benadering van onderzoek in regionale anesthesie met behulp van stamceltechniek wordt besproken in **sectie 4** van deze thesis.

Deze thesis beoogde de volgende onderzoeksvragen te beantwoorden:

- Hoe beïnvloedt diabetes mellitus als co-morbiditeit regionale anesthesie?
- Kan de obturator zenuw effectief worden geblokkeerd tijdens een fascia iliaca-compartimentblok? Kunnen takken van de nervus ischiadicus worden bereikt bij het toepassen van een saphenusblok?
- Hoeveel volume lokale verdoving is nodig voor een saphenusblok? En is een adductorkanaalblok een alternatief voor een femoraalblok bij de behandeling van postoperatieve pijn na kruisbandoperatie in dagbehandeling?
- Welke rol kunnen stamcellen spelen bij het bestuderen van regionale anesthesie?

In Sectie 1 werd diabetes mellitus besproken in relatie tot regionale anesthesie.
In **Hoofdstuk 2** bespraken we relevante literatuur met betrekking tot regionale anesthesie bij patiënten bekend met diabetes mellitus (DM) en formuleerden we aanbevelingen voor de klinische praktijk. De pathofysiologische mechanismen van diabetische perifere polyneuropathie (DPN) zijn multifactorieel en hoofdzakelijk gebaseerd op ontsteking, oxidatieve stress en mitochondriale disfunctie veroorzaakt door langdurige hyperglycemie. Dit leidt uiteindelijk tot veranderde zenuw excitabiliteit als gevolg van gewijzigde natriumstromen en microvasculaire schade. Diabetische neuropathie beïnvloedt regionale anesthesie in verschillende opzichten. De drempel voor elektrische stimulatie van de zenuw is aanzienlijk verhoogd, wat mogelijk het risico op naalddislocatie bij stimulator-geleide zenuwblokkades verhoogt. Deze verhoogde drempel kan niet nauwkeurig worden voorspeld uit de anamnese of gedetailleerd neurologisch onderzoek. Bovendien is de inwerkduur

van het blok langer en lijkt de regressietijd van de blokkade aanzienlijk langer te zijn bij slecht gecontroleerde diabetes. De oorzaken voor de verlengde blokkadeduur zijn niet volledig opgehelderd, maar zowel farmacodynamische (natriumstromen zijn gevoeliger) als farmacokinetische (verminderde zenuwbloedstroom leidt tot een langere verblijfstijd van lokale anesthetica in de zenuw) mechanismen worden gesuggereerd. Hoewel er gespeculeerd wordt dat lokale anesthetica meer toxisch zouden kunnen zijn bij diabetische neuropathie, is het bewijs niet conclusief en mag dit geen reden zijn om regionale anesthesie te onthouden aan patiënten met een geldige indicatie. Het gebruik van perifere zenuwkatheters bij patiënten met diabetes is een onafhankelijke risicofactor is voor kathetergerelateerde infecties.

Zowel de farmacodynamische als de farmacokinetische hypotheses zoals beschreven in het vorige hoofdstuk, werden bestudeerd in **Hoofdstuk 3**. We voerden experimenten uit met een blokkade van de nervus ischiadicus bij Zucker Diabetic Fatty (ZDF) ratten. De minimale lokale verdovingsconcentratie (MLAC) van lidocaïne voor een blokkade van de nervus ischiadicus werd in vivo bepaald, waarbij de duur van de motorblokkade significant werd verlengd bij de diabetische ZDF-ratten in vergelijking met de controlegroep. Diabetische dieren vertoonden een significante verlaging van de minimale lokale verdovingsdosis (ED50) voor een door lidocaïne geïnduceerde motorblokkade (0,9%) in vergelijking met de controledieren (1,4%) (P < 0,018, CI 0,58 tot 0,57). Deze waarneming werd ondersteund door *in vitro* patch clamp-onderzoeken van natriumkanaalstromen, waaruit bleek dat het remmende effect van een specifieke lidocaïneconcentratie significant sterker was bij primair sensorische neuronen verkregen van diabetische ratten in vergelijking met die van de controlegroep. Diabetische ganglia van de dorsale wortel (DRG's) vertonen hyperexcitabiliteit, zoals blijkt uit een hoger aantal actiepotentialen tijdens depolariserende pulsen in vergelijking met controlegroep DRG's. Ze zijn echter ook meer vatbaar voor onderdrukking door lokale anesthetica: metingen op enkelvoudige cellen toonden een lagere benodigde concentratie van lidocaïne aan voor het blokkeren van natriumstromen in neuropathische neuronen vergeleken met controle-neuronen. Om de farmacokinetiek te bestuderen, werd intraneuraal radiogelabelde 14C-lidocaïne aangebracht bij de blokkade van de nervus ischiadicus bij 24 controledieren en 25 diabetische ratten en over tijd gevolgd. We observeerden dat na 60 minuten de neurale radioactief gelabelde lidocaïne-inhoud in zenuwen van controledieren (gemiddeld log) 5,4 was, tegenover 7,1 bij diabetische dieren (P = 0,005, CI −2,88 tot 0,52). We illustreerden een verhoogde responsiviteit van de diabetische neuropathische

zenuw op lokale anesthetica, evenals een langere retentie van lokale anesthetica in de diabetische neuropathische zenuw. Zo speelden zowel farmacodynamische als farmacokinetische mechanismen een rol bij het verlengen van de duur van de zenuwblokkade in dit knaagdiermodel van neuropathie.

Diabetische perifere neuropathie is een veelvoorkomende complicatie van zowel type 1 als type 2 DM en de meest voorkomende neuropathie in de westerse wereld. Diabetespatiënten ondergaan vaker een operatie dan patiënten zonder diabetes. Verschillende chirurgische ingrepen voor typische complicaties van langdurige DM, bijvoorbeeld het creëren van een arterioveneuze fistel bij patiënten met eindstadium nierziekte, worden bij voorkeur uitgevoerd onder regionale anesthesie. Anesthesiologen komen dagelijks patiënten tegen met diabetische perifere neuropathie, maar er ontbreekt nog steeds begrip met betrekking tot zowel preventie als behandeling. We tonen aan dat de farmacodynamiek en farmacokinetiek van lokale anesthetica invloed uitoefenen op regionale zenuwblokkades bij diabetische neuropathie. Toekomstig onderzoek is nodig voor het bepalen van gedetailleerde dosis-responscurven bij diabetische neuropathie. Specifiek zou dit onderzoek zich kunnen richten op de vraag of de gevoeligheid voor lokale anesthetica, die zich manifesteert bij diverse neuronale subgroepen, specifiek is voor bepaalde natriumstromen en varieert bij verschillende lokale anesthetica.

Sectie 2. Bestudeerde toegepaste anatomie van de saphenous en obturatorius zenuw voor zenuwblokkades in de heup en knie regio.

In **Hoofdstuk 4** voerden we een radiologische kadaverstudie uit om de incidentie van betrokkenheid van de nervus ischiadicus na verschillende technieken van het adductorenkanaalblok (ACB) te onderzoeken, welke klinisch wordt gebruikt bij knie- en onderste extremiteitschirurgie. Achttien niet-geconserveerde menselijke kadavers, in een verse en niet-bevroren toestand, werden willekeurig toegewezen om echografisch geleide zenuwblokkades te ondergaan in de "distale femorale driehoek" danwel het "distale adductorenkanaal" met twee verschillende injectievolumes. Geen betrokkenheid van de nervus ischiadicus, de nervus tibialis of de nervus profundus werd gevonden bij een van de kadavers. Verspreiding van contrast naar de popliteale fossa werd waargenomen bij drie van de 36 kadaverzijden. Zo bleken technieken voor het blokkeren van het adductorenkanaal niet de nervus ischiadicus of zijn belangrijkste takken te blokkeren, zelfs bij gebruik van grotere volumes. Bovendien bereikte het lokale anestheticum in een minderheid van de gevallen de popliteale

fossa, en het blijft onzeker of hierdoor een klinisch analgetisch effect wordt bereikt. Een blokkade van de nervus saphenus kan dus veilig worden uitgevoerd wanneer na de operatie geen spierzwakte gewenst is.

De vraag, relevant voor analgesie bijvoorbeeld bij heupchirurgie, of het fascia iliaca-compartimentblok de nervus obturatorius (NO) betrekt, is een onderwerp van controverse. De mate van betrokkenheid kan afhangen van de verspreiding van het lokale anestheticum in de craniale richting. Daarom hebben we in **hoofdstuk 5** de supra-inguïnale naaldpositionering al dan niet gecombineerd met hydrodissectie op betrokkenheid van de NO en craniale verspreiding van het lokale anestheticum bestudeerd. Zeventien verse, niet-bevroren en niet-geconserveerde menselijke kadavers werden geïncludeerd om 34 blokkades uit te voeren en gerandomiseerd toegewezen aan een supra-inguïnale of infra-inguïnale techniek. Noch de supra-inguïnale naaldbenadering met hydrodissectie, noch enige andere techniek gericht op het fascia iliaca compartiment leidde tot betrouwbare betrokkenheid van de NO, en als zodanig lijkt de NO geen betrokkenheid te hebben bij blokkades gericht op het fascia iliaca compartiment. Toevoeging van een selectieve blokkade van de NO bij het iliaca facialis compartiment (of een blokkade met groot volume) moet worden overwogen wanneer dit klinisch geïndiceerd is.

Translationeel anatomisch onderzoek met een klinische uitkomstmaat in regionale anesthesie is uitdagend vanwege de aanzienlijke anatomische variatie; de translatie van neuroanatomie in kadavers naar de mate van klinische analgesie is vaak geen eenvoudige één-op-één-correlatie. Illustratief is dat de nervus ischiadicus niet betrokken is bij de kadaverstudie van een ACB in Hoofdstuk 4, terwijl in Hoofdstuk 6 mogelijke sensorische betrokkenheid een bijkomende bevinding is. De literatuur beschrijft doorgaans de verspreiding naar de popliteale fossa na een ACB, maar specifieke details over de diepte van verspreiding binnen deze fossa worden zelden besproken. Toekomstig onderzoek zal moeten uitwijzen of het lokale anestheticum consistent sensorische zenuwen bereikt bij het bereiken van de popliteale fossa om de inconsistente klinische analgetische effecten te verklaren. Voor het verdoven van de NO moeten toekomstige studies uitsluitsel geven hoe anesthesie van de NO binnen het retroperitoneale compartiment betrouwbaar kan worden bereikt.

Sectie 3 bepaalde het minimale volume voor de verdoving voor een saphenusblok, en de effectiviteit van een saphenusblok in voortse kruisbandchirurgie in dagbehandeling.
In **Hoofdstuk 6** onderzochten we het saphenusblok (SB) bij vrijwilligers om de verspreiding van sensibiliteitsverlies vast te stellen en het minimale volume van lokale verdoving (MlaV) te bepalen die nodig is om deze anesthesie te bereiken. Volgens het Dixon-dosismodel waren de gemeten MlaV-doses die effectief waren bij 50% (eD50) en de berekende MlaV-effectieve dosis bij 95% (eD95) voor een volledig SB respectievelijk 1,5 en 1,9 ml. De cutane verspreiding van de selectieve zenuwblokkade vertoont aanzienlijke individuele variabiliteit, met name met betrekking tot de innervatie van de dorsale en mediale voet. Er was geen duidelijke correlatie tussen het volume lokale verdoving en het begin of de duur van de selectieve SB.

In **Hoofdstuk 7** randomiseerden we 53 patiënten in een multicenter superioriteitsstudie die een operatie ondergingen voor reconstructie van de voorste kruisband in dagbehandeling. Deze patiënten werden gerandomiseerd voor een femoraalblok (FB) of een ACB voor de postoperatieve pijnstilling. Beide groepen ondergingen een echogeleide zenuwblokkade vóór de inductie van algemene anesthesie. Er was geen significant verschil tussen de twee zenuwblokgroepen wat betreft gereedheid voor ontslag (FB mediaan 1,8 uur (95% CI 1,0 - 3,5) uur, vs. ACB 2,9 uur (CI 1,5 - 4,7); p = 0,3). Motorblokkades en incidentie van (bijna) vallen werden echter vaker gemeld bij patiënten met een FB in vergelijking met die met een ACB. Er waren geen verschillen tussen de groepen in postoperatieve pijnscores in de loop van de tijd. Op dezelfde manier werden bij de follow-up-beoordelingen na zes weken en twaalf weken geen verschillen tussen de groepen waargenomen met betrekking tot het voorkomen van (bijna) vallen en de beoordeling van de knie door de orthopedisch chirurg. Bovendien toonden lange termijn patiënt gerapporteerde uitkomstmetingen geen verschillen tussen de groepen. Een FB heeft daarom een minder gunstig veiligheidsprofiel dan een ACB, gekenmerkt door meer motorblokkades en (bijna) vallen.

Nader onderzoek is nodig om te bepalen of er een correlatie bestaat tussen de toegediende dosis lokale anesthetica in het adductorenkanaal en de duur van postoperatieve analgesie, omdat dit een meer klinisch relevante vraagstelling is. Vanuit een klinisch oogpunt erkennen we dat de patiëntenpopulatie die een reconstructie van de kruisband ondergaat zeer heterogeen is. Toekomstige onderzoek is nodig

naar voorspellende factoren voor postoperatieve pijn binnen deze groep om vooraf patiënten te identificeren die baat zouden kunnen hebben bij deze interventie.

Sectie 4 Stamcellen worden geïntroduceerd.
Deze sectie vormt het deel van het proefschrift dat de discussie moet voeden over de richting waarin het onderzoek naar regionale anesthesie zou moeten gaan. De overgang van dierstudies naar het gebied van stamcellen is een opwindende onderneming; het onderkennen van de principes van stamcellen en het ontwikkelen van een functioneel model dat toepasbaar is in de anesthesiologie.

Hoofdstuk 8 geeft een overzicht van hoe geïnduceerde pluripotente stamcellen (iPSC's) zich positioneren binnen de context van bruikbare stamcelmodellen. We beschrijven de regressie voor het maken van iPSC's naar een pluripotente toestand van somatische cellen, zoals huidfibroblasten. Deze cellen hebben het vermogen te differentiëren tot elk celtype in het lichaam (pluripotentie) en onveranderde dochtercellen te produceren (zelfvernieuwing). De neuronale inductie van de pluripotente stamcel wordt beschreven, evenals de stappen van differentiatie tot een perifeer neuron. Deze uit iPSC afgeleide nociceptoren zijn functioneel volwassen nociceptieve neuronen die de neurotransmitter substantie P afscheiden, elektrisch actief zijn en samensmelten tot ganglionachtige structuren. Het veld zou kunnen profiteren van dit onderzoek model dat de complexe aspecten van pijn signalering bij mensen nauwkeuriger weerspiegelt in vergelijking met de bestaande diermodellen, en heeft potentieel voor farmaceutisch onderzoek.

Uiteindelijk illustreerde **Hoofdstuk 9** een functionele studie waarin we iPSC-afgeleide DRG-nociceptoren differentieerden uit commerciële Human iPSC-Derived Sensory Neuron Progenitors. iPSC's differentiatie volgt stadia die embryonale ontwikkeling nauw nabootsen, gaande van een beginstadium dat lijkt op de ontwikkeling van de neurale buis, tot een volgende subfase van de neurale lijst, en uiteindelijk in 21-28 dagen een toestand bereiken die lijkt op nociceptieve dorsale wortelganglion (DRG) neuronen. Het gebruik van immunofluorescentie bevestigde de perifere sensorische neuronale identiteit voor β3-tubuline en BRN3A. Bovendien bleken neuronen alle verwachte markers van nociceptie tot expressie te brengen, inclusief spanningsafhankelijke natriumkanalen 1.7 en 1.8, transient receptor potential cation channels ankyrin 1 (TRPA1) en vanilloid 1 (TRPV1), en de neurotransmitter substance P. Daarna hebben we de impact van lidocaïne op elektrische activiteit en mogelijke cytotox-

iciteit bestudeerd. Met behulp van MEA toonden we een bijna volledige blokkade aan van de elektrische activiteit na toepassing van lidocaïne, met een toename van LDH ten opzichte van onbehandelde controle. We demonstreerde een door iPSC afgeleid model van DRG-nociceptoren dat morfologisch, moleculair en functioneel lijkt op hun tegenhangers in vivo.

Ons model werd gevalideerd door de gevoeligheid voor de effecten van het gangbare lokale anestheticum lidocaïne te aan te tonen. In de toekomst kunnen experimentele procedures worden aangepast om aanvullende functionele assays (bijv. patch-klemmen of calciumbeeldvorming) en toxicologische assays (bijv. detectie van caspase-enzymactivatie) op te nemen voor een uitgebreid preklinisch onderzoek van nieuwe of gevestigde analgetica. Het model kan ook worden gebruikt voor ziektemodellering van (chronische) pijnomstandigheden en biedt mogelijk een meer gepersonaliseerde benadering van regionale anesthesie, aangezien de genetische code van de donor (inclusief mutaties en variaties) wordt behouden tijdens de iPSC-reprogrammering.

In conclusie heeft deze thesis cruciale vragen behandeld op het gebied van regionale anesthesie, waarbij diverse onderwerpen aan bod kwamen, variërend van diabetes mellitus als co-morbiditeit tot de toepassing van stamcellen op dit gebied. We hebben ons gericht op de klinische relevantie van diabetes mellitus op regionale anesthesie. Farmacodynamische en farmacokinetische aspecten werden onderzocht van lokale anesthetica bij zenuwblokkades bij diabetische ratten, wat inzicht gaf in verhoogde gevoeligheid en verlengde retentie van lokale anesthetica in diabetische neuropathische zenuwen. Bevindingen over de toegepaste anatomie van de saphenus- en obturatorzenuwen voor zenuwblokkades leverden waardevolle inzichten op met betrekking tot verwaarloosbare betrokkenheid van beide zenuwen bij de overeenkomstige blokkades. Het minimale volume lokale verdoving dat nodig is voor een saphenusblok werd bepaald in vrijwilligers, terwijl we het femoraalblok en het adductorkanaalblok vergeleken in dagchirurgie aan de voorste kruisband. De resultaten gaven de voorkeur aan de laatste vanwege een gunstiger veiligheidsprofiel. Het laatste deel van deze scriptie introduceerde stamcellen in het onderzoek naar regionale anesthesie. Het potentieel van geïnduceerde pluripotente stamcellen (iPSC's) werd besproken als een model voor pijn-signalering, We presenteerden een functionele studie met iPSC-afgeleide DRG-nociceptoren, waarbij hun responsivi-

teit op lidocaïne werd aangetoond en een model werd voorgesteld voor preklinisch onderzoek.

Met dit proefschrift hoop ik naast het beantwoorden van specifieke onderzoeksvragen ook een bijdrage te hebben geleverd aan toekomstperspectieven op het gebied van regionale anesthesie. De integratie van stamcelonderzoek opent nieuwe wegen voor het begrijpen van pijnmechanismen en het ontwikkelen van innovatieve benaderingen voor dit medische domein.

Appendices

List of publications W ten Hoope

Comparison of Postoperative Neurocognitive Function in Older Adult Patients with and without Diabetes Mellitus.
van Zuylen ML, van Wilpe R, **Ten Hoope W**, Willems HC, Geurtsen GJ, Hulst AH, Hollmann MW, Preckel B, DeVries JH, Hermanides J.
Gerontology. 2023;69(2):189-200.

Adductor canal block techniques do not lead to involvement of sciatic nerve branches: a radiological cadaveric study.
Smulders PS, **Ten Hoope W**, Baumann HM, Hermanides J, Hemke R, Beenen LFM, Oostra RJ, Marhofer P, Lirk P, Hollmann MW.
Reg Anesth Pain Med. 2023 Jun 29:rapm-2022-104227.

Amputation and prosthetics of the lower extremity: The 2020 Dutch evidence-based multidisciplinary guideline.
Fard B, Persoon S, Jutte PC, Daemen JHC, Lamprou DA, **Hoope WT**, Prinsen EC, Houdijk H, Olsman J, Holling T, De Wever HPPR, Schrier E, Donders N, Rietman JS, Geertzen JHB.
Prosthet Orthot Int. 2023 Feb 1;47(1):69-80.

A radiological cadaveric study of obturator nerve involvement and cranial injectate spread after different approaches to the fascia iliaca compartment block.
Ten Hoope W, Smulders PSH, Baumann HM, Hermanides J, Beenen LFM, Oostra RJ, Marhofer P, Lirk P, Hollmann MW. Sci Rep. 2023 Jul 26;13(1):12070.

The Effectiveness of Adductor Canal Block Compared to Femoral Nerve Block on Readiness for Discharge in Patients Undergoing Outpatient Anterior Cruciate Ligament Reconstruction: A Multi-Center Randomized Clinical Trial.
Ten Hoope W, Admiraal M, Hermanides J, Hermanns H, Hollmann MW, Lirk P, Kerkhoffs GMMW, Steens J, van Beek R. J Clin Med. 2023 Sep 17;12(18):6019.

Prospective comparison of three methods for detecting peri-operative neurocognitive disorders in older adults undergoing cardiac and non-cardiac surgery.
van Zuylen ML, Kampman JM, Turgman O, Gribnau A, **Ten Hoope W**, Preckel B, Willems HC, Geurtsen GJ, Hermanides J. Anaesthesia. 2023 May;78(5):577-586.

Psychometric evaluation of the Dutch 40-item Quality-of-Recovery scale.
Wensing AGCL, van Cuilenborg VR, Breel JS, Heineman DJ, Hermanides J, Hollmann MW, **Ten Hoope W.**
Br J Anaesth. 2022 Jan;128(1):e6-e8.

Investigating Peripheral Regional Anesthesia Using Induced Pluripotent Stem Cell Technology: Exploring Novel Terrain.
Smulders PSH, van Zuylen ML, Hermanides J, Hollmann MW, Weber NC., **Ten Hoope W**
Anesth Analg. 2022 Sep 1;135(3):659-662.

Perioperative cerebrospinal fluid sorbitol and fructose concentrations in patients undergoing thoracic aortic surgery.
van Zuylen ML, Peters van Ton AM, Duindam HB, Scholten E, van Dongen EPA, **Ten Hoope W**, Plummer MP, DeVries JH, Preckel B, Scheffer GJ, Abdo WF, Hermanides J.
Br J Anaesth. 2022 Sep;129(3):e73-e76.

Use of a human induced pluripotent stem cell-derived dorsal root ganglion neurone model to study analgesics in vitro: proof of principle using lidocaine.
Smulders PSH, **Ten Hoope W**, Bernardino Morcillo C, Hermanides J, Hollmann MW, Weber NC. Br J Anaesth. 2022 Dec;129(6):e172-e175.

Effects of surgery and general anaesthesia on sleep-wake timing: CLOCKS observational study.
van Zuylen ML, Meewisse AJG, **Ten Hoope W**, Eshuis WJ, Hollmann MW, Preckel B, Siegelaar SE, Stenvers DJ, Hermanides J.
Anaesthesia. 2022 Jan;77(1):73-81.

Perioperative cerebrospinal fluid sorbitol and fructose concentrations in patients undergoing thoracic aortic surgery.
van Zuylen ML, Peters van Ton AM, Duindam HB, Scholten E, van Dongen EPA, **Ten Hoope W**, Plummer MP, DeVries JH, Preckel B, Scheffer GJ, Abdo WF, Hermanides J.
Br J Anaesth. 2022 Sep;129(3):e73-e76.

Optimal Perioperative Pain Management in Esophageal Surgery: An Evaluation of Paravertebral Analgesia.
Feenstra ML, **Ten Hoope W**, Hermanides J, Gisbertz SS, Hollmann MW, van Berge Henegouwen MI, Eshuis WJ.
Ann Surg Oncol. 2021 Oct;28(11):6321-6328.

The role of intraoperative hypotension on the development of postoperative cognitive dysfunction: a systematic review.
van Zuylen ML, Gribnau A, Admiraal M, **Ten Hoope W**, Veelo DP, Hollmann MW, Preckel B, Hermanides J.
J Clin Anesth. 2021 Sep;72:110310.

Registration of attentional function as a predictor of incident delirium (the RAPID study).
van Zuylen ML, Hermanides J, **Ten Hoope W**, Preckel B, van de Beek D, van Gool WA, Schoenmaker N.
Alzheimers Dement (N Y). 2020 Jun 16;6(1):e12031.

Paravertebral catheter versus EPidural analgesia in Minimally invasive Esophageal resectioN: a randomized controlled multicenter trial (PEPMEN trial).
Kingma BF, Eshuis WJ, de Groot EM, Feenstra ML, Ruurda JP, Gisbertz SS, **Ten Hoope W**, Marsman M, Hermanides J, Hollmann MW, Kalkman CJ, Luyer MDP, Nieuwenhuijzen GAP, Scholten HJ, Buise M, van Det MJ, Kouwenhoven EA, van der Meer F, Frederix GWJ, Cheong E, Al Naimi K, van Berge Henegouwen MI, van Hillegersberg R.
BMC Cancer. 2020 Feb 22;20(1):142.

Driving Pressure During General Anesthesia for Open Abdominal Surgery (DESIGNATION): study protocol of a randomized clinical trial.
DESIGNATION–investigators.
Trials. 2020 Feb 18;21(1):198.

Safety of epidural drugs: a narrative review.
van Zuylen ML, **Ten Hoope W**, Bos E, Hermanides J, Stevens MF, Hollmann MW.
Expert Opin Drug Saf. 2019 Jul;18(7):591-601.

Pharmacodynamics and Pharmacokinetics of Lidocaine in a Rodent Model of Diabetic Neuropathy.
Ten Hoope W, Hollmann MW, de Bruin K, Verberne HJ, Verkerk AO, Tan HL, Verhamme C, Horn J, Rigaud M, Picardi S, Lirk P.
Anesthesiology. 2018 Mar;128(3):609-619.

Minimum local anesthetic volumes for a selective saphenous nerve block: a dose-finding study.
Ten Hoope W, Hollmann MW, Atchabahian A, Rigaud M, Kerkhoffs GM, Lirk P, Baumann HM.
Minerva Anestesiol. 2017 Feb;83(2):183-190.

Regional anesthesia in diabetic peripheral neuropathy.
Ten Hoope W, Looije M, Lirk P.
Curr Opin Anaesthesiol. 2017 Oct;30(5):627-631.

Effects of early and late diabetic neuropathy on sciatic nerve block duration and neurotoxicity in Zucker diabetic fatty rats.
Lirk P, Verhamme C, Boeckh R, Stevens MF, **ten Hoope W**, Gerner P, Blumenthal S, de Girolami U, van Schaik IN, Hollmann MW, Picardi S.
Br J Anaesth. 2015 Feb;114(2):319-26.

Localization of the potential zonal marker clusterin in native cartilage and in tissue-engineered constructs.
Malda J, **ten Hoope W**, Schuurman W, van Osch GJ, van Weeren PR, Dhert WJ.
Tissue Eng Part A. 2010 Mar;16(3):897-904.

Zonal chondrocyte subpopulations reacquire zone-specific characteristics during in vitro redifferentiation.
Schuurman W, Gawlitta D, Klein TJ, **ten Hoope W**, van Rijen MH, Dhert WJ, van Weeren PR, Malda J.
Am J Sports Med. 2009 Nov;37 Suppl 1:97S-104S.

List of Co-author's

Markus W Hollmann
Department of Anesthesiology
Amsterdam UMC, AMC Amsterdam

Arthur Atchabahian
Department of Anaesthesiology
New York University School of Medicine
New York, USA

Marcel Rigaud
Department of Anaesthesiology
Medical University Graz
Graz, Austria

Gino M Kerkhoffs
Department of Orthopedic Surgery
Amsterdam UMC, AMC Amsterdam

Philip Lirk
Department of Anesthesiology
Brigham and Women's Hospital
Harvard Medical School
Boston Massachusetts, USA

Holger M Baumann
Department of Anesthesiology
Amsterdam UMC, AMC Amsterdam

Kora de Bruin
Department of Nuclear Medicine
ARIA-IWO laboratorium
Amsterdam UMC, AMC Amsterdam

Hein J Verberne
Department of Nuclear Medicine
Amsterdam UMC, AMC Amsterdam

Arie O Verkerk
Department of Cardiology
Department of Anatomy, Embryology and Physiology
Amsterdam UMC, AMC Amsterdam

Hanno L Tan
Department of Cardiology
Amsterdam UMC, AMC Amsterdam

Camiel Verhamme
Department of Neurology
Amsterdam UMC, AMC Amsterdam

Janneke Horn
Department of Intensive Care
Laboratory of Experimental Anesthesiology and Intensive Care (LEICA)
Amsterdam UMC, AMC Amsterdam

Susanne Picardi
Department of Anesthesiology
University of Heidelberg
Heidelberg, Germany

Pascal SH Smulders
Department of Anesthesiology
Amsterdam UMC, AMC Amsterdam

Mark L van Zuylen
Department of Anesthesiology
Amsterdam UMC, AMC Amsterdam

Jeroen Hermanides
Department of Anesthesiology
Amsterdam UMC, AMC Amsterdam

Nina C Weber
Department of Anesthesiology
Laboratory of Experimental Anesthesiology and Intensive Care (LEICA)
Amsterdam UMC, AMC Amsterdam

Carmen Bernardino Morcillo
Department of Anesthesiology
Laboratory of Experimental Anesthesiology and Intensive Care (LEICA)
Amsterdam UMC, AMC Amsterdam

Robert Hemke
Department of Radiology
Amsterdam UMC, AMC Amsterdam

Ludo FM Beenen
Department of Radiology
Amsterdam UMC, AMC Amsterdam

Roelof-Jan Oostra
Department of Medical Biology
Amsterdam UMC, AMC Amsterdam

Peter Marhofer
Department of Anesthesiology & Intensive Care Medicine
Medical University of Vienna
Vienna, Austria

Manouk Admiraal
Department of Anesthesiology
Amsterdam UMC, AMC Amsterdam

Henning Hermanns
Department of Anesthesiology
Amsterdam UMC, AMC Amsterdam

Jeroen Steens
Department of Orthopedics
Dijklander Ziekenhuis, Hoorn

Rienk van Beek
Department of Orthopedics
Dijklander Ziekenhuis, Hoorn

Marjoleijn Looije
Department of Anesthesiology
Amsterdam UMC, AMC Amsterdam

PhD Portfolio

PhD student: Werner ten Hoope
Supervisors: Prof. dr. M.W. Hollmann en Prof. dr. J. Hermanides
PhD period: 2014 – 2024

PHD Training	Year	ECTS
Courses		
Basiscursus regelgeving klinisch onderzoek (BROK)	2013	0,9
Course Laboratory Animal Science to obtain art. 9 certificate	2017	18,75
Hercertificering BROK	2018	0,25
Hercertificering BROK	2022	0,25
Presentations		
Effects of early and late diabetic neuropathy on sciatic nerve block duration and neurotoxicity in Zucker diabetic fatty rats. NVA jaarvergadering	2017	0,5
Local anesthetics: pharmacodynamics and pharmacokinetics in models of diabetic neuropathy. Euroanaesthesia Copenhagen	2018	0,5
Pharmacodynamic and pharmacokinetic aspects of regional anesthesia in neuropathy *DARA Annual meeting*	2020	0,5
International conferences		
American Society of Anesthesiologists Annual Meeting, San Francisco	2013	0,75
Euroanaesthesia Stockholm	2014	0,5
Euroanaesthesia Berlin	2015	0,5
DARA Annual conference	2016	0,5
DARA Annual conference	2017	0,5
Euroanaesthesia Copenhagen	2018	0,5
DARA Annual conference	2018	0,5
Euroanaesthesia Vienna	2019	0,5
DARA Annual conference	2019	0,5
Euroanaesthesia Virtual	2020	0,5
DARA Annual conference	2021	0,5
Euroanaesthesia Milan	2022	0,5
DARA Annual conference	2023	0,5
DARA Annual conference	2024	0,5

Teaching		
Key speaker AO-symposium regional anesthesia in Thorax Trauma	2019	0,75
Other		
Richtlijn ontwikkeling NVA/ FMS Amputatie en prothesiologie onderste extremiteit	2018-2019	1
Supervising		
P. Smulders, IPSC in regional anesthesia	2022 - 2024	4
Department of Anesthesia, Amsterdam UMC	2018	0,75
Grants		
Innovation Grant AMC €100.000	2018	1
ESRA Research Support Grant €10.000	2019	0,1
BBraun Education Grant €8000	2019	2
ZonMW Paravertebral catheter versus Epidural in Minimally Invasive Esophageal Resection: a randomized controlled multicenter trial (PEPMEN trial) €392.960		
Awards and Prizes		
Ritsema van Eck Award NVA, First author	2019	
Matthieu Gielen Award DARA, First author	2018	
Publications		
Peer reviewed 22		
Book chapter 2		
Probleem georiënteerd denken in de anesthesiologie, Hoofdstuk lokaal anesthetica 2016		
Regional Anesthesia - From Anatomy to Clinical Practice, Chapter 63 Cambridge University Press 2024 (in press)		
A&I 2020 Paravertebrale pijnstilling: Een vergeten techniek maakt een comeback		
A&I 2020 Locoregionale anesthesie bij diabetische polyneuropathie		

Biography

Werner ten Hoope, born on June 22, 1979, in 's-Gravenhage, spent most of his childhood in Zoetermeer. He completed his education at the Alfrink College in Zoetermeer and started on his educational journey by pursuing a degree in Physical Therapy at Hogeschool Utrecht. Subsequently, he pursued a master's course in General Health Science at Utrecht University for two years. In 2005, he enrolled in the Selective Utrecht Medical Master course (SUMMA) at Utrecht University, a comprehensive 4-year program integrating medical practice and research. He earned his master's degree in medicine in 2009.

Werner gained valuable clinical experience by working as a resident, not in training, for two years in the Department of Surgery and subsequent Intensive Care Medicine at Isala Clinics in Zwolle. In 2011, he commenced his residency as an Anesthesiologist in training at the Amsterdam Medical Center, University of Amsterdam, culminating in a fellowship in Intensive Care Medicine completed in 2017. Concurrently, during his residency, he began working part-time as a PhD candidate at the Laboratory of Experimental Intensive Care and Anesthesiology. This marked the beginning of his current research focus on stem cell research, clinical research and regional anesthesia. After four years as a senior consultant in Anesthesiology, he transitioned to Rijnstate Hospital in Arnhem, where he continues his professional contributions.

Dankwoord

De route naar het behalen van een doctoraat kent zelden een strak verloop, en dus ook mijn traject heeft diepe dalen en hoge beklimmingen gekend. Dit proefschrift heb ik kunnen schrijven dankzij de bijdragen van velen; en het is juist de samenwerking met deze mensen die het bereiken van de top waardevol heeft gemaakt. Ik wil graag uitgebreid mijn dank uitspreken naar eenieder die zich hierin herkent. Hoewel ik ongetwijfeld tekort zal schieten in mijn streven naar volledigheid, is mijn oprechte dankbaarheid ook jegens deze mensen niet minder gemeend. Een aantal mensen wil ik in het bijzonder bedanken, om te beginnen mijn promotieteam.

Markus, ik wil mijn diepe waardering uitspreken voor jouw als promotor en persoon tijdens mijn promotietraject. Je hebt destijds ingestemd met mijn plan om een onderzoek op te zetten dat zowel fundamentele als klinische aspecten omvatte. Hoewel je de risico's en uitdagingen niet verbloemde, stond je vanaf het begin achter mij. Binnen de opleiding kreeg ik alle ruimte om mezelf als onderzoeker te ontplooien. Vervolgens schonk je mij het vertrouwen voor een stafplek binnen jouw afdeling. Zelfs toen ik naar een ander ziekenhuis vertrok, bleef je mij niet alleen steunen, maar ook herinneren, bevragen, verwonderen en uitdagen. Maar bovenal bleef je mij steunen. Zonder jou zou dit promotietraject niet mogelijk zijn geweest. Ik wil je oprecht bedanken voor het vertrouwen, de vrijheid en het geduld dat je mij hebt geschonken om mijn ideeën te ontwikkelen. Ik had geen betere promotor kunnen wensen en kijk uit naar de mogelijkheden in de toekomst. Bedankt voor de afgelopen jaren!

Jeroen, de precieze timing van jouw betrokkenheid bij mijn onderzoek is enigszins vaag. Jij vond je passie in de suiker met mensen, terwijl ik mij bezighield met suikerratten. Deze complementariteit heeft wellicht de interesse in elkaars onderzoek aangewakkerd. Vanaf het begin wist ik jou te vinden om samen de wetenschappelijke paden te bewandelen; je was als het ware mijn onofficiële copromotor. Geleidelijk groeide onze relatie uit tot een vriendschap die het vanzelfsprekend maakte dat jij een co-promotor plaats moest vervullen. Samen begonnen we te fantaseren, publiceerden we en ontwikkelden we samenwerkingslijnen met andere afdelingen. Maar bovenal wist ik jou altijd te vinden voor steun en gezelligheid, zelfs tot in de late uurtjes. Recent ben jij heel terecht benoemd tot professor en kon je in het team de plek van promotor innemen. Ik ben jou buitengewoon dankbaar voor de academische reis die we samen hebben gemaakt, voor alle inzichten, tijd en ideeën die je

hebt gedeeld, de concerten en borrels die we hebben beleefd en voor alles wat ons onderzoek ons gezamenlijk heeft gebracht. Bedankt makker!

Beste Arie, mijn oprechte dank voor het aanvaarden van je rol als co-promotor. Niet meer dan een terechte plek. Jouw betrokkenheid bij mijn onderzoeken is vanaf het allereerste begin essentieel geweest. In eerste instantie bij de rattenstudies, en nog steeds ben jij van onschatbare waarde bij de ontwikkeling van de stamcelmodellen. Zonder jouw inzet zou er geen fundamenteel onderzoek in mijn proefschrift zijn opgenomen. Ik heb altijd bijzonder gewaardeerd hoe ik te allen tijde kon aankloppen bij jou, en jij niet alleen de weg wist naar andere experts, maar ook de faciliteiten van jouw laboratorium ter beschikking hebt gesteld. Jouw inbreng en betrokkenheid hebben een cruciale rol gespeeld in de totstandkoming van dit proefschrift.

Beste Mark, in de wereld van wederkerigheid is het credo "voor wat, hoort wat". Gedurende jouw promotieonderzoek mocht ik jou ondersteunen om tot een prachtig proefschrift te komen. Niet dat mijn begeleiding doorslaggevend was, maar er is een punt bereikt waarop jij om kon kijken met een afgerond proefschrift. Vanaf toen kon ik op jou rekenen mijn proefschrift tot een goed einde te brengen. Jouw immer gulle lach, grenzeloze inzet en de mooie momenten, zowel inhoudelijk als in de kroeg, hebben een onschatbare waarde toegevoegd aan mijn proefschrift. Hartelijk dank voor alles, in de ruimste zin van het woord.

Beste Philipp, zelden heb ik een onderzoeker ontmoet die zo bevlogen en tegelijkertijd betrokken bij de klinische praktijk is als jij. Samen hebben we initieel mijn onderzoek vorm kunnen geven, en mocht ik jouw laboratoriumonderzoek overnemen. Jij hebt mij de nuances van het onderzoek bijgebracht, mij geïnspireerd en gevormd in de wetenschap. Jouw hulp is niet alleen waardevol, maar onmisbaar geweest. Toen jij de kans kreeg om je carrière voort te zetten aan Harvard, had je mij voldoende bagage gegeven om het onderzoek succesvol voort te zetten. Ik hoop oprecht dat er in de toekomst weer mogelijkheden zijn om samen te werken. Jouw begeleiding heeft van mij een betere onderzoeker gemaakt, waarvoor ik je buitengewoon dankbaar ben. Ik wens je nog steeds alle geluk toe in de US.

Geachte leden van de leescommissie – prof. dr J.H de Vries, prof. dr M.B. Vroom, prof. dr A.P.J. Vlaar, prof. dr J. Bruhn, prof. dr. M.M.P.J. Reijnen en dr. E. Bos - veel dank

voor het beoordelen van mijn proefschrift en uw bereidheid om zitting te nemen in mijn commissie.

Pascal, jouw onderzoek vormt een naadloze voortzetting van onze onderzoekslijn. Vanuit de polikliniek in Arnhem weggekaapt, heb jij je met volle overgave gestort op het terrein van stamcelonderzoek, en nu blijkt al snel dat dit buitengewoon succesvol is. Ik ben ontzettend trots dat we samen het model verder hebben kunnen ontwikkelen; zonder jouw toewijding zou dat zeker niet zo ver zijn gekomen. Ik heb alle vertrouwen dat we gezamenlijk in staat zullen zijn om een diabetisch neuropathisch stamcelmodel te creëren. Ik bewonder je eigenzinnigheid, je vastberadenheid en je zelfvertrouwen waarmee je door het leven gaat en trouw blijft aan jezelf. Dank voor alles!

Nina, ook jouw rol als hoofdonderzoeker op het LEICA lab is van onschatbare waarde geweest voor het laatste deel van het proefschrift. Voor jou was dit eveneens een onderzoeksveld met talloze uitdagingen, zeker gezien de moeizame opstart door de invloed van COVID-19. Jouw ongelofelijke inzet en toewijding aan de begeleiding op het laboratorium zijn ongeëvenaard; zonder jouw inbreng zouden we nu niet staan waar we staan. Heel veel dank hiervoor, en ik kijk ernaar uit om onze samenwerking nog lang voort te zetten.

Voor de realisatie van dit proefschrift is nauw samengewerkt met het Dijklanderziekenhuis in Hoorn. Aan Rienk en Jeroen wil ik mijn oprechte dank betuigen voor hun waardevolle bijdrage, betrokkenheid en de tijd die zij hebben geïnvesteerd in de studie.

Ik wil graag mijn oud-collega AIOS hartelijk bedanken voor hun deelname als proefpersoon, zoals beschreven in hoofdstuk 6. Dit onderzoek heeft zelfs de Raad van Bestuur van het AMC bereikt, waarbij er aandacht werd besteed aan de ethische grenzen van afhankelijkheid bij dergelijk onderzoek onder het personeel. Nogmaals mijn oprechte dank aan iedereen die heeft bijgedragen!

Mijn paranimfen Mart en Michiel. Jullie kenden elkaar al voordat ik me bij jullie aansloot tijdens een briljante cursus in Botswana. Die tijd was ongelooflijk mooi en heeft een stevig fundament gelegd voor prachtige momenten, fijne spijzen en genietmomenten met mooie wijnen. Samen met Charlotte en Joyce zijn jullie ontzet-

tend belangrijk in zowel goede als minder goede tijden. Bedankt voor jullie warme vriendschap.

Graag wil ik mijn collega's van het AMC en het Rijnstate Ziekenhuis, coauteurs, mijn familieleden, schoonfamilie en vrienden hartelijk bedanken voor alle steun die ik heb ontvangen gedurende het proces van dit proefschrift. Ook zonder jullie zou deze promotie niet mogelijk zijn geweest.

In het bijzonder Wim en Jose. Zonder jullie inspanningen, toewijding, liefde, geduld en geluk zou mijn leven nooit tot dit punt zijn gekomen. Samen met Elske kijken we terug op een tijd die ons onbetaalbare herinneringen heeft geschonken.

Lieve Marin, mijn trots en toeverlaat, altijd sta je klaar om mij te ondersteunen en te faciliteren bij de dromen die we samen waar willen maken. De vrijheid en ruimte die je mij geeft in alles wat ik aanpak lijkt grenzeloos. Dit geldt ook voor dit proefschrift. Jij hebt minstens net zoveel tijd en energie gestoken om het voor mij mogelijk te maken de promotie tot een goed einde te brengen. De druk van ons beider werk, wetenschap, het gezin en beide een fijn sociaal leven trekt soms best een wissel op onze tijd samen. Ik ben ontzettend trots op jou, op wat we samen bereiken met onze lieve kinderen, we ons droomhuis hebben gevonden op onze boerderij en ons thuis hebben gevonden in de Achterhoek. Een dikke zoen voor jou, Siemen, Jelte, Plien en Jolie.

Dankjewel lieve Stefanie, altijd het gevoel je heel dichtbij mee te dragen fluister je mij zelfvertrouwen in.


ANESTHESIESWIDERZOEKERS
UNITED